Thesis submitted for the degree
of Doctor of Philosophy at the
University of Leicester

by

Oliver Zaccheo
MRC Toxicology Unit/Department of Genetics
University of Leicester

Submitted April 2003

ProQuest LLC
789 East Eisenhower Parkway
P.O. Box 1346
Ann Arbor, MI 48106-1346

Analysis of the Yeast Homologue of Neuropathy Target Esterase

Oliver Zaccheo

Abstract

Neuropathy Target Esterase (NTE) is an essential protein implicated in mammalian neural development and was first identified as the target for those organophosphates (OPs) that cause a delayed neuropathy. NTE has esterase activity, allowing it to hydrolyse the artificial substrate phenyl valerate *in vitro*: this can be followed in a simple assay. OPs inhibit this activity by reacting with the essential active site serine of NTE. Recent evidence suggests the physiological substrate of NTE to be a lysophospholipid. Previous work has shown that a region of 489 amino acids towards the C-terminal of NTE forms a domain that is sufficient for catalysis. The N-terminal portion of NTE contains regions that show similarity to cAMP-binding domains. These may contribute a regulatory role but have yet to be proved functional.

On the basis of sequence data, NTE belongs to a family of proteins whose members are found in organisms ranging from bacteria to man. The previously uncharacterised protein Yml059c of the baker's yeast *Saccharomyces cerevisiae* belongs to the NTE family of proteins, displaying 58% similarity and 38% identity to NTE over the catalytic domain (NTE residues 727-1216) and also possessing a putative cAMP-binding motif.

This study has shown that *YML059c* is not essential for cell viability; deletion or overexpression of *YML059c* failed to cause any obvious phenotype. Visualisation by green fluorescent protein tagging revealed the protein to be associated with an undetermined intracellular organelle. Experiments described here show that Yml059c possesses a similar biochemical activity to mammalian NTE. Like NTE, it was able to hydrolyse phenyl valerate in an organophosphate-sensitive manner and had lysophospholipase activity. The catalytic activity of Yml059c was also dependent upon a serine residue, in an equivalent location to that of NTE's active site. In addition, Yml059c appeared able to bind radioactively labelled cAMP, suggesting a possible mechanism whereby the catalytic activity of this family of proteins may indeed be regulated by cAMP. The tentative conclusion can be drawn that Yml059c performs a similar cellular role in yeast as NTE does in mammals.

Acknowledgements

I would like to thank my two supervisors Paul Glynn and Peter Meacock for their unending advice, support and enthusiasm throughout the course of this project.

Many thanks must go to Glen, Kezza, Marcus, Ray, Rob, Stu and all other past and present crew of the good ship Biocentre for sensible and constructive scientific advice at times and less sensible shenanigans most of the rest of the time.

The biggest thanks of all must go to Mandy who's been a pillar of support and encouragement over the last three-and-a-bit years, especially during the preparation of this thesis when it was certainly needed the most!

Abbreviations

[^{3}H]	Tritiated
A	Adenine
$A_{(260)}$	Absorbance at (260)nm
AAP	4-aminoantipyrine
AchE	Acetylcholinesterase
Amp	Ampicillin
ANP	D-(−)-threo-2-amino-1-[p-nitrophenyl]-1,3-propanediol
APS	Ammonium persulphate
ATP	Adenosine-5'-triphosphate
BCIP	5-bromo-4-chloro-3-indolyl phosphate
bp	Base pairs
BSA	Bovine serum albumin
C	Cytosine
cAMP	Cyclic adenosine monophosphate
CAP	Catabolite gene activator protein
cdc	Cell division cycle
CHAPS	3-[(3-cholamidopropyl)dimethylammonio]-1-propane-sulfonate
CMVIE	Cytomegolovirus immediate early promoter
CoA	coenzyme A
dATP	Deoxyadenosine 5'-triphosphate
dCTP	Deoxycytidine 5'-triphosphate
DEPC	Diethyl pyrocarbonate
DFP	Di-isopropylfluorophosphate
dGTP	Deoxyguanosine 5'-triphosphate
DMF	Dimethylformamide
DMSO	Dimethylsulfoxide
DNA	Deoxyribonucleic acid
DNP	Dinitrophenol
DOPC	Dioleoylphosphatidylcholine
DPM	Disintegrations per minute
DTT	Dithiothreitol
dTTP	Deoxythymidine 5'-triphosphate
ECL	Enhanced chemiluminescence
EDTA	Ethylenediamine tetra acetic acid
EOPF	Ethyl octylphosphonofluoridate
ER	Endoplasmic reticulum
FFA	Free fatty acid
G	Guanine
GDP	Glyceraldehyde-3-phosphate dehydrogenase
GFP	Green fluorescent protein
GPCR	G-protein coupled receptor
GPI	Glycosyl-phosphatidylinositol

GTP	Guanosine triphosphate
HEPES	4-(2-Hydroxyethyl)piperazine-1-ethanesulfonic acid
IBMX	3-Isobutyl-1-methylxanthine
IMS	Industrial methylated spirit
$iPLA_2$	Calcium independent phospholipase A_2
IPTG	Isopropyl-β-D-thiogalactopyranoside
Kan	Kanamycin
kb	Kilobase pairs
kDa	Kilo Daltons
LB	Luria Bertani
LGT	Low gelling temperature
LYSO-PL	Lysophospholipid
MAFP	Methyl arachidonyl fluorophosphonate
MOPS	4-morpholinepropanesulfonic acid
mRNA	Messenger RNA
NBT	Nitro blue tetrazolium
NEST	NTE esterase domain
NTE	Neuropathy Target Esterase
OLB	Oligo labelling buffer
OP	Organophosphorus esters
ORF	Open reading frame
PA	Phosphatidic acid
PBC	Phosphate binding cassette
PC	Phosphatidylcholine
PCR	Polymerase chain reaction
PE	Phosphatidylethanolamine
PI	Phosphatidylinositol
PI-PLC	Phosphatidylinositol-specific phospholipase C
PKA	Protein kinase A
PKA-R1α	Protein kinase A regulatory subunit 1α
PLA_2	Phospholipase A_2
PLB	Phospholipase B
PLC	Phospholipase C
PLD	Phospholipase D
PLPC	1-palmitoyl-lysophosphatidylcholine
PMSF	Phenyl methylsulphonylfluoride
PS	Phosphatidylserine
psi	Pounds per square inch
PSP	Phenyl saligenin phosphate
PV	Phenyl valerate
PVDF	Polyvinylidene fluoride
RNA	Ribonucleic acid
S9B	1-(saligenin cyclic phosphoro)-9-biotinyl-diaminononane
SCM	Synthetic complete media
SD	Synthetic defined

SDS	Sodium dodecylsulphate
SDS-PAGE	sodium dodecylsulphate polyacrylamide gel electrophoresis
SLAD	Synthetic low ammonia dextrose
SLAG	Synthetic low ammonia galactose
SSC	sodium chloride/sodium citrate
STRE	Stress response element
SWS	Swiss cheese
T	Thymine
TAE	Tris-acetate EDTA
TBHB	2,4,6-tribromo-3-hydroxy-benzoic acid
TBS	Tris buffered saline
TE	Tris/EDTA
TEMED	N,N,N',N'-Tetramethylethylenediamine
TOCP	Tri-o-cresyl phosphate
Tris	2-amino-2-(hydroxymethyl)-1,3-propanediol
UTP	Uridine triphosphate
UV	Ultra violet
v/v	Volume by volume
w/v	Weight by volume
YNB	Yeast nitrogen base
YNEST	Yeast NTE esterase domain
YPD	Yeast peptone dextrose

Table of Contents

Figures and Tables

Chapter 1: General Introduction

1.1 Yeast as a model organism for the study of higher eukaryotes

In this study, the baker's yeast *Saccharomyces cerevisiae* is used as a model organism to investigate the biochemical role of Neuropathy Target Esterase (NTE); the target protein for organophosphate induced delayed neuropathy (OPIDN) and putatively involved in mammalian neural development (Glynn, 2000). *S.cerevisiae* is a single-celled fungus with a range of features that make it ideally suited as a model organism for the study of fundamental gene functions in higher eukaryotes. Despite being separated by some 1.5 billion years of evolution, many biochemical pathways and cellular processes remain conserved between *S.cerevisiae* and humans (Wang *et al.*, 1999b). *S.cerevisiae* was the first eukaryote to have its entire genome sequenced (Goffeau *et al.*, 1996) simplifying the identification of possible yeast homologues to mammalian genes. By exploiting yeast's efficient system of homologous recombination, simple protocols have been devised for rapid and accurate gene disruption. The genome of *S.cerevisiae* also contains relatively few introns simplifying the cloning of any gene of interest by the polymerase chain reaction (PCR). Under ideal conditions laboratory yeast cells divide every ninety minutes and will stably exist in a haploid or diploid form until mated or induced to undergo meiosis. Yeast will readily take up plasmid DNA and can be manipulated to overexpress a protein of interest with post-translational modifications more similar to that of a higher eukaryote than would be achieved in a bacterial system. With many of the cellular processes of yeast already well understood, investigation of an unknown gene may place it in a biochemical pathway that has been previously characterised.

There are many examples of yeast research that has led to an enhanced understanding of mammalian systems. Much of what is known about the eukaryotic cell cycle started with the identification of conditional cell division cycle (cdc) mutants in *S.cerevisiae* (Hartwell, 1974). Using a similar approach, mutants of the fission yeast *Schizosaccharomyces pombe* that prematurely entered mitosis were isolated and from this screen two genes, wee1 and cdc2 were identified that controlled progression into M-phase (Nurse *et al.*, 1976). Cdc2 was shown to have kinase activity (Simanis and Nurse, 1986) and was found to have a central role in the fission yeast cell cycle as it also controls the onset of S-phase (Nurse and Bissett, 1981). The equivalent key gene in the regulation of the human cell division cycle was cloned by functional complementation of a temperature sensitive cdc2 mutant in fission

yeast (Lee and Nurse, 1987). This shows the potential power of yeast genetics and also serves as an example of the conservation of gene function across such diverse systems.

A recent example where yeast has proved a useful model system for human neural development is in the study of the juvenile neuronal ceroid-lipofuscinoses or Batten disease. This is a progressive neurodegenerative disease, with an incidence as high as 1 in 12,500 live births (Banerjee *et al.*, 1992) and is characterised by a decline in mental abilities, increased severity of untreatable seizures, blindness, loss of motor skills and premature death. By positional cloning, mutation of the human CLN3 gene was shown to be responsible for Batten disease with most sufferers carrying a major deletion of this gene (The International Batten Disease Consortium, 1995). However, the function of the CLN3 protein and the molecular basis of the disease remain undetermined. At the cellular level Batten disease results in an accumulation of autofluorescent material in the lysosomes of neurons and some other cell types (Koenig *et al.*, 1964). The major component of these accumulations has since been shown to be subunit *c* of the mitochondrial ATP synthase (Hall *et al.*, 1991; Palmer *et al.*, 1992). Normally CLN3 is localised to the lysosome so the defect is presumed to be there rather than in the mitochondria (Jarvela *et al.*, 1998; Jarvela *et al.*, 1999). Putative homologues to CLN3 can be found in a variety of species including mouse, dog, rabbit, *C.elegans* and *S.cerevisiae.* The yeast gene *BTN1* is non-essential and encodes a protein that is 39% identical and 59% similar to human CLN3 (Pearce and Sherman, 1997). Yeast lacking the *BTN1* gene have been shown to cause a pH decrease in the growth media, providing resistance to D-(–)-threo-2-amino-1-[p-nitrophenyl]-1,3-propanediol (ANP). This change in extracellular pH is brought about by an increase in activity of the plasma membrane H^+-ATPase, which in turn is in response to an imbalance of pH homeostasis within the cell caused by an abnormally acidic vacuole (Pearce *et al.*, 1999). The ANP resistant phenotype could be complemented with the human CLN3 gene. Point mutations within *BTN1*, equivalent to point mutations of CLN3 identified in less severe forms of Batten disease caused a corresponding decreased level of ANP resistance (Pearce and Sherman, 1998). Thus, the gene products of *BTN1* and CLN3 are inferred to be required for correct regulation of the pH of the vacuole or lysosome, respectively. This example shows again the possible conservation of gene function between yeast and man, and provides a model by which ongoing studies may facilitate the further understanding of the function of CLN3 and the molecular basis of human neurodegeneration.

With the discovery and subsequent characterisation of the [*URE3*] and [*PSI*$^+$] determinants as yeast prions by Wickner (1994) yeast may also provide an amenable model system for enhancing our understanding of human prions and the spongiform encephalopathies.

1.2 Neuropathy Target Esterase and organophosphate induced delayed neuropathy

In humans and some other vertebrates, exposure to di-isopropylfluorophosphate (DFP) or certain other organophosphates (OPs) causes a delayed degeneration of the long axons of the peripheral nerves and spinal cord, termed Organophosphate Induced Delayed Neuropathy (OPIDN). Unlike acute cholinergic syndrome, caused by OP inhibition of acetylcholinesterase (AchE) for which the clinical signs are almost immediate, this neuropathy is characterised by a latent phase of 1-2 weeks followed by initial sensory disorders progressing to weakness and eventual flaccid limb paralysis some 1-3 weeks after exposure (Lotti, 1991).

Although such a delayed neuropathy had been occasionally observed in tuberculosis patients treated with phosphocreosote (Johnson, 1987), the toxicity of such compounds was not realised until a major poisoning outbreak in 1930. More than 10,000 people suffered symptoms of OPIDN, after consuming a contaminated liquor ("Ginger Jake"). Using the adult hen as an experimental model, the causative agent was found to be the OP, tri-*o*-cresyl phosphate (TOCP) (Smith *et al.*, 1930) (for the structure of TOCP and some of the compounds used in the study of NTE and OPIDN see Figure 1.1). Other examples of compounds containing potentially neuropathic OPs include some older pesticides, aircraft lubricants and industrial plasticizers, although potently neuropathic pesticides are no longer in use.

Organophosphorus compounds such as phosphonates and phosphates are known to inhibit members of the serine hydrolase superfamily of proteins. This family includes serine esterases, proteases, lipases and amidases. These enzymes are all characterised by an active site serine, at the centre of a Gly-X-Ser-X-Gly motif, that participates covalently in catalysis and most employ a "catalytic triad" consisting of this serine, a histidine and an acidic residue (either aspartate or glutamate). The serine esterase family (including AchE) hydrolyse carboxylate esters by the formation of a covalent acyl-enzyme intermediate expelling an alcohol moiety. Water, acting as a nucleophile subsequently disrupts this intermediate releasing a carboxylic acid and regenerating the free enzyme (see Figure 1.2). OPs inhibit serine esterases by binding in an analogous reaction, generating a phosphorlyated enzyme that is greatly more resistant to hydrolysis. Some OPs are able to undergo a second reaction once bound to the enzyme. This reaction is termed 'aging' and involves loss of one of the OP's R groups, leaving the enzyme's active site carrying a negative charge. This arrangement of enzyme covalently bound to a negatively charged

OP is considerably more resistant to reactivation by nucleophiles. Only those OPs that undergo this aging reaction cause OPIDN (Johnson, 1974).

The target for the neuropathic OPs that cause OPIDN was discovered to possess esterase activity and was defined as the remaining sites in chicken brain homogenates that bind radiolabelled DFP or hydrolyse the artificial substrate phenyl valerate (PV), after preincubation with a non-neuropathic OP (Johnson, 1969a; Johnson, 1969b). This protein was subsequently named Neuropathy Target Esterase. The internationally recognised assay for NTE is defined as the portion of a sample's PV hydrolase activity that is resistant to the non-neuropathic OP paraoxon and sensitive to the neuropathic OP mipafox (Johnson, 1977). Using a combination of this assay and radiolabelling with [^{3}H]DFP it was shown that, in brain, NTE is associated with microsomal membranes (Richardson *et al.*, 1979) and has a subunit size of 155 kilo Daltons (kDa) (Williams and Johnson, 1981). The highest NTE activity in the adult chicken is present in the brain with lowered but detectable activity in the spinal cord and sciatic nerve. Lower levels of NTE can also be found in some non-neural tissues including intestine, spleen and thymus (Johnson, 1982).

1.3 Purification, cloning and sequencing of NTE

Efforts to characterise NTE and to determine the mechanism of its involvement in OPIDN had been hampered by the lack of a suitable method for its purification. Isolation of native NTE proved difficult due to its low abundance (0.03% of brain microsomal protein; Williams and Johnson, 1981), membrane bound nature, loss of activity upon solubilisation and inactivation during purification. Detergent is required for solubilisation of NTE and the enzyme's PV hydrolase activity is inhibited by even low concentrations of detergent (Johnson, 1982). Thomas *et al.* (1990) demonstrated that loss of catalytic activity upon solubilisation could be restored by the inclusion of phospholipid. Pope and Padilla (1989a) also demonstrated that certain phospholipids could stimulate the catalytic activity of partially purified NTE. This evidence clearly indicates that the catalytic activity of NTE requires lipid.

Purification of NTE had been attempted by various strategies with limited success (Ishikawa *et al.*, 1983; Chemnitius *et al.*, 1984; Pope and Padilla, 1989b; Thomas *et al.*, 1989; Thomas *et al.*, 1990; Thomas *et al.*, 1993). One strategy which achieved a degree of purification involved differential centrifugation, detergent phase partitioning, anion exchange and preparative SDS-PAGE of a [^{3}H]DFP-labelled hen brain homogenate (Ruffer-Turner *et al.*, 1992). Purification was finally achieved through the use of a novel biotinylated organophosphate; 1-(saligenin cyclic phosphoro)-9-biotinyl-diaminononane (S9B) (Glynn *et al.*, 1994). Paraoxon treated hen brain microsomes were incubated with S9B before boiling in SDS, binding to avidin-Sepharose and boiling in SDS to elute. As well as a 155kDa

polypeptide, two endogenously biotinylated polypeptides were also eluted. These were removed by purifying the 155kDa product by preparative SDS-PAGE. Using the same procedure, sufficient NTE protein was purified from pig brain microsomes to enable digestion with endoproteinase Glu-C and N-terminal peptide sequencing of 11 peptide fragments. The sequence of one peptide fragment was homologous to the translation of a human expressed sequence tag cDNA; this was then used as a starting point for screening a human foetal brain cDNA library, from which a 4.4 kilobase (kb) clone was isolated and sequenced (Lush *et al.*, 1998).

1.4 The protein features of NTE

The NTE gene encodes a polypeptide 1327 amino acids in length, with Ser^{966} lying at the centre of the GXSXG motif common to all serine hydrolases. The transmembrane helix prediction program TMpred (Hofmann and Stoffel, 1993) predicts NTE to possess 4 membrane-spanning segments (see Figure 1.5), the most N-terminal of which is the strongest candidate. By expressing truncated regions of NTE in *E.coli,* amino acids 727-1216 were found to represent the catalytic domain, termed NEST (NTE esterase domain). Lysates of *E.coli* expressing this portion potently hydrolyse phenyl valerate and react with covalent inhibitors in a manner similar to chicken brain microsomes (Atkins and Glynn, 2000). Detergent is required at all stages of purification of NEST resulting in a loss of PV hydrolase activity; this activity was restored by incorporation into dioleoylphosphatidylcholine (DOPC) liposomes while removing the detergent by dialysis. NEST-containing liposomes were labelled with [^{3}H]DFP, Glu-C treated and the radioactivity associated with individual residues liberated by successive Edman degradation was determined; by this method Ser^{966} was confirmed as the active site serine. Using site directed mutagenesis amino acid residues His^{860}, His^{885}, Asp^{960}, Asp^{1086} and Ser^{966} were all found to be critical to the catalytic activity of NEST. Despite lacking the most probable TM segment of NTE, NEST separates into the detergent phase during phase partitioning experiments, a property usually associated with an integral membrane protein (Atkins and Glynn, 2000). TMpred analysis predicts that the active site serine is located within a membrane-spanning segment. If this were the case, NEST would need to form a pore structure to permit sufficient access to water to enable catalysis. However, radiation inactivation experiments have shown that NEST is active as a monomer (Atkins *et al.*, 2002); with NEST possessing only 3 predicted TM domains this would seem too few to establish a membrane-spanning pore. Therefore, it appears unlikely that TM2, 3 and 4 (Figure 1.5) are true transmembrane segments and indeed, standard hydropathy analysis only detects the amino terminal transmembrane segment (TM1 in Figure 1.5).

As well as the C-terminal catalytic domain, sequence analysis shows that the N-terminal region of NTE has similarity to the cyclic adenosine monophosphate (cAMP) binding domain of the regulatory subunit of protein kinase A (PKA); this suggests the possibility that NTE's catalytic activity might be modulated by cAMP (Lush *et al.*, 1998).

1.5 NTE catalyses the hydrolysis of membrane lipids

Studies into the inhibition of NTE's PV hydrolase activity with a series of saligenin cyclic phosphonates (Wu and Casida, 1992) and alkyl-thiotrifluoromethyl ketones (Thomas *et al.*, 1990) suggested that the active site of NTE has a preference for carboxylate esters with a alkyl chain length of at least 9-10 carbon atoms. This, coupled with the fact that the region of NTE immediately up and downstream of its active site serine has modest sequence similarity (28% identity over a 160 residue region) to the active site of calcium independent phospholipase A_2 ($iPLA_2$), led van Tienhoven *et al.* (2002) to pursue whether the physiological substrate of NTE could be a lipid or phospholipid (see Figure 1.6 for the structure of phospholipids and the action of phospholipases). Van Tienhoven *et al.* (2002) discovered that incorporation of NEST into DOPC liposomes resulted in the liberation of free fatty acid (FFA), whereas no free fatty acid was detected when the same procedure was conducted using NEST lacking the active site serine. Using differentially [^{14}C]-labelled phosphatidylcholines, NEST was shown to hydrolyse diacylphospholipids, although considerably more slowly than PLA_2; and whereas PLA_2 quantitively converts dioleoylphosphatidylcholine to oleic acid and lysophosphatidylcholine by hydrolysis of the oleic acid at the *sn*-2 position, NEST mediates a slow cleavage of the *sn*-2 bond followed by rapid hydrolysis of the resulting lysophospholipid. Indeed NEST was found to hydrolyse lysophospholipids (LYSO-PLs) the most rapidly of all of the lipid substrates, liberating free fatty acid from 1-palmitoylphosphatidylcholine with a V_{max} approximately 10 fold greater than that reported for recombinant human brain lysophospholipid-specific lysophospholipase (Wang *et al.*, 1999a). NEST can also cleave fatty acid from monoacylglycerols with a preference for the 1-acyl isomer but has no activity towards di- or triacylglycerols (van Tienhoven *et al.*, 2002).

1.6 The NTE family of proteins

Sequence database searches showed that NTE represents a member of a new family of proteins, with potential NTE homologues existing in organisms ranging from bacteria to man (Lush *et al.*, 1998)(see Figure 1.3 and Figure 1.4). Like NTE, each of the homologues present in fruit fly, nematode, yeast and *E.coli,* possess a number of putative transmembrane domains and all have a serine residue at an equivalent location to the active site serine of NTE, also within a GXSXG motif. All of the residues shown to be critical for NEST's catalytic activity (Atkins and Glynn, 2000) are conserved within the

eukaryotic members, with the exception of His^{860} that is conserved only in the yeast homologue. The predicted protein YCHK of *E.coli* is homologous to a 189 residue region spanning NTE's active site; as well as the active site serine, residues corresponding to NTE's essential Asp^{960} and Asp^{1086} are present. Being the shortest of this family of proteins, the NTE-like portion of YCHK might represent the minimum region required for activity. Each of the eukaryotic members of this family also possesses a putative cAMP-binding domain that is not present in YCHK. It is therefore possible that the regulation of YCHK may differ from that of the eukaryotic members. With homologues spanning the whole diversity of evolution, NTE and its family members must presumably carry out a function with fundamental biochemical importance, which has yet to be determined.

Null mutants of both the mouse and the *Drosophila melanogaster* homologues may provide clues as to the physiological function of NTE. A screen for *Drosophila* with visible brain defects identified a mutation that caused an age dependent neurodegeneration characterised by the development of large vacuoles in the adult brain and hence named *swiss cheese* (*sws*) (Heisenberg and Bohl, 1979). The neurons of wild type *Drosophila* are tightly wrapped by a single layer of glial cells, whilst the neurons of the *swiss cheese* mutant are loosely wrapped by multiple glial layers. This leads to apoptosis of both neurons and glia and the subsequent development of the characteristic vacuolated brain. The beginnings of this defect can be detected in newly eclosed mutant flies and by day 20 (incubated at 25°C) widespread vacuoles are visible throughout the brain. The SWS protein that is mutated in this condition has since been identified and the gene cloned (Kretzschmar *et al.*, 1997). The amino acid sequence of this protein was found to be 44% identical to that of human NTE. Three different *swiss cheese* mutant strains were used in the above study. One carries a point mutation causing an amino acid substitution within the core 200 amino acid region of the catalytic domain (glycine to aspartate at residue 956), one carries a point mutation causing a substitution in the putative cAMP binding domain (glycine to arginine at residue 648), at a residue conserved in the cAMP binding domain of PKA regulatory subunits. The third carries a nonsense mutation producing a truncated protein ¼ of the wildtype length. It is interesting that each of these three confer a phenotype of equal severity.

Sws mutant flies, when transformed with a wild type copy of the *sws* gene display a wild type phenotype. However, the wild type phenotype is not restored if the transformed copy of *sws* contains a mutation that causes the protein to lack the active site serine. This evidence proves that esterase activity is essential to the function of SWS. The SWS protein does indeed appear to share some functional homology with NTE, as NTE appears equally capable as sws to restore the phenotype (Kretzschmar *et al.* unpublished work). These

observations taken with the level of sequence similarity suggest that NTE's physiological role is also in neural development. Indeed, *in situ* hybridisation shows that *Nte* is expressed in mouse neurons from their first appearance in the developing nervous system (Moser *et al.*, 2000). However, *Nte* knockout mice die by day 10 in the embryo due to defective formation of the placenta in these animals (Moser *et al.*, 2003). Although this evidence strongly suggests a vital role for NTE in development, the significance of its esterase or lipase activity remains unknown.

In situ hybridisation shows the *sws* transcript to be present in the neurons but absent from the glia (Kretzschmar *et al.*, 1997). The fact that defects in the *sws* mutant fly are first detectable in the glia and not the neurons implies a possible cell-signalling role for SWS; perhaps SWS is required to signal to the glia to stop the wrapping process. Through immunohistochemistry of frozen chicken brain sections, NTE was also found to be localised to the neurons with none detectable in cells with glial morphology (Glynn *et al.*, 1998). Detection of *Nte* transcript in mouse brain sections through *in situ* hybridisation agrees with this expression pattern (Moser *et al.*, 2000). With a similar expression pattern to that of *swiss cheese*, perhaps NTE is also required for neuron to glial signalling.

1.7 Yml059c: the putative yeast homologue of NTE

Yml059c of the budding yeast *Saccharomyces cerevisiae* is a previously uncharacterised putative homologue of NTE. *YML059c* is a conceptual gene identified by the genome sequencing program. It is 5040 base pairs (bp) in length, encoding a putative protein of 1679 amino acids. This protein has two regions that show a high degree of sequence similarity to NTE. The C-terminal half of Yml059c (residues 797-1646) is 32% identical and 51% similar to NTE and a small N-terminal proximal segment (residues 409-470) is 40% identical and 64% similar to NTE (Figure 1.5). Sequence analysis of the remaining 769 residues failed to identify any functional domains outside of the NTE-like segments. Like NTE, Yml059c possesses a region with similarity to the cAMP binding domains of the regulatory subunit of PKA (see Figure 1.7) and a number of possible transmembrane helices, within one of which lies the putative active site serine. This high level of similarity implies some degree of conservation of biochemical function and cellular role between these two proteins.

1.8 The putative regulatory domains of NTE and Yml059c retain the essential features of known cAMP binding domains

Both NTE and Yml059c contain a putative regulatory region with significant sequence similarity to the cAMP binding domains of the regulatory subunits of protein kinase A

(Shabb and Corbin, 1992), the catabolite gene activator protein (CAP) of *E.coli* (McKay *et al.*, 1982) and the recently discovered cAMP-activated guanine nucleotide exchange factor Epac2 (de Rooij *et al.*, 2000); with each containing two adjacent cAMP binding sites. The sequence similarity of each site is also conserved in the single cAMP binding site of Epac1 (de Rooij *et al.*, 1998). The crystal structures of CAP, PKA-R1α and Epac2 have all been solved and indicate a high degree of structural similarity, with each binding site possessing a 15 residue motif, termed the phosphate binding cassette (PBC) situated within an 8-strand β barrel. This motif interacts with the phosphate and ribose moieties of cAMP (McKay *et al.*, 1982; Weber and Steitz, 1987; Su *et al.*, 1995; Rehmann *et al.*, 2003). Three glycines, a glutamate and an arginine residue are conserved between CAP and all known PKA-R subunits. The three glycine residues are also conserved in Epac and are assumed to be essential structural features linking individual β strands (Shabb and Corbin, 1992); of these three, the one adjacent to the PBC has been experimentally determined to be essential for the function of PKA-R (Ogreid *et al.*, 1988). The conserved glutamate and arginine residues lie within the PBC and in the case of PKA-R1α bind directly to cAMP and are essential for its function (Bubis *et al.*, 1988; Woodford *et al.*, 1989; Su *et al.*, 1995). Interestingly Epac also employs a corresponding arginine for direct cAMP interaction but lacks the glutamate residue; this may be responsible for Epac's reduced affinity for cAMP compared to that of PKA-R (Rehmann *et al.*, 2003). Although a degree of sequence similarity to these established cAMP binding domains is apparent across both 'A' and 'B' sites of Yml059c and NTE, it seems most likely that only the 'B' site is functional in each protein as both 'A' sites lack the important arginine and glutamate residues. The 'B' sites of NTE and Yml059c are 30% and 28% identical and 50% and 48% similar to PKA-R1α respectively and possess 3 glycines and an arginine residue at corresponding locations to those conserved between PKA-R, CAP and Epac. Interestingly, the Yml059c 'B' site also has an equivalent glutamate to that conserved amongst PKA-Rs, whereas NTE, like Epac does not (see Figure 1.7). With this conservation of the critical residues in the B sites of NTE and Yml059c and an overall significant level of sequence similarity apparent between known cAMP binding domains and the putative regulatory domains of these two proteins, it seems a reasonable hypothesis that each is able to bind cAMP. This being the case it would suggest a possible regulatory mechanism whereby the catalytic activity of NTE and Yml059c is modulated by the presence of cAMP.

1.9 cAMP mediated processes in yeast

The only identified function for cAMP in *S.cerevisiae* is in cAMP-dependent protein kinase A pathways which regulate a number of cellular processes in response to prevailing nutrient availability. The common upstream part of these pathways is activated by an increase in adenylate cyclase (encoded by *CYR1*) activity raising the intracellular levels of cAMP, which

in turn act by binding to the regulatory domain of PKA, releasing it from and therefore activating the catalytic subunit (Broach, 1991). In yeast, there is a single PKA regulatory subunit, encoded by *BCY1* and three PKA catalytic subunits, Tpk1, Tpk2 and Tpk3 (Toda *et al.*, 1987).

Low activity of the cAMP-PKA pathway has long been implicated in the signalling of nutrient exhaustion. Mutations that confer reduced levels of activity such as temperature sensitive mutations in *RAS2* or *CYR1* cause entry into stationary phase (G_0) and acquisition of stationary phase characteristics such as accumulation of trehalose and glycogen and increased resistance to heat shock, osmotic or oxidative stress and sporulation (in diploid cells) on rich media. Conversely an overactive cAMP-PKA pathway causes sensitivity to heat shock and nutrient starvation, low levels of the storage carbohydrates trehalose and glycogen, failure to arrest properly at G1 during nutrient depletion, inability to grow on non-fermentable carbon sources and failure of diploids to sporulate (for reviews see Broach and Deschenes, 1990; Broach, 1991; Thevelein, 1994; Thevelein and de Winde, 1999).

The mechanism as to how nutrient depletion is signalled through the cAMP-PKA pathway still remains unclear, as nutrient depletion is not accompanied by a decrease in intracellular cAMP (Ma *et al.*, 1997). Identification of the GTP-binding proteins Ras1 and Ras2 and the guanine nucleotide exchange factor protein Cdc25 as regulators of adenylate cyclase had led to the conclusion that nutrient sensing signals were transmitted through Ras (Toda *et al.*, 1985). However, recent work has clarified this pathway's role in glucose sensing with the identification of a G-protein coupled receptor (GPCR) system consisting of the receptor Gpr1 and its associated Gα protein Gpa2 that activate the cAMP-PKA pathway in response to the presence of glucose (Colombo *et al.*, 1998; Kraakman *et al.*, 1999). It now seems that for the transduction of the glucose-sensing signal, GTP-bound Ras is required for activity of adenylate cyclase and that this activity is modulated through Gpr1 and Gpa2, rather than by signalling through Ras itself (Thevelein and de Winde, 1999).

A key role for the cAMP-PKA pathway now seems to be in the sensing of sufficient glucose (or other related fermentable carbon source) levels to allow fermentation to take place in medium that contains all other nutrients required for growth (Thevelein, 1991; Giots *et al.*, 2003). Addition of glucose to cells grown on a non-fermentable carbon source results in a transient increase in intracellular cAMP which is apparently sufficient to activate downstream events (van der Plaat, 1974). Downstream targets for activated PKA include the enzyme trehalase and the transcription factors Msn2 and Msn4 whose function is to transcribe those stress response genes whose promoters contain stress response elements (STREs), including trehalase. Thus, activated PKA brings about the metabolism of the

storage carbohydrate trehalose by post-translational activation of trehalase (Thevelein, 1984; Zahringer *et al.*, 1998) and, through inactivation of Msn2 and Msn4, a decrease in transcription of genes required for resistance to oxidative and osmotic stress and heat shock (Schmitt and McEntee, 1996; Boy-Marcotte *et al.*, 1998; Smith *et al.*, 1998; Norbeck and Blomberg, 2000; Zahringer *et al.*, 2000; Hasan *et al.*, 2002).

The cAMP-PKA pathway has also been implicated in the control of sporulation and pseudohyphal growth. During conditions of nitrogen starvation *S.cerevisiae* is able to undergo a dimorphic transition and grow not in its typical yeast form but as pseudohyphae (Gimeno *et al.*, 1992). Pseudohyphal growth is characterised by elongated cells, budding in a unipolar manner with buds failing to separate, thereby forming filamentous chains. This produces characteristic macroscopic structures emanating away from the colony. It is believed that the purpose of this change in morphology is to allow foraging for scarce nutrients. Although some haploid strains are capable of forming pseudohyphae this pattern of growth is more readily observed in diploids.

Formation of pseudohyphae is regulated through both the MAP kinase cascade and the cAMP-PKA pathway (Robertson and Fink, 1998; Pan and Heitman, 1999). These pathways interact via the GTP-binding protein Ras2 and converge to regulate the cell-surface flocculin Flo11 required for pseudohyphal formation (discussed in the review by Gancedo, 2001). Lorenz *et al.* (2000) have shown that pseudohyphal differentiation requires not only a limited nitrogen source but also the presence of a good fermentable carbon source, the detection of which requires Gpr1.

Under conditions of both carbon and nitrogen starvation diploid yeast cells initiate meiosis and sporulate. This process has been demonstrated to be dependent upon a functional cAMP-PKA pathway in that mutations of the adenylate cyclase gene, *cyr1* (*cdc35*) or *ras2* that result in low cAMP levels cause sporulation to occur even in rich medium (Shilo *et al.*, 1978; Toda *et al.*, 1985). Also, mutation of the PKA regulatory subunit *bcy1* that causes the constitutive activation of the PKA catalytic subunit, results in a deficiency of meiosis and sporulation (Matsumoto *et al.*, 1983). The cAMP-PKA pathway exerts its effect upon the decision to enter meiosis through Ime1, a transcriptional activator of meiotic genes (Rubin-Bejerano *et al.*, 1996). Regulation of *IME1* is controlled at the transcriptional level by the repressor Sok2 and the activators Msn2 and Msn4; all of which are direct targets for phosphorylation by PKA. As stated above Msn2 and Msn4 are inactivated by phosphorylation whereas phosphorylation positively regulates Sok2 (Sagee *et al.*, 1998; Shenhar and Kassir, 2001). Thus, high PKA activity represses transcription of *IME1* and

prevents meiosis and sporulation, whereas low PKA activity activates transcription of *IME1* and induces meiosis and sporulation.

If Yml059c does bind cAMP then its cellular role might conceivably be to act as an esterase that functions during any one of these cAMP dependent cellular processes, with its catalytic activity being directly regulated by cAMP levels.

1.10 Are all cAMP effects in yeast mediated via the regulatory subunit of PKA?

There is mounting evidence in a number of mammalian cell types (leukocytes, thyroid and pancreas) that not all cAMP-regulated events are mediated via PKA (de la Rosa *et al.*, 2001; Iacovelli *et al.*, 2001; Kashima *et al.*, 2001; Gasperini *et al.*, 2002; Eliasson *et al.*, 2003). In some cases, these events may involve direct activation of the guanine nucleotide exchange factor, Epac by cAMP (Iacovelli *et al.*, 2001; Kashima *et al.*, 2001). As noted above, in *S.cerevisiae* cAMP regulation of fermentation and colony morphology appear to be mediated through adenylate cyclase and PKA (Thevelein and de Winde, 1999). However, in the filamentous fungus *Aspergillus nidulans*, recent studies of these phenotypes in adenylate cyclase or PKA mutants strongly suggest that not all cAMP regulated pathways involve the regulatory subunit of PKA (Fillinger *et al.*, 2002). Similarly, in the plant fungus *Magnaporthea grisea*, different cAMP signalling pathways regulating growth and pathogenesis not relying on PKA have been proposed (Adachi and Hamer, 1998). A BLAST search using the sequence of human Epac1 as the query detected possible homologues in insects, chordates and nematodes but none in fungi. As putative NTE homologues can be identified in both *A.nidulans* and *M.grisea*, it is possible that NTE protein family members may have a role in these cAMP-dependent PKA-independent processes.

As well as Bcy1, two other proteins capable of binding cAMP have been suggested to exist in *S.cerevisiae* (Muller and Bandlow, 1991). Both are anchored to lipid membrane by glycosyl-phosphatidylinositol (GPI) but their function remains unknown (Muller *et al.*, 1992). These proteins have been shown to be separate entities from Bcy1 as Bcy1-specific antibodies do not react with either of these peptides. Also, the properties of these novel proteins can still be detected in *bcy1Δ* mutant yeast and peptide maps generated using V8 protease or trypsin have been used to show that these proteins are similar to each other but unrelated to Bcy1 (Muller and Bandlow, 1991). However, their respective genes have not been identified, precluding further characterisation.

1.11 Yeast phospholipids and phospholipases

NTE has been shown to hydrolyse membrane lipids with a preference for lysophospholipid (see section 1.5). If Yml059c also catalyses the liberation of free fatty acid from phospholipid it is necessary to consider the phospholipid composition of *S.cerevisiae* and those previously identified enzymes for which phospholipids are the substrate.

The phospholipid composition of yeast membranes is consistent with that of higher eukaryotes. The relative abundance of each phospholipid class in yeast is as follows: phosphatidylcholine (PC, ≈45%), phosphatidylethanolamine (PE, ≈20%), phosphatidylinositol (PI, ≈20%), phosphatidylserine (PS, ≈5%), phosphatidic acid (PA, ≈4%), cardiolipin (≈2%) and lysophospholipid (≈1%) (Daum *et al.*, 1999). However, as *S.cerevisiae* is unable to synthesise polyunsaturated fatty acids the fatty acids that comprise yeast phospholipids are rather more simple than those of higher eukaryotes and consist of the following (with the length of the carbon chain, the number of unsaturations and the relative abundance indicated): palmitoleic acid (C16:1, ≈40%), oleic acid (C18:1, ≈40%), palmitic acid (C16:0, ≈15%) and stearic acid (C18:0, ≈5%) (Wagner and Paltauf, 1994). As with higher eukaryotes, saturated fatty acids most frequently occupy the *sn*-1 position (Wagner and Paltauf, 1994).

To date, only a small number of yeast enzymes have been characterised for which phospholipid is the cellular substrate (see Figure 1.6 for definition of phospholipase classes). Two phospholipase Cs (PLC) have so far been identified, Plc1 and Isc1. *PLC1* encodes a phosphatidylinositol-specific phospholipase C (PI-PLC) that binds to the receptor Gpr1 and is required for pseudohyphal differentiation (Ansari *et al.*, 1999). *ISC1* encodes an inositol phosphosphingolipid phospholipase C (IPS-PLC); the first identified yeast enzyme for which complex sphingolipids are the substrate (Sawai *et al.*, 2000). *SPO14* encodes the only characterised phospholipase D (PLD) in yeast; an enzyme with an apparent role in secretion, sporulation and the formation of mating projections (Rose *et al.*, 1995; Sreenivas *et al.*, 1998; Hairfield *et al.*, 2001). However, these PLCs and PLDs act by cleaving the phosphodiester bonds of phospholipids and, assuming Yml059c has a similar activity to that of NTE, have little relevance to the possible role of Yml059c.

Only three yeast enzymes have been identified that catalyse the liberation of free fatty acid from phospholipid; these are Plb1, Plb2 and Plb3. (Lee *et al.*, 1994; Fyrst *et al.*, 1999; Merkel *et al.*, 1999). All three are highly similar to each other on the basis of peptide and DNA sequence and all are predominantly active in the plasma membrane and periplasmic space. The cellular function of these phospholipases has not been determined; all are non-

essential and indeed disruption of all three does not affect viability. The only established mutant phenotypes for these are that the *plb2* mutant is somewhat sensitive to exogenous lysophosphatidylcholine, the *plb1 plb2 plb3* triple mutant is highly sensitive to lysophosphatidylcholine and has a reduced growth rate compared to the wildtype under anaerobic conditions in which the phospholipid 1-palmitoyl-2-oleoyl-phosphatidylcholine is the only source of fatty acid (Merkel *et al.*, 1999). Characterisation of their enzymatic activity has shown that all are phospholipase Bs (PLBs), hydrolysing free fatty acid from both diacylphospholipids and lysophospholipids. Their substrate specificities differ in that Plb1 and Plb2 can hydrolyse phosphatidylserine, phosphatidylinositol, phosphatidylcholine and phosphatidylethanolamine, whereas Plb3 can hydrolyse only PS and PI with no detectable activity towards PC or PE. Also, the lysophospholipase activity of Plb1 and Plb2 towards lysophosphatidylcholine greatly exceeds their diacylphospholipase activity, whereas Plb3 has only minor lysophospholipase activity. In addition to this, all three displayed some degree of transacylase activity in that they catalyse the production of diacylphospholipids from a lysophospholipid substrate (Lee *et al.*, 1994; Merkel *et al.*, 1999); a common property of phospholipase Bs. Plb1, Plb2 and Plb3 are most likely to be serine hydrolases with each containing the GXSXG motif and a putative catalytic triad formed by appropriately positioned arginine and aspartate residues.

1.12 Project aims

At the beginning of this project, sequence similarity between human NTE and yeast Yml059c suggested that the two proteins might be orthologues. The esterase activity of NTE was well established and, more recently, lysophospholipids were shown to be substrates *in vitro*. Although both NTE and Yml059c have moderate sequence similarity to cAMP-binding proteins, as yet, neither have been shown to bind this nucleotide. Thus, the objectives of the project were (1) to ascertain whether Yml059c and NTE have similar properties and therefore to what extent yeast can provide a suitable model for the study of NTE; specifically, does Yml059c react with substrates and inhibitors in a similar fashion to NTE and does it bind cAMP? (2) To investigate the function of Yml059c in yeast in order to gain clues as to the physiological function of NTE; specifically, can a phenotype be detected for *yml059c* null yeast?

Figure 1.1. Compounds used in the study of NTE and OPIDN

The structures of some of the compounds used in the study of NTE and OPIDN. OPs are shown with the leaving group ("X" in Figure 1.2) to the left of the phosphorus atom.

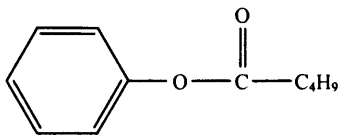

Phenyl Valerate

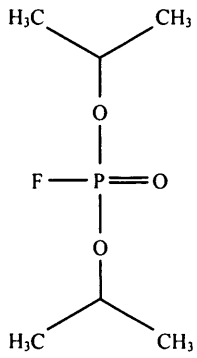

DFP

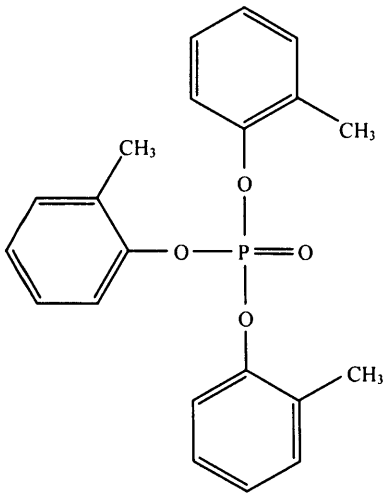

TOCP

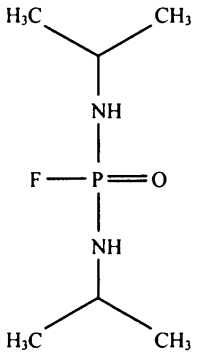

Mipafox

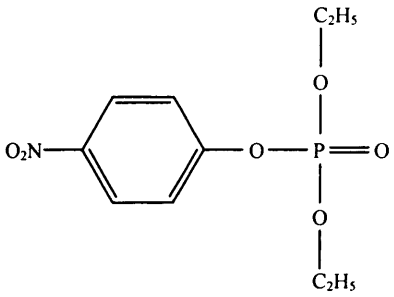

Paraoxon

Figure 1.2. Catalytic mechanism of serine esterases and inhibition by organophosphates

(Adapted from Glynn, 2000) **A.** The hydroxyl group of the enzyme's active site serine makes a nucleophilic attack on the ester's acyl carbon atom forming an acyl-enzyme intermediate. This is rapidly hydrolysed to form a carboxylic acid and regenerate the free enzyme. **B.** OPs react with the enzyme in an analogous reaction. The resultant organophosphorylated enzyme is hydrolysed much more slowly. 'Aging' of the OP results in the loss of one R group, leaving a negative charged species bound to the enzyme's active site.

A.

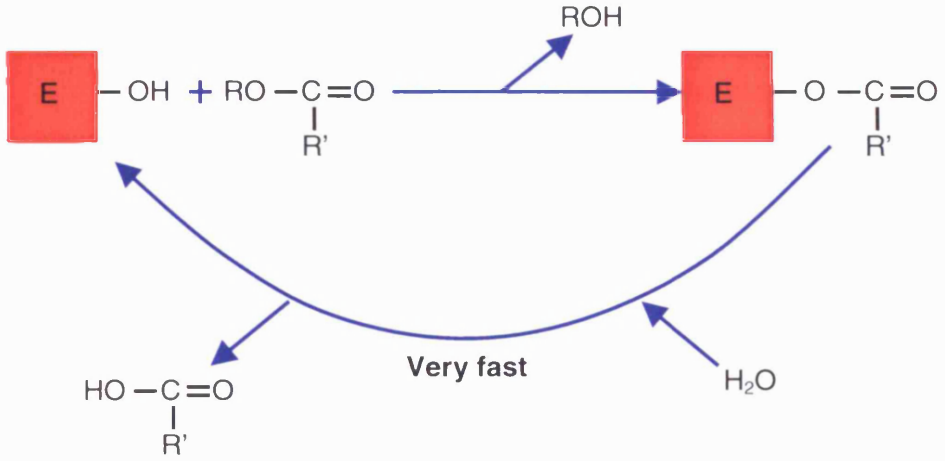

B.

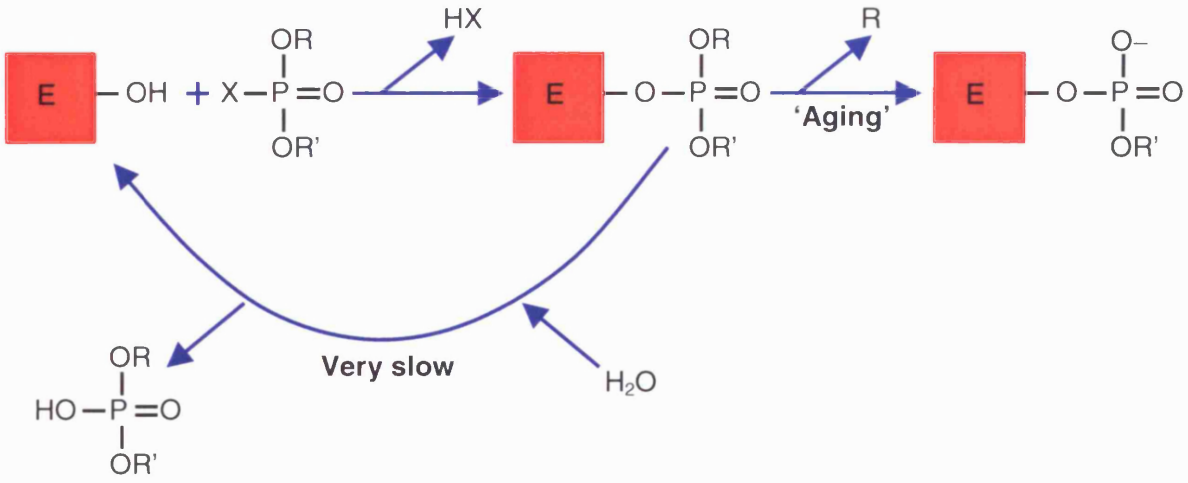

Figure 1.3. The NTE family of proteins

Members of the NTE family of proteins from human, fruit fly, nematode, yeast and *E.coli*. The region similar to NTE is indicated in each case, as is the location of the putative active site serine, and any possible transmembrane helices and cAMP binding domains

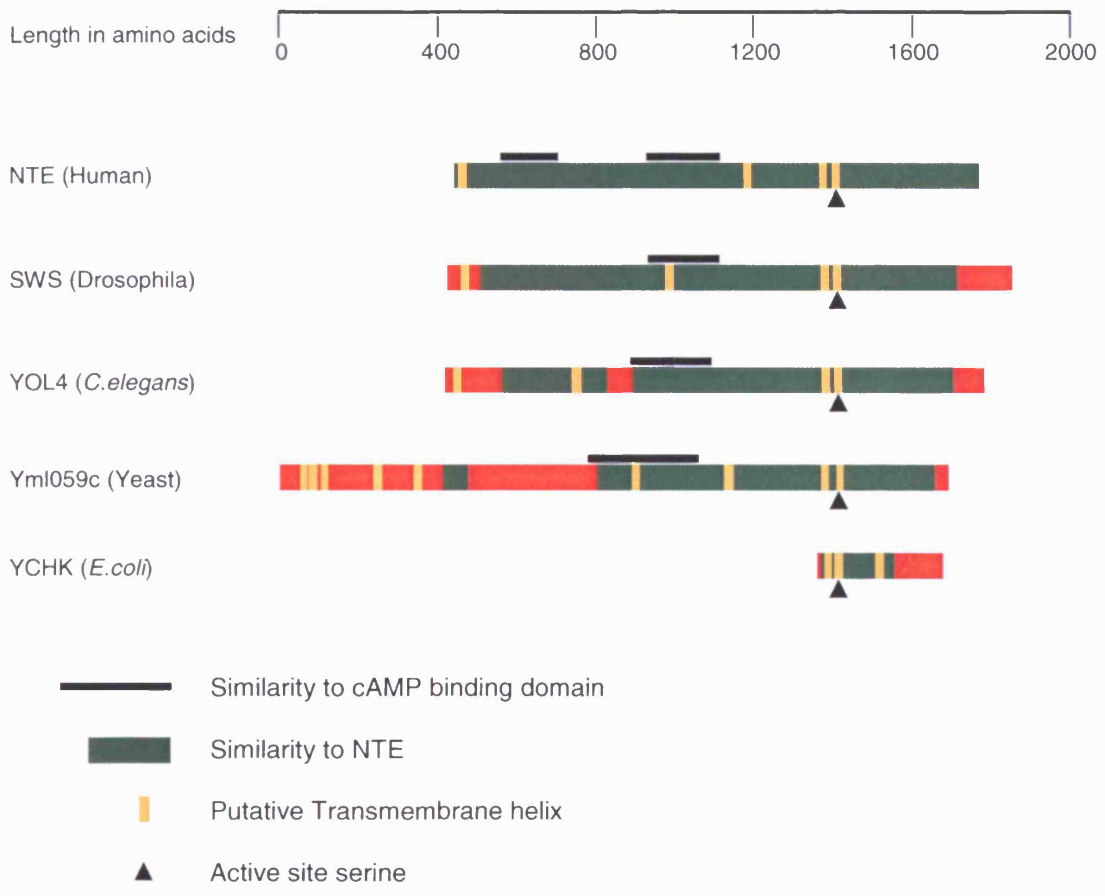

Figure 1.4. Sequence similarity of the NTE protein family

Clustal W alignment (Thompson *et al.*, 1994) of the NEST region of NTE (amino acids 727-1216) with the putative homologues SWS (*Drosophila melanogaster*), Yol4 (*C.elegans*), Yml059c (*S.cerevisiae*) and YCHK (*E.coli*). Shading indicates related amino acids in 3 out of 5 sequences (white-on-black for identical residues, white-on-grey for similar). Those residues shown to be essential to the catalytic activity of NEST are numbered (with 4 denoting the active site serine).

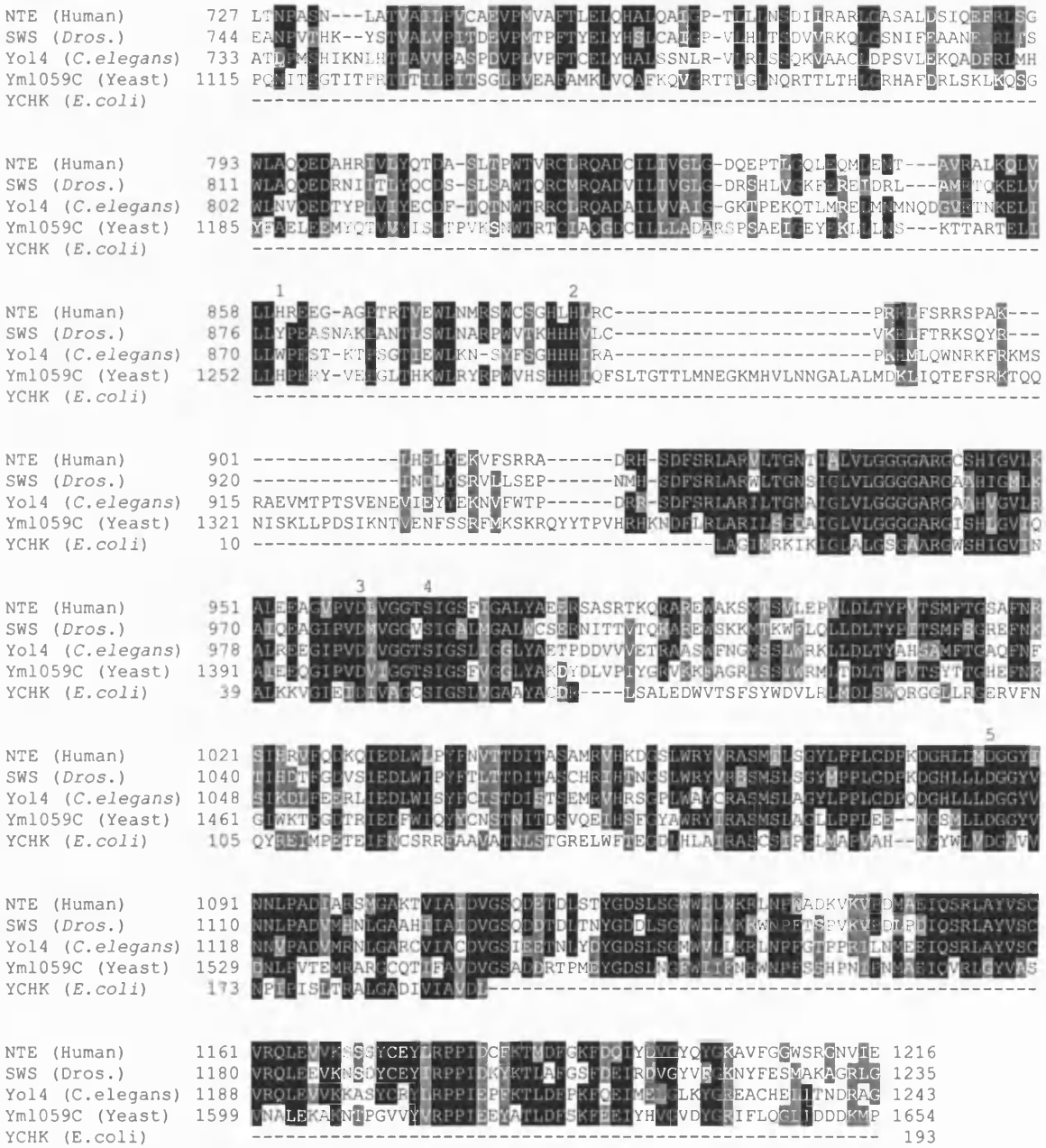

Figure 1.5. The features and similarities of NTE and Yml059c

A comparison of the protein features of human NTE and Yml059c of yeast. The location of the conserved regions are indicated. The TMpred scores of the numbered putative transmembrane segments are shown in the table below.

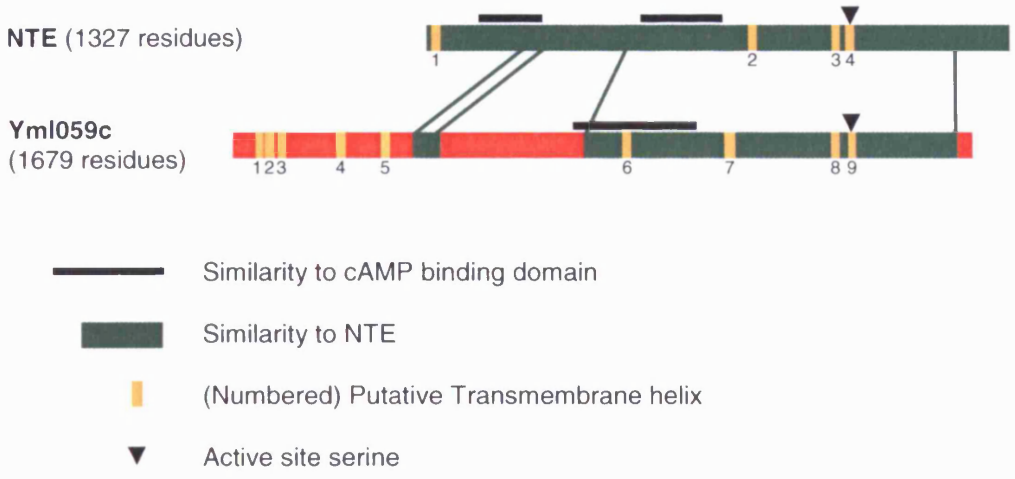

Putative Transmembrane helix	TMpred scores	
	NTE	Yml059c
1	2375	1708
2	958	755
3	1087	2899
4	1276	895
5	-	674
6	-	1472
7	-	621
8	-	871
9	-	686

Figure 1.6. The general structure of phospholipids/lysophospholipids and the action of phospholipases

A. Shows the general structure of a phospholipid, with two fatty acids esterified to a glycerol backbone and a polar head group of either choline, ethanolamine, serine or inositol (X), attached by a phosphodiester linkage. **B**. Shows the related lysophospholipid with only one fatty acid.
The specific bond cleaved by each class of phospholipase is indicated.

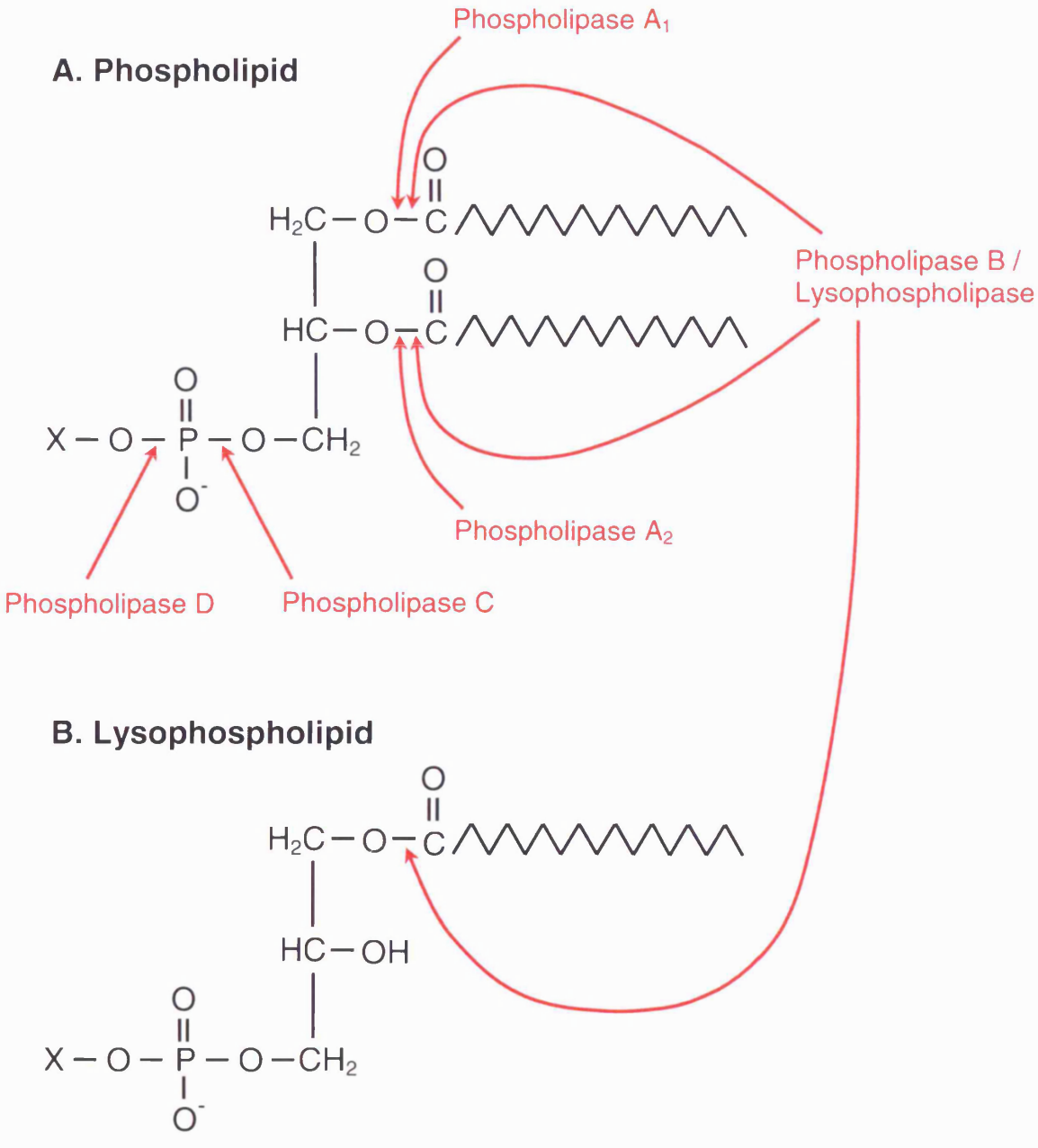

Figure 1.7 The putative cAMP binding domains of NTE and Yml059c

Clustal W alignment (Thompson *et al.*, 1994) of the 2 putative cAMP binding sites of NTE and Yml059c with those of yeast PKA regulatory subunit (Bcy1), human PKA regulatory subunits (PKAR-1α and PKAR-2α) and the cAMP regulated guanine nucleotide exchange factor Epac1. Shading indicates related amino acids in 3 or more sequences (white-on-black for identical residues, white-on-grey for similar). The 'A' and 'B' binding sites of Yml059c and NTE are arbitrarily aligned with the A and B sites of the PKA regulatory subunits; the single binding site of Epac1 is arbitrarily aligned with the A sites. Amino acids previously suggested to be important for the function of cAMP binding sites are indicated with arrows. The boxed area shows those residues that form the phosphate binding cassette. For clarity, the small region of approximately 30 residues that connects the two cAMP binding domains in each protein (with the exception of Epac1) has not been shown.

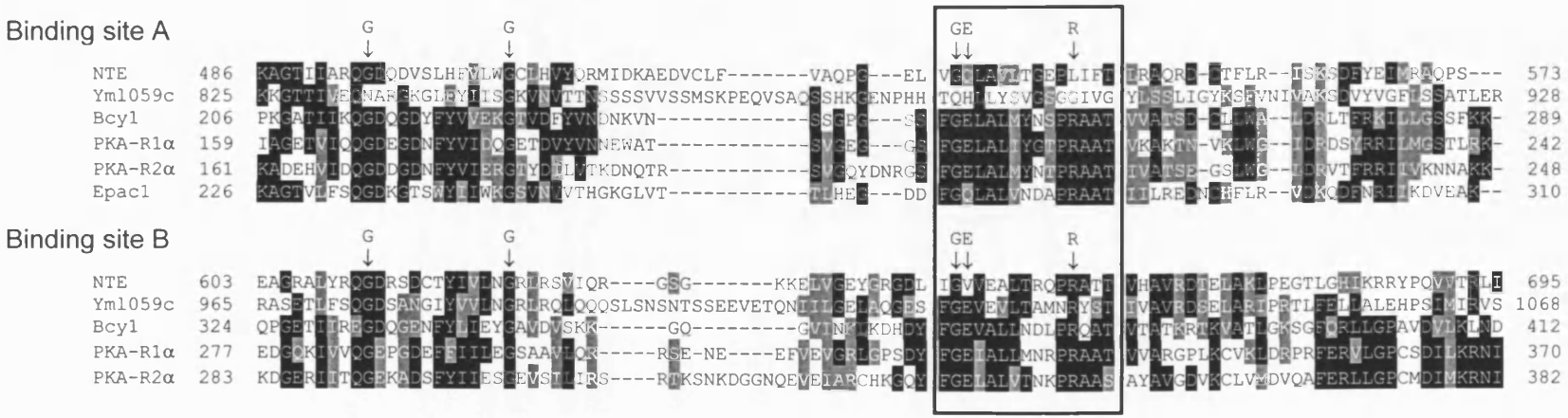

Chapter 2: Materials and Methods

2.1 Strains and Plasmids

2.1.1 Yeast Strains (*Saccharomyces cerevisiae*)

Table 2.1. Yeast strains used in this study

Strain	Genotype	Source or Reference
BY4741	*MAT a, his3Δ1, leu2Δ0, met15Δ0, ura3Δ0*	(Brachmann *et al.*, 1998) Euroscarf Accession No: Y00000
BY4742	*MAT α, his3Δ1, leu2Δ0, lys2Δ0, ura3Δ0*	(Brachmann *et al.*, 1998) Euroscarf Accession No: Y10000
BY4741 *Yml059cΔ*	*MAT a, his3Δ1, leu2Δ0, met15Δ0, ura3Δ0, yml059c::kanMX4*	Euroscarf Accession No: Y00511
BY4742 *Yml059cΔ*	*MAT α, his3Δ1, leu2Δ0, lys2Δ0, ura3Δ0; yml059c::kanMX4*	Euroscarf Accession No: Y10511
BY4743	*MAT a/α, his3Δ1/his3Δ1, leu2Δ0/leu2Δ0, met15Δ0/MET15, LYS2/lys2Δ0, ura3Δ0/ura3Δ0*	(Brachmann *et al.*, 1998) Euroscarf Accession No: Y20000
BY4733	*MAT a, his3Δ200, leu2Δ0, met15Δ0, trp1Δ63, ura3Δ0*	(Brachmann *et al.*, 1998)
BY4743 *Yml059cΔ/Δ*	*MAT a/α, his3Δ1/his3Δ1, leu2Δ0/leu2Δ0, met15Δ0/MET15, LYS2/lys2Δ0, ura3Δ0/ura3Δ0, yml059c::kanMX4/yml059c::kanMX4*	This study
BY4743 *YML059c-GFP/+*	*MAT a/α, his3Δ1/his3Δ1, leu2Δ0/leu2Δ0, met15Δ0/MET15, LYS2/lys2Δ0, ura3Δ0/ura3Δ0, YML059c-GFPS65T-HIS3MX6/YML059c*	This study
BY4743 *P_{gal1}-GFP-YML059c/+*	*MAT a/α, his3Δ1/his3Δ1, leu2Δ0/leu2Δ0, met15Δ0/MET15, LYS2/lys2Δ0, ura3Δ0/ura3Δ0, HIS3MX6-P_{gal1}-GFPS65T-YML059c/YML059c*	This study
BY4743 *P_{gal1}-YML059c/+*	*MAT a/α, his3Δ1/his3Δ1, leu2Δ0/leu2Δ0, met15Δ0/MET15, LYS2/lys2Δ0, ura3Δ0/ura3Δ0, KanMX6-P_{gal1}-YML059c/YML059c*	This study
BY4743 *P_{gal1}-YML059c-GFP/+*	*MAT a/α, his3Δ1/his3Δ1, leu2Δ0/leu2Δ0, met15Δ0/MET15, LYS2/lys2Δ0, ura3Δ0/ura3Δ0, KanMX6-P_{gal1}-YML059c-GFPS65T-HIS3MX6/YML059c*	This study
BY4743 *P_{gal1}-GFP-YML059c/ P_{gal1}-GFP-YML059c*	*MAT a/α, his3Δ1/his3Δ1, leu2Δ0/leu2Δ0, met15Δ0/MET15, LYS2/lys2Δ0, ura3Δ0/ura3Δ0, HIS3MX6-P_{gal1}-GFPS65T-YML059c/HIS3MX6-P_{gal1}-GFPS65T-YML059c*	This study
BY4741 *P_{gal1}-GFP-YML059c*	*MAT a, his3Δ1, leu2Δ0, met15Δ0, ura3Δ0, HIS3MX6-P_{gal1}-GFPS65T-YML059c*	This study
BY4742 *P_{gal1}-GFP-YML059c*	*MAT α, his3Δ1, leu2Δ0, lys2Δ0, ura3Δ0, HIS3MX6-P_{gal1}-GFPS65T-YML059c*	This study
MW1076 (Σ1278b derivative)	*MAT a, ura3-52, leu2::hisG, his3::hisG, trp1::hisG*	M. Werner-Washburne University of New Mexico
MW1077 (Σ1278b derivative)	*MAT α , ura3-52, leu2::hisG, his3::hisG trp1::hisG*	M. Werner-Washburne University of New Mexico
MW1076/7 (Σ1278b derivative)	*MAT a/α, ura3-52/ura3-52, leu2::hisG/leu2::hisG, his3::hisG/his3::hisG, trp1::hisG/trp1::hisG*	This study
MW1076 *Yml059cΔ* (Σ1278b derivative)	*MAT a, ura3-52, leu2::hisG, his3::hisG, trp1::hisG, yml059c::HIS3MX6*	This study

MW1077 *Yml059cΔ* (Σ1278b derivative)	*MAT α , ura3-52, leu2::hisG, his3::hisG trp1::hisG, yml059c::TRP1*	This study
MW1076/7 *Yml059cΔ/Δ* (Σ1278b derivative)	*MAT a/α, ura3-52/ura3-52, leu2::hisG/leu2::hisG, his3::hisG/his3::hisG, trp1::hisG/trp1::hisG, yml059c::HIS3MX6/yml059c::TRP1*	This study
DC14	*MAT a, his1*	Lab stocks
DC17	*MAT α, his1*	Lab stocks

2.1.2 Bacterial Strains (*Escherichia coli*)

Table 2.2. Bacterial strains used in this study

Strain	Genotype	Source or Reference
BL21(DE3)pLysS	*E.coli* B F- *dcm ompT hsdS*(r_B- m_B-) *gal λ* (DE3) [pLysS Cam^r]^a	Novagen
DH5α	ϕ80*lacZ*ΔM15,*recA*1, *endA*1, *gyrA*96, *thi*-1, *hsd*R17 (r_K^- ,m_K+), *sup*E44, *rel*A1, *deo*R,Δ (*lac*ZYA-*arg*F) U169	(Hanahan, 1983)
XL-10 gold	Tet^r *Δ(mcrA)183 Δ(mcrCB-hsdSMR-mrr)173 endA1 supE44 thi-1 recA1 gyrA96 relA1 lac* Hte [F' *proAB lacI^{q}ZΔM15 Tn10* (Tet^r) Amy Cam^r]^a	Stratagene
XL1-BLue	*recA1 endA1 gyrA96 thi-1 hsdR17 supE44 relA1 lac* [F'*proAB lacI^{q}ZΔM15 Tn10* (Tet^r)]	Stratagene

2.1.3 Plasmids and Vectors

Table 2.3. Bacterial, yeast and mammalian plasmids used in this study

Plasmid	Genotype	Source or Reference
pBS-Actin	*ori, Amp^R, ACT1*	Lab stocks
pEGFP-N1	*ori, Amp^R, Neo^R, SV40 ori,* P_{CMVIE}	Clontech
pEGFP-NTE	NTE carried on pEGFP-N1	Gift from Yong Li
pEGFP-Yml059c	*YML059c* carried on pEGFP-N1	This Study
pEMBLyex4	*ori, Amp^R, URA3, leu2-d, 2-μm ori,* $P_{CYC-GAL}$	(Baldari and Cesareni, 1985)
pEMBL-NTE	NTE carried on pEMBLyex4	This Study
pEMBL-*YML059c*	*YML059c* carried on pEMBLyex4	This study
pET21b	*ori, Amp^R,* P_{T7}, *lacI*	Novagen
pET-YNEST	YNEST carried on pET21b (as described in text)	This study

pFA6a-GFP(S65T)-*HIS3MX6*	*ori, Amp^R, GFP(S65T)-HIS3MX6*	(Wach *et al.*, 1997)
pFA6a-*HIS3MX6*	*ori, Amp^R, HIS3MX6*	(Wach *et al.*, 1997)
pFA6a-*HIS3MX6*-P_{gal1}-GFP	*ori, Amp^R, HIS3MX6-P_{gal1}-GFP(S65T)*	(Longtine *et al.*, 1998)
pFA6a-KanMX6-P_{gal1}	*ori, Amp^R*, KanMX6-P_{gal1}	(Longtine *et al.*, 1998)
pFA6a-*TRP1*	*ori, Amp^R, TRP1*	(Longtine *et al.*, 1998)
pG3	*ori, Amp^R, TRP1, 2-μm ori,* P_{GPD}	(Bitter and Egan, 1984)
pG3-*YML059c*	*YML059c* carried on pG3	This study
pRS416	*ori, Amp^R, LacZ, CEN6, ARSH4, URA3*	(Brachmann *et al.*, 1998)
pRS416-P_{gal1}-*YML059c*	P_{gal1}-*YML059c* carried on pRS416 (as described in text)	This study
pRS416-P_{gal1}-GFP-*YML059c*	P_{gal1}-GFP-*YML059c* carried on pRS416 (as described in text)	This study
pRS416-P_{gal1}-GFP-*YML059c*(S1406A)	pRS416-P_{gal1}-GFP-*YML059c* altered by site directed mutagenesis (as described in text)	This study
pTARGET-NTE	*ori, Amp^R, Neo^R, SV40 ori,* P_{CMV}-NTE	Gift from Yong Li
pYC2/CT	*ori, Amp^R, URA3, CEN6, ARSH4,* P_{gal1}	Invitrogen
pYC2/CT-*BCY1*	*BCY1* carried on pYC2/CT	This study
pYC2/CT-NTE-GFP	NTE-GFP carried on pYC2/CT	This study
pYES2/CT	*ori, Amp^R, URA3, 2-μm ori,* P_{gal1}	Invitrogen
pYES2/CT-NTE-GFP	NTE-GFP carried on pYES2/CT	This study

2.2 Growth Media and Conditions

For solid media 2% w/v agar was added. Bacterial strains were incubated at 37°C. Yeast strains were incubated at 30°C unless otherwise stated.

2.2.1 Luria Broth (LB)

E.coli was propagated in LB medium consisting of 1% w/v bacto-tryptone, 0.5% w/v bacto-yeast extract and 0.5% w/v NaCl, adjusted to pH7.2 with NaOH. Selection of antibiotic resistant *E.coli* was achieved by addition of the relevant antibiotic; ampicillin at 50μg ml^{-1} (LB/Amp) or kanamycin at 10μg ml^{-1} (LB/Kan)(Sambrook *et al.*, 1989).

2.2.2 Yeast Peptone (YP) Medium

Where no nutritional selection was required yeast were typically grown using yeast peptone dextrose (YPD) medium. This consisted of 1% w/v yeast extract, 2% w/v bacto-peptone and 2% w/v glucose (Guthrie and Fink, 1991). For the induction of galactose regulated promoters 2% w/v galactose was added in place of glucose as a carbon source. Other carbon sources were used for phenotypic tests, for concentrations see Table 4.1.

For the phenotypic test of response to low pH, agar plates at pH7, 5, 4, 3 and 1 were achieved by adding 0, 50, 100, 200 and 400µl of 6M HCl respectively to 25ml of molten YP agar before pouring. The pH was confirmed using pH indicator strips.

For selection of G418 resistance, G418 was added to YPD at 200mg l^{-1} (Wach *et al.*, 1994).

2.2.3 Synthetic Defined (SD) Medium

SD medium consisted of 0.17% w/v yeast nitrogen base (with ammonium sulphate, without amino acids) and 2% w/v glucose (or galactose for the induction of galactose regulated promoters). For nutritional selection the required supplements were added at the following final concentrations: uracil 20mg l^{-1}, tryptophan 20mg l^{-1}, histidine 20mg l^{-1}, methionine 20mg l^{-1}, leucine 20mg l^{-1} and lysine 30mg l^{-1}.

2.2.4 Synthetic Complete Medium (SCM)

For nutritional selection SCM dropout powder mixes were added to SD medium at 2g l^{-1}. Dropout mixes were prepared as follows, omitting the supplement for which selection was required (Rose *et al.*, 1990):

Adenine	0.5g (21mg l^{-1})	L-leucine	4.0g (171mg l^{-1})
L-alanine	2.0g (86mg l^{-1})	L-lysine	2.0g (86mg l^{-1})
L-arginine	2.0g (86mg l^{-1})	L-methionine	2.0g (86mg l^{-1})
L-asparagine	2.0g (86mg l^{-1})	p-aminobenzoic acid	0.2g (9mg l^{-1})
L-aspartic acid	2.0g (86mg l^{-1})	L-phenylalanine	2.0g (86mg l^{-1})
L-cysteine	2.0g (86mg l^{-1})	L-proline	2.0g (86mg l^{-1})
L-glutamine	2.0g (86mg l^{-1})	L-serine	2.0g (86mg l^{-1})
L-glutamic acid	2.0g (86mg l^{-1})	L-threonine	2.0g (86mg l^{-1})
L-glycine	2.0g (86mg l^{-1})	L-tryptophan	2.0g (86mg l^{-1})
L-histidine	2.0g (86mg l^{-1})	L-tyrosine	2.0g (86mg l^{-1})
Inositol	2.0g (86mg l^{-1})	Uracil	2.0g (86mg l^{-1})
L-isoleucine	2.0g (86mg l^{-1})	L-valine	2.0g (86mg l^{-1})

The final working concentration for each supplement is indicated in parentheses.

2.2.5 SLAD and SLAG media

SLAD and SLAG media were used for the induction of pseudohyphal growth. SLAD consisted of 0.17% w/v yeast nitrogen base (without ammonium sulphate or amino acids), 50μM ammonium sulphate, 2% glucose and 2% agar, SLAG consisted of 0.17% w/v yeast nitrogen base (without ammonium sulphate or amino acids), 50μM ammonium sulphate, 2% galactose and 2% agar (Gimeno *et al.*, 1992). Each were supplemented with the required bases and amino acids at the concentrations described above for SD.

2.2.6 Presporulation and KAc media

Presporulation media consisted of 5% w/v glucose, 3% w/v nutrient broth (Difco), 1% w/v yeast extract and 2% w/v agar. KAc sporulation media consisted of 1% w/v potassium acetate, 0.01% w/v adenine, 0.01% w/v uracil, 0.1% w/v yeast extract, 0.05% w/v glucose and 1.3% w/v agar.

2.2.7 Anaerobic Conditions

Growth of yeast under anaerobic conditions was achieved in a BBL GasPak chamber containing oxoid gas-generating sachet. Growth was on YPD agar containing Tween 80 (0.9ml l^{-1}) and ergosterol (30mg l^{-1}).

2.3 Manipulations in yeast

2.3.1 PCR mediated gene disruption and gene tagging

PCR mediated gene disruption was carried out by the method described by Wach *et al.* (1994). A selectable marker was amplified from one of the pFA6a plasmid series to generate the desired disruption cassette. The primers were designed to include approximately 40bp overhangs homologous to the flanking regions of the gene to be disrupted. Typically 5μg of the amplification product was transformed into the yeast (see section 2.3.2). With the appropriate selection, only those yeast cells in which homologous recombination has replaced the targeted gene with the selectable marker will form colonies (see Figure 2.1). Successful gene disruption was confirmed by PCR. With genomic DNA from knockout candidates used as template, PCR was performed using pairs of primers that would indicate the presence or absence of the disrupted gene or the correctly integrated knockout cassette (see the relevant results section for specific details). Integration of the *GAL1* promoter and generation of green fluorescent protein (GFP) fusion constructs was performed in a similar manner, with primers being designed for the amplification of an appropriate tag/promoter and insertion of the integrating cassette with little or no replacement of native sequence (see the relevant results section for specific details).

2.3.2 High efficiency transformation

High efficiency transformation of yeast was carried out using the method described by Gietz *et al.* (1995). Yeast cells were grown to approximately 2×10^7 cells ml^{-1} in YPD, harvested by spinning in a bench-top centrifuge (3,500rpm for 7min) and washed twice in sterile water. Cells were then washed once and resuspended in 100mM lithium acetate in TE pH8, at 2×10^9 cells ml^{-1} and incubated at 30°C for 15min. To 50µl cell aliquots was added 5µl of 10mg ml^{-1} single stranded salmon sperm DNA (Sigma), 300µl of freshly prepared 40% (w/v) polyethelene glycol 3350 in 100mM lithium acetate/TE pH8 and transforming DNA. For routine plasmid transformation this was typically 100ng, for gene disruption/tagging approximately 5µg was used. Samples were incubated at 30°C for 30min, heat shocked at 42°C for 20min then plated onto selective media and incubated for 2-3 days. For G418 selection, samples were incubated for 2 hours in 3ml of YPD at 30°C with shaking, before plating onto YPD containing G418.

2.3.3 Small scale preparation of genomic DNA

A 10ml yeast culture was grown in YPD overnight. Cells were then harvested in a bench-top centrifuge (3,500rpm for 7min) before being resuspended in 0.5ml of water and transferred to screw-top microfuge tubes. Cells were pelleted in a microcentrifuge (13,000rpm for 2min) and resuspended in 200µl of breaking buffer (2% w/v Triton X-100, 1% w/v SDS 100mM NaCl, 10mM Tris-HCl pH8 and 1mM EDTA pH8) to which 200µl of phenol/chloroform/isoamyl alcohol (in the ratio 25:24:1) was added. 425-600µm acid washed glass beads were added up to the meniscus and the tubes were vortexed for 7min. 200µl of TE was added, the tubes were briefly vortexed and spun in a microcentrifuge at (13,000rpm for 5min). To remove residual phenol the aqueous layer was then transferred to a fresh tube containing 200µl of chloroform/isoamyl alcohol (24:1), vortexed, centrifuged again and the aqueous layer transferred to 1ml of 100% ethanol and mixed by inversion. The solution was then spun in a microcentrifuge (13,000rpm for 3min), the supernatant removed and the pellet resuspended in 0.4ml of TE, to which 3µl of RNAse A (10mg ml^{-1}) was added and incubated for 1 hour at 37°C. To precipitate the genomic DNA, 10µl of 4M ammonium acetate and 1ml of 100% ethanol was added and mixed by inversion. The mixture was spun in a microcentrifuge (13,000rpm for 3min), the supernatant aspirated and the pellet air-dried before resuspending in 100µl of TE (Hoffman, 1997).

2.3.4 Preparation of total RNA

Small scale preparations of total yeast RNA were conducted by the method of Schmitt *et al.* (1990). All solutions were made up using Diethyl pyrocarbonate (DEPC)-treated water (DEPC was added at 0.1% v/v to deionised water, shaken and left overnight before

autoclaving at 121°C, 15psi for 20min). A 50ml culture of yeast was grown in SD or YP media using 2% w/v glucose as the carbon source (or 2% w/v galactose for the induction of galactose inducible promoters) to approximately 1×10^7 cells ml^{-1}. Cells were harvested in a bench-top centrifuge (3,500rpm for 7min), resuspended in 400µl of AE buffer (50mM sodium acetate pH5.3, 10mM EDTA) and transferred to microfuge tubes. 80µl of 10% SDS was added and vortexed for 30s followed by addition of 440µl of phenol (equilibrated to pH5.3 with AE buffer) and vortexed again for 30s. Tubes were freeze-thawed by 3 repeated cycles of incubation in a 65°C water bath for 4min followed by rapid chilling in a dry ice/IMS bath for 3min. Tubes were then spun in a microcentrifuge (13,000rpm for 2min) and the aqueous phase transferred to a tube containing 0.5ml of phenol/chloroform/isoamyl alcohol (in the ratio 25:24:1) before being briefly vortexed and spun in a microcentrifuge (13,000rpm for 10min). The phenol extraction was repeated and the aqueous phase was transferred to a tube containing 40µl of 3M sodium acetate and 1ml of 100% ethanol. Total RNA was then precipitated on dry ice for 1 hour before being pelleted in a microcentrifuge (13,000rpm for 10min). The pellet was then rinsed with 1ml of 80% ethanol, spun in a microcentrifuge (13,000rpm for 5min), aspirated, air dried and resuspended in 50µl of DEPC-treated water.

2.3.5 Preparation of crude homogenates

50ml of culture was grown in YP or SD broth (with 2% w/v galactose as the sole carbon source for the induction of galactose inducible promoters) to approximately 1×10^7 cells ml^{-1}. Cells were harvested in a bench-top centrifuge (3,500rpm for 7min), resuspended in 1ml of sterile water and transferred to microfuge tubes. Cells were pelleted in a microcentrifuge (13,000rpm for 2min) and resuspended in 250µl of glass bead disruption buffer (20mM Tris-HCl pH7.9, 10mM $MgCl_2$ 1mM EDTA 5% v/v glycerol 1mM dithiothreitol) and 0.5g of 425-600µm acid washed glass beads were added. Tubes were shaken at 4°C for 5min using a Disruptor Genie (Scientific Industries). The crude extract was removed from the glass beads using a P1000 pipette tip. The glass beads were then rinsed with 0.5ml of glass bead disruption buffer and the extracts were pooled. Extracts were then spun at 100*g* for 5min to remove cellular debris.

2.3.6 Preparation of soluble and particulate fractions

A crude homogenate was prepared as above and spun at 100,000*g* for 45min. The supernatant was removed as the soluble fraction and the particulate fraction was prepared by resuspending the pellet in TE pH8 using a 0.5ml syringe with a 27G needle.

Where the effect of varying pH on PV hydrolase activity was being tested the crude homogenate was prepared using water instead of glass bead disruption buffer and the final

particulate fraction was resuspended in the following buffers: 50mM glycine-HCl (pH3), 50mM sodium acetate (pH4), 50mM sodium acetate (pH5), 50mM sodium phosphate (pH6), 50mM sodium phosphate (pH7) or 50mM Tris-HCl (pH8) each containing 1mM EDTA.

Where the preparation was to be used for western blotting or reacting with [^{3}H]DFP a fungal protease inhibitor cocktail (Sigma) was added to the glass bead disruption buffer and the TE at 1:100.

2.3.7 Sporulation of diploids and dissection of tetrads

Diploids were patched onto presporulation medium and incubated for 2 days at 30°C before being removed from the plate using a sterile toothpick and patched on KAc media and incubated at 22°C for approximately 10 days. Cells were then resuspended in 100µl of water to which 5µl of β-glucuronidase was added. The mixture was incubated at room temperature for 5min to digest the asci walls. Meiotic tetrads were then dissected using a Singer MSM Micromanipulator on YPD plates poured using a level platform. Plates were then incubated for 3 days.

2.3.8 Assessing markers and mating types

For the assessment of nutritional markers and mating types of the dissected spores, each was picked and patched in grids on YPD and incubated at 30°C for 2 days. To determine which selectable markers were present in each spore this plate was then replicated onto relevant selective media and incubated for 2-3 days. Growth on a selective media lacking a supplement indicated the presence of this selectable marker.

Mating types were determined using mating type tester strains that can complement all the nutritional markers of the strains on test. The following procedure was used to determine the mating type of each spore: 1ml cultures of the two mating type tester strains, DC14 and DC17 (see Table 2.1 for genotypes), were spread onto YPD plates and incubated overnight. The gridded plate of test samples was then replicated onto two fresh YPD plates, onto each of which one of the test strain plates was also replicated. Plates were then incubated for 4 hours before replicating onto SD without any supplements and incubating for 2 days. Growth of a spore indicates the opposite mating type to the tester strain, and failure to grow indicates the same mating type as the tester strain. Haploid strains with the desired mating type and selectable markers were retained.

2.3.9 Generation of diploid yeast strains

Generally 'a' and 'α' type haploids were mated by mixing a colony of each on a YPD plate and incubating overnight. Where selection of a diploid was possible an area of this mixture

was picked and streaked onto an SD plate containing those supplements that would allow only the growth of the diploid. After a two-day incubation one colony from this plate was picked and streaked to single colonies on the same media to purify a single clone.

Direct selection of diploids was not possible when generating MW1076/7. In this case the MW1076/MW1077 mating mixture was streaked to single colonies and incubated for 2 days on YPD. Twenty single colonies were picked from this plate and gridded on YPD for determination of mating type as above; haploids MW1076 and MW1077 were included on the grid as controls. Successful diploids were those that could mate with neither 'a' nor 'α' mating tester strain. These were further confirmed as diploids by inducing them to sporulate (see section 2.3.7).

2.4 Phenotypic tests

Phenotypic tests were carried out in one of two ways:-

Method 1: The first method was to grow cultures of both BY4741 and BY4741 *yml059cΔ* to an equal density, and make 1, 1/10, 1/100 and 1/1000 serial dilutions of each. For the anaerobic growth test 1, 1/5, 1/25, 1/125 and 1/625 serial dilutions were used. 5μl (2.5μl for anaerobic growth test) of each dilution was then spotted on to an agar plate containing the condition on test and the plate was incubated at 30°C, unless otherwise stated. After 1-4 days the growth of each strain was compared to see if either was more sensitive/resistant to the condition on test. For each test a control plate was included. Unless otherwise indicated the control consisted of each dilution being spotted onto a standard YPD plate and incubated at 30°C to ensure that the two strains on test would grow in an equal fashion in the absence of any test condition. The level of growth for each yeast spot was given a score from ranging from 5, for dense confluent growth down to 1 indicating few, poorly growing individual colonies. A score of 0 indicates no visible growth.

Method 2: Generally the second method entailed producing 2 plates of YPD, onto which top agar was poured that contained either BY4741 or BY4741 *yml059cΔ*, in an equal concentration of approximately 1×10^7 cells ml^{-1}. For the sensitivity to phenyl saligenin phosphate (PSP) test, 3 YPgal plates were used onto which top agar was poured containing either BY4743, BY4743 *yml059cΔ/yml059cΔ* or BY4743 P_{gal1}-*GFP-YML059c*/P_{gal1}-*GFP-YML059c*. A disc of filter paper impregnated with the inhibitor on test was then placed on to each plate, and the plates were then incubated at 30°C. The diameter of the zone of inhibition, within which yeast would not grow was then measured and compared for each strain.

2.4.1 Induction of pseudohyphal growth

Yeast were streaked to single colonies on duplicate plates of SLAD media (or SLAG media for the induction of galactose regulated promoters) and incubated at 30°C for 10-14 days.

2.5 Manipulations in *E.coli*

2.5.1 Preparation of competent *E.coli* DH5α

Competent *E.coli* DH5α were prepared by the calcium chloride method of Mandel and Higa (1970). Using a 1ml overnight culture as the inoculum, 100ml of DH5α was grown in LB to an A_{650} of 0.4-0.6. The culture was poured into 4 pre-chilled 25ml universal tubes and placed on ice for 10min before harvesting at 3,500rpm and 4°C for 10min. Each pellet was then resuspended in 10ml of sterile 0.1M calcium chloride and left on ice for a minimum of 1 hour. Cells were then pelleted as above before resuspending in a total of 6ml of freezer mix (15% v/v glycerol 0.1M $CaCl_2$). 300μl aliquots were then flash frozen in a bath of dry ice and IMS before storing at -80°C for future use.

2.5.2 Transformation

When transforming DH5α, 100μl of competent cells were added to DNA ligation mixes or 100ng of plasmid and incubated at 30°C for 30min. Cells were then heat shocked at 42°C for 2min; the volume made up to 1ml with LB and re-incubated at 37°C for 1 hour. Cells were pelleted in a microfuge (13,000rpm for 1min) resuspended in 100μl LB, plated onto selective medium and incubated overnight.

For XL-1 Blue, XL-10 Gold and BL21(DE3)pLysS, 40μl of thawed cells were placed in pre-chilled 15ml polypropylene tubes to which the transforming DNA was added. Tubes were incubated on ice for 20min before being heat shocked at 42°C for 45s and immediately returned to ice. 0.46ml of LB containing 20mM glucose was added to each tube and shaken at 37°C, for 90min. 100ul of each reaction was then plated on selective media and incubated at 37°C overnight.

2.5.3 Plasmid DNA preparations

Mini-Prep, Midi-Prep and Hi-speed Midi-Prep plasmid purification kits (supplied by Qiagen) were used to obtain plasmid DNA. Procedures were carried out in accordance with the manufacturers' instructions.

2.5.4 Preparations of bacterial homogenates

Crude homogenates of BL21(DE3)pLysS were obtained in order to determine the presence, solubility and any PV hydrolase activity of the YNEST polypeptide being expressed using the pET21b vector. Overnight LB/Amp cultures of BL21(DE3)pLysS carrying pET-YNEST were diluted 6-fold in LB/Amp and shaken at 37°C for 45min. Expression was then induced by addition of IPTG to 1mM followed by a further 3 hour incubation. To confirm the presence of the polypeptide by western blot analysis 1ml of this culture was harvested and the pellet boiled for 5min in 200µl of 2% SDS-PAGE sample buffer (60mM Tris-HCl, pH6.8, 2% w/v SDS, 2% v/v glycerol, 2% w/v DTT, 0.002% w/v bromophenol blue). For the determination of any PV hydrolase activity and for the assessment of the solubility of the polypeptide, cells were broken by freeze-thawing pellets of induced culture.

2.6 Mammalian cell culture

2.6.1 Transient transfection of COS-7 and Hela cells

8×10^5 cells were plated in 10cm petri dishes in 10ml of medium (Dulbecco's MEM with Glutamax-I (Life Technologies), 10% v/v foetal calf serum, 2% w/v penicillin, 2% w/v streptomycin) and incubated overnight. The following day, cells were rinsed once with PBS and covered with 10ml of fresh medium. For each transfection, 4µg of the transfecting plasmid was mixed in a 15ml tube with 25µl of Polyfect reagent (Qiagen) and left to react at room temperature for 5-10min, before being mixed in 1ml of medium and added to the cells. Plates were swirled to mix and incubated for 48 hours.

2.6.2 Preparation of microsomes from transfected COS-7 and Hela cells

Transfected cells were rinsed once with PBS and covered with 10ml of trypsin (0.5mg ml^{-1} with 0.5mM EDTA in PBS), left at room temperature for 5min then scraped from the dish with a rubber policeman. Cells were harvested in 25ml universals (300*g* for 5min) and rinsed once with PBS. Each pellet was homogenised in 1ml of TE using a 0.5ml syringe. The homogenate was spun at 200*g* for 5min to remove cellular debris and the resulting supernatant was centrifuged at 100,000*g* for 45min. The supernatant was discarded and the pellet was homogenised in 100µl of TE using a 0.5ml syringe with a 27G needle.

2.7 Nucleic Acid Manipulations

2.7.1 Quantification of nucleic acid

The concentration of single stranded DNA, double stranded DNA or RNA in aqueous solution was determined by measuring the absorbance of a diluted (typically 50- or 100-fold)

solution of the nucleic acid in a quartz cuvette at 260nm. The concentration was calculated using the following formula (Sambrook *et al.*, 1989):

$$\text{Nucleic acid concentration } (\mu g\ ml^{-1}) = A_{260} \times \text{dilution} \times X$$

Where X = 50 for double stranded DNA, 33 for single stranded DNA and 40 for RNA.
The concentration of oligonucleotide primers was determined using the following formula (Sambrook *et al.*, 1989):

$$\text{Primer concentration } (pmol\ \mu l^{-1}) = A_{260} \times \text{dilution} \times \frac{100}{1.5\,N_A + 0.71\,N_C + 1.2\,N_G + 0.84\,N_T}$$

Where N is the number of A, C, G and T bases.

2.7.2 Restriction enzyme digests

Restriction enzymes were obtained from Gibco-BRL or New England Biolabs. Digestions were carried out in accordance with the suppliers' instructions.

2.7.3 DNA agarose gel electrophoresis

DNA fragments were separated by agarose gel electrophoresis, typically using 1% w/v high gelling temperature agarose in TAE buffer (0.04M Tris-acetate, 2mM EDTA). After running, gels were stained in a 0.5mg ml^{-1} ethidium bromide solution and visualised under UV light (Sambrook *et al.*, 1989).

2.7.4 RNA agarose gel electrophoresis

RNA was separated by electrophoresis using formaldehyde denaturing gels (Lehrach *et al.*, 1977). Samples were prepared by combining 10-20μg of RNA, 2.5μl of 10×MOPS buffer (200mM MOPS, 83mM sodium acetate, 1mM EDTA pH7), 10μl of deionised formamide and 3.5μl of formaldehyde in a final volume of 20μl. Samples were denatured by heating to 65°C for 10min then immediately cooled on ice before adding 2μl of loading buffer (0.4% w/v bromophenol blue, 0.4% w/v xylene cyanol, 50% v/v glycerol, 1mM EDTA) and 1μl of 1mg ml^{-1} ethidium bromide. Samples were loaded onto 1.5% w/v agarose gels (made in MOPS buffer) containing 3% v/v formaldehyde and run in MOPS buffer at 100 volts for 2-3 hours and visualised under UV light, noting the position of the markers.

2.7.5 Recovery of DNA fragments from agarose gels

DNA fragments were recovered from agarose gels with Qiagen Gel Extraction, Qiagen Mini-Elute Gel Extraction and Millipore Ultrafree-DA kits, in accordance with the manufacturers' instruction.

2.7.6 Phosphatase treatment of DNA

Dephosphorylation of DNA was achieved using Shrimp Alkaline Phosphatase (supplied by Amersham Biosciences) and carried out in accordance with the manufacturers instructions.

2.7.7 DNA ligation

DNA ligation was performed using T4 DNA ligase and 5×ligation buffer (supplied by Gibco BRL). A typical reaction consisted of 20-100ng of vector DNA, insert DNA, 1μl of T4 DNA ligase (1 unit) and 4μl of 5×ligation buffer in a total volume of 20μl. In order to include approximately equal molar quantities of insert and vector DNA samples of each were visually quantified by agarose gel electrophoresis.

2.7.8 Site directed mutagenesis

Site directed mutagenesis was carried out using the QuikChange kit (supplied by Stratagene) and performed in accordance with the manufacturers' instructions (see section 3.7 for details), using the primers indicated in Table 2.4.

2.7.9 Northern blot hybridisation

Following electrophoresis (see section 2.7.4) RNA was transferred onto Hybond N+ nylon membrane by capillary action from a reservoir of 10×SSC (1.5M sodium chloride, 0.15M sodium citrate pH7 (Thomas, 1980). The RNA was then fixed onto the membrane using an RPN2500 UV crosslinker (Amersham) set to 70mJ cm^{-2}. Prior to hybridisation, membranes were rotated in hybridisation tubes containing 20ml Church-Gilbert buffer (0.5M sodium phosphate, 7% w/v SDS, 1mM EDTA pH7.4) (Church and Gilbert, 1984) for 6 hours at 65°C. A radiolabelled oligonucleotide probe (see section 2.7.10) was then added to the tube and incubation continued overnight. Membranes were then washed four times with 3×SSC, 0.1% w/v SDS at 65°C before covering with Saran wrap and visualising by autoradiography.

2.7.10 Radiolabelling of oligonucleotide probes

Oligonucleotide probes were radiolabelled using random hexanucleotide primers, based on the method of Feinberg and Vogelstein (1983).

Oligo labelling buffer (OLB) was prepared by combining A (18% v/v β-mercaptoethanol, 5mM dATP, dTTP, dGTP, 0.125M $MgCl_2$, 1.25M Tris-HCl pH8), B (2M HEPES-NaOH pH6.6) and C (Hexanucleotides at 90 A_{260} ml^{-1} in TE) at a ratio of 10:25:15. 20ng of DNA to be labelled (in 15μl of water) was denatured at 100°C for 5min then immediately cooled on ice. To this, 5μl OLB, 1μl (1 unit) klenow enzyme, 1μl 10mg ml^{-1} bovine serum albumin

(BSA) and 2.5µl of [^{32}P]dCTP were added and incubated at room temperature for 6 hours. Unincorporated nucleotides were removed using prepacked Sephadex G-50 NICK columns (Amersham).

The probe used for the detection of *YML059c* by northern blot was generated by amplifying the first 494bp of *YML059c* by PCR, using BY4741 genomic DNA as template and primers YML5 and P8 (see Table 2.4). The probe for the detection of the *BYC1* transcript consisted of the final 287bp of *BCY1*, obtained by restriction digestion of pYC2/CT-*BCY1* using *EcoR*I and *Bgl*II. The probe for *ACT1* was a 342bp restriction fragment obtained by digestion of pBS-Actin using *Kpn*I and *Hind*III.

2.7.11 Polymerase chain reaction

PCR amplification was performed using a Hybaid Omn-E thermal cycler. Reactions were carried out in the following solution: 45mM Tris-HCl pH8.8, 11mM ammonium sulphate, 4.5mM magnesium chloride, 6.7mM β-mercaptoethanol, 4.5µM EDTA pH8.0, 1mM dATP, 1mM dCTP, 1mM dGTP, 1mM dTTP, 113 µg ml^{-1} BSA and each primer at 0.2µM. A 100µl reaction included 100ng of template DNA and 1µl of polymerase. Using either Taq polymerase (supplied by Abgene) or BIO-X-ACT (supplied by Bioline).

Generally PCR was performed using the following program:

	Temperature (°C)	Time (min)	No. of cycles
Denaturing	94	2	1
Denaturing	94	1	35
Annealing	50-58.5	1	
Extension	72	1min kb^{-1} amplified	
Extension	72	10	1

For amplifying products of 5kb or greater extension times were increased to 10min and denaturing times were decreased to 30s.

For the amplification of gene knockout/tagging cassettes the following two-step program was used (adapted from Brachmann *et al.* 1998) in which early rounds of amplification are performed at a low stringency to allow the annealing of primers with long overhangs:

	Temperature (°C)	Time (min)	No. of cycles
Denaturing	94	2	1
Denaturing	94	1	10
Annealing	55	1	
Extension	72	1min kb^{-1} amplified	
Denaturing	94	1	30
Annealing	65	1	
Extension	72	1min kb^{-1} amplified	
Extension	72	10	1

2.7.12 Oligonucleotide primers

Oligonucleotide primers were synthesised by the Protein and Nucleic Acid Chemistry Laboratory, University of Leicester and supplied in ammonia solution. Before use primers were ethanol precipitated as follows: 200µl of stock primer was combined with 20µl of 3M sodium acetate and 500µl of 100% ethanol in a microfuge tube and placed on dry ice for 10min. Tubes were then spun in a microcentrifuge at 13,000rpm and 4°C for 10min before aspirating the supernatant and washing the pellet twice with 1ml of 70% ethanol. Pellets were then dried at 65°C for 10min before resuspending in 200µl of sterile water. See Table 2.4 for a list of primers used in this study.

Table 2.4. Oligonucleotides used in this study

Oligo Name	Oligo Sequence (5'→3')	Function	Annealing coordinates (5'→3')
5GFPL	AAACAAGAAAAGAATAGAAAGG CTTGGCTCTAGTTTTTGCGAATT CGAGCACGTTTAAAC	Amplification of P_{gal1} cassette with or without GFP tag	-41bp to -1bp, relative to ATG of *YML059c*
5GFPR	TATTGTTGGTGTTGTTCGTAGTG CAATTCATTGAACGCATTTTGTA TAGTTCATCCATGC	Amplification of P_{gal1}-GFP cassette	+40bp to +1bp, relative to ATG of *YML059c*
BCYF	CCCAAGCTTATGGTATCTTCTTT GCC	Amplification of *BCY1* ORF for cloning	+1bp to +17bp relative to ATG of *BCY1*
BCYR	CCCGCCTTCATGTCTTGTAGGA TCATTGAGC	Amplification of *BCY1* ORF for cloning	-4bp to -25bp relative to stop codon of *BCY1*
GALB	CCTCTATACTTTAACGTCAAGG	Confirmation of *GAL1* promoter and GFP insertion	Anneals within *GAL1* promoter: -46bp to -25bp relative to fusion junction
GALR	TATTGTTGGTGTTGTTCGTAGTG CAATTCATTGAACGCATTTTGAG ATCCGGGTTTT	Amplification of P_{gal1} cassette	+40bp to +1bp relative to ATG of *YML059c*
GALYMLF	GGGGAGCTCACAGATCTGTAAA GAGCCC	Amplification of overexpression constructs	-2bp to +17bp relative to the *Bgl*II site that denotes the beginning of the *GAL1* promoter
GALYMLR	GGGCTCGAGCTTAAAAAGTCAT AGTAAATACC	Amplification of overexpression constructs	+219bp to +194bp relative to the stop codon of *YML059c*

GFPA	CCAGTGAAAAGTTCTTCTCC	Confirmation of *GAL1* promoter and GFP insertion	Anneals within GFP tag: +47bp to +28bp relative to GFP fusion junction with *YML059c*
GFPL	TCAAGTTCCTGAGTTTTTATTAC ATAGAAGAAATAGTATTCGGATC CCCGGGTTAATTAA	Amplification of C-terminal GFP tagging cassette	-43bp to -4bp relative to stop codon of *YML059c*
GFPR	ACAAAAAACGGTCACCAAGGCG TTGGAAGATAGAAATCTAGAATT CGAGCTCGTTTAAAC	Amplification of C-terminal GFP tagging cassette	+40bp to +1bp relative to stop codon of *YML059c*
KOYMLF	AAACAAGAAAAGAATAGAAAGG CTTGGCTCTAGTTTTTGCCGGAT CCCCGGGTTAATTAA	Amplification of gene disruption cassettes for genetic knockout of *YML059c*	-40bp to -1bp relative to ATG of *YML059c*
KOYMLR	ACAAAAAACGGTCACCAAGGCG TTGGAAGATAGAAATCTAGAATT CGAGCTCGTTTAAAC	Amplification of gene disruption cassettes for genetic knockout of *YML059c*	+40bp to +1bp relative to stop codon of *YML059c*
P15	CCTGGTTCACAAGAAACC	Confirmation of *yml059c* gene disruption and chromosomal fusions	Anneals within *YML059c*: -72bp to -55bp relative to stop codon of *YML059c*.
P16	CAATAGATGGGGTCGCCTACC	Confirmation of *yml059c* gene disruption and chromosomal fusions	Anneals downstream of *YML059c*: +879bp to +859bp relative to stop codon of *YML059c*
P3	CAATAGATGGGGTCGCCTACC	Confirmation of *yml059c* gene disruption and chromosomal fusions	Anneals within KanMX4 and *HIS3MX6* cassettes: +220bp to +200bp for *HIS3MX6* and KanMX4 disruption cassettes, +1164bp to +1144bp for GFP-*HIS3MX6* fusion cassette. All relative to fusion junction.
P4	CGCCTCGACATCATCTGCCC	Confirmation of *yml059c* gene disruption and chromosomal fusions	Anneals within KanMX4 and *HIS3MX6* cassettes, -140bp to -121bp relative to fusion junction i
P7	GGGTTAAGGCCTTGGTCCATGG	Confirmation of *yml059c* gene disruption and chromosomal fusions	Anneals upstream of *YML059c*: -527bp to -506bp relative to ATG of *YML059c*
P8	GGCGCGTTGGCTGACTGAGTG G	Confirmation of *yml059c* gene disruption and chromosomal fusions, and amplification of *YML059c* hybridisation probe	Anneals within *YML059c*: +494bp to +473bp relative to ATG of *YML059c*
S1406AF	CGACGTTATTGGAGGAACAGCG ATTGGTTCC	Site directed mutagenesis of active site serine to alanine	+4197bp to +4227bp relative to ATG of *YML059c*
S146AR	GGAACCAATCGCTGTTCCTCCA ATAACGTCG	Site directed mutagenesis of active site serine to alanine	+4227bp to +4197bp relative to ATG of *YML059c*
SC-R1	CTCGAGCTCGAGACCATAGTCT ACACCCACATG	Amplification of the region encoding the catalytic domain of Yml059c for cloning into pET21b	+4921bp to +4900bp relative to ATG of *YML059c*
SERSEQ	GCGAGAGGTATTAGTCATTTGG	Sequencing primer for confirmation of serine to alanine mutagenesis	+4138 to +4159bp relative to ATG of *YML059c*
TP1	CCTTAATTAACCCGGGGATCCG	Confirmation of *yml059c* gene disruption from pseudohyphal strain	Anneals within *HIS3MX6* and *TRP1* cassettes: +1bp to + 22bp relative to fusion junction
TP2	TTGACCCGGTTATTGCAAGG	Confirmation of *yml059c* gene disruption from pseudohyphal strain	Anneals within *TRP1* cassette: -633bp to -613bp relative to fusion junction

YF2	GAGCTCGAGCTCGGCCCAAAGT TCACACAAGGGT	Amplification of the region encoding the catalytic domain of Yml059c for cloning into pET21b	+2608bp to +2628bp relative to ATG of *YML059c*
YML3	GGGCTCGAGTCAAATACTATTTC TTCTATG	Amplification or full length *YML059c* for cloning	-1bp to -21bp relative to stop codon of *YML059c*
YML3.3	CAAGGTACCCCAATACTATTTCT TCTATG	Amplification of *YML059c* for cloning into pEGFP-N1	-4bp to -21bp relative to stop codon of *YML059c*
YML5	GGGTGATCAATGCGTTCAATGA ATTGC	Amplification of *YML059c* hybridisation probe and full length *YML059c* for cloning	+1bp to +18bp relative to ATG of *YML059c*
YML5.3	GGGGAGCTCATGCGTTCAATGA ATTGC	Amplification of *YML059c* for cloning into pEGFP-N1	+1bp to +18bp relative to ATG of *YML059c*

2.7.13 DNA sequencing

Sequencing was performed by the Protein and Nucleic Acid Chemistry Laboratory, University of Leicester on an ABI 377 sequencer following a cycle sequencing reaction using Big Dye Terminator ready mix. For each reaction the following reagents were combined: Big Dye Terminator Ready Mix (8μl), template DNA (1μg for a plasmid, 75ng for a PCR product) and sequencing primer (3.2pmol) in a total volume of 20μl of sterile water and overlaid with mineral oil. Cycling reactions were carried out in a Hybaid Omn-E thermal cycler using the following program:

	Temperature (°C)	Time	No. of cycles
Denaturing	96	5min	1
Denaturing	96	30s	45
Annealing	50-58.5	15s	
Extension	72	4min	

After temperature cycling the reactions were removed from beneath the mineral oil layer by pipetting and transferred to a microfuge tube containing 2μl of 3M sodium acetate (pH4.6) and 50μl of 100% ethanol. Tubes were then mixed and placed on ice for 10min to precipitate the extension products and spun in a microcentrifuge at 13,000rpm for 30min. The supernatant was aspirated and the pellet rinsed with 250μl of 70% ethanol. After centrifuging again as above, the supernatant was aspirated and the pellet air-dried before submitting for sequencing.

2.8 Biochemical techniques

2.8.1 Protein concentration determination

The determination of protein concentrations was achieved using the Bio-Rad *DC* protein assay. Based on the Lowry assay, this method of determining protein concentrations relies

on the reaction of protein with an alkaline copper tartrate solution and the Folin reagent, producing a characteristic blue colour (Lowry *et al.*, 1951). Duplicate test samples (typically duplicate 4 and 8µl samples were used for determining the concentration of yeast particulate fractions) were pipetted into assay tubes, as were 0, 20, 40, 60, 80 and 100µg of BSA, to obtain a standard linear plot. 125µl of copper tartrate solution was added to each tube and vortexed briefly. To each tube 1ml of Folin reagent was added and vortexed again. Tubes were then left to stand for 10min before measuring the absorbance at 750nm relative to the 0µg standard. Using a plot of BSA absorbance values versus concentration of BSA, the concentrations of the test samples were determined.

2.8.2 SDS-polyacrylamide gel electrophoresis

1.5mm thickness 7.5% polyacrylamide gels were used for the separation of proteins by SDS-PAGE. The following volumes of each solution (ml) were combined to achieve the desired percentage gel, including the 4% stack gel:

	7.5% resolving gel	4% stack
30% w/v acrylamide and bis-acrylamide (29:1)	6.25	1.3
1.5M Tris-HCl, pH8.8	6.25	-----
0.5M Tris-HCl, pH6.8	-----	2.5
10% SDS	0.25	0.1
10% APS (made fresh each time)	0.125	0.05
TEMED	0.013	0.01
H_2O	12.2	6.1

For both the resolving and stacking gel, the acrylamide, Tris-HCl, SDS and water were mixed before polymerisation was initiated by addition of the ammonium persulphate (APS) and TEMED. The resolving gel was pipetted into a Bio-Rad gel cassette and approximately 1ml of iso-propanol was layered on top to prevent air bubbles. After the gel had set the iso-propanol was rinsed off with distilled water and the excess water was absorbed with Whatman 3MM filter paper. The comb was then inserted before the stacking gel was pipetted onto the resolving gel.

Samples were boiled for 5min in a final concentration of 2% SDS-PAGE sample buffer (60mM Tris-HCl, pH6.8, 2% w/v SDS, 2% v/v glycerol, 2% w/v DTT, 0.002% w/v bromophenol blue) before loading 20µl of each. Gels were run in SDS-PAGE running buffer

(25mM Tris, 190mM glycine, 0.1% SDS) at 200V until the dye front had reached the bottom of the gel. Gels were then either transferred to a membrane or Coomassie stained. Gels were stained for 10min using 0.25% Coomassie brilliant blue in 50% v/v methanol, 10% v/v acetic acid. Gels were then destained using several changes of 50% v/v methanol, 10% v/v acetic acid (or overnight using 25% v/v methanol, 10% v/v acetic acid) before rehydrating in 10% v/v acetic acid for 1hour.

2.8.3 Western blotting

For the detection of polypeptides by western blot, gels were transferred to nitrocellulose by the method of Towbin *et al.* (1979). Having been presoaked in transfer buffer (20% v/v methanol, 25mM Tris, 190mM glycine) the following were set up, in the order stated, between the negative and positive terminals of a Mini Trans-Blot cell (Bio-Rad): sponge, Whatman 3MM filter paper, polyacrylamide gel, nitrocellulose, Whatman 3MM filter paper, sponge. The cell was then filled with transfer buffer and run at 80 volts for 45min.

After transfer was complete the nitrocellulose membrane was stained for 2min using 0.25% w/v Ponceau S in 1% v/v acetic acid and rinsed with distilled water until the markers were sufficiently visible for their position to be noted. The blot was then incubated for 30min at 37°C in 2% w/v Marvel/TBS (50mM Tris-HCl, 150mM NaCl pH7.4) before being rinsed in cold tap water and deionised water and incubated (in a heat-sealed bag) with diluted primary antibody (1:10,000 for the T7 antibody and 1:1,000 for the GFP antibody in 2% w/v marvel/TBS) for 2 hours at room temperature (or 4°C overnight). After which the blot was rinsed with distilled water and rocked in blot wash (0.005% v/v Tween 20 in TBS) for 5min. The blot was then rinsed in cold tap water and deionised water before being incubated (in a heat-sealed bag) with diluted peroxidase- or alkaline phosphatase-labelled secondary antibody (1:1,000 in 2% w/v marvel/TBS) for 2 hours at room temperature (or 4°C overnight). The blot was washed again as above and developed.

The alkaline phosphatase conjugated was visualised by covering with 150µl BCIP (16.5mg ml^{-1} in 100% DMF) and 150µl NBT (33mg ml^{-1} in 70% DMF) in 15ml alkaline phosphatase buffer (0.1M Tris-HCl pH9.5, 0.1M sodium chloride, 5mM magnesium chloride) until bands were visible before washing with distilled water and drying.

The peroxidase conjugate was visualised by autoradiography after overlaying the blot with 2ml of freshly mixed Pierce ECL reagent and incubating on the bench for 2min.

GFP tagged polypeptides were detected using a polyclonal rabbit anti-GFP antibody (Clontech). T7 tagged polypeptides were detected using polyclonal anti-T7 antibody (Novagen).

2.8.4 Determining solubility of recombinant YNEST in SDS and Triton X-100

Pellets obtained from 2×4ml IPTG induced cultures of BL21(DE3)pLysS carrying pET-YNEST were resuspended in 0.9ml of TE, frozen on dry ice for ½ hour and thawed. To each sample either 0.1ml of 10% SDS or 10% Triton X-100 was added and rotated for 1 hour at room temperature. Samples were then centrifuged at 100,000*g* for 45min. The supernatant was then removed and assessed for the presence of the YNEST polypeptide by western blot using an anti-T7 antibody.

2.8.5 Phenyl valerate hydrolase assay

Hydrolysis of phenyl valerate was assayed by the colorimetric determination of liberated phenol based on the assay developed by Johnson (1977). 1ml samples diluted in TE were assayed in duplicate, for each assay a reaction blank consisting of 1ml of TE was included. 1ml of substrate (0.5mg ml^{-1} phenyl valerate in 0.03% Triton X-100) was added to each sample before a 20min incubation at 37°C, after which the reaction was stopped by the addition of 1ml SDS/APP (3.4% SDS w/v, 0.25mg ml^{-1} 4-aminoantipyrine in TE) and 0.5ml 0.4% w/v potassium ferricyanide. After 10min on the bench the A_{486} for each reaction was measured by spectrophotometer. For each reading the A_{486} for the TE blank was subtracted and the following equation was used to determine the rate of PV hydrolysis:

$$\text{Rate of hydrolysis (nmol of phenol min}^{-1}\text{ mg}^{-1}) = \frac{A_{486}}{E_m} \times \frac{v}{t \times p} \times 10^6$$

Where: A_{486} = the absorbance of the sample minus that of TE blank, at 486nm

E_m = the molar extinction coefficient (16,470)

v = the total assay volume (ml)

t = the time of the incubation with the substrate (min)

p = the quantity of protein in the reaction (mg)

2.8.6 Phenyl valerate hydrolase assay at varied temperature and pH

When investigating the effect of altered temperature on PV hydrolase activity the assay was performed as above with the incubation temperature set at either 30°C or 37°C.

The above assay was altered to investigate the affect of varying pH on PV hydrolase activity in the following ways: (i) by diluting the samples in the relevant pH buffer (see section 2.3.6) in place of TE, and (ii) by the addition of 100µl of 1.5M Tris-HCl pH8.8 after the 20min incubation to ensure that low pH would not alter the colour change.

2.8.7 Inhibition of phenyl valerate hydrolase activity

Samples were incubated with the inhibitor on test for 20min at 37°C after which the PV hydrolase activity was determined as above. The following inhibitors were tested at the indicated final concentrations: Phenyl methylsulfonylfluoride (PMSF 0, 0.01, 250, 500, 1000 and 2000µM) mipafox (0, 0.01, 12, 25, 50 and 100µM), di-isopropyl fluorophosphate (0, 0.01, 0.75, 1.5, 3, 6, 12 and 25µM) and phenyl saligenin phosphate (0, 0.01, 0.06, 0.12, 0.25, 0,5 and 1µM). DFP and PMSF stock solutions were made up in dry dimethylformamide (DMF). PSP was made up in dimethylsulfoxide (DMSO) and mipafox was made up in Tris-citrate pH6.0. Inhibitors were added to the reaction such that the solvent concentration did not exceed 1%.

2.8.8 Lysophospholipase assay

Liberation of free fatty acid from 1-palmitoyl-lysophosphatidylcholine (PLPC) was used to determine the lysophospholipase activity of particulate fractions of yeast. This was carried out by the following procedure:

Duplicate 0.5ml reactions were set up in 0.15% w/v CHAPS in PEN buffer (50mM sodium phosphate pH7.8, 0.5mM EDTA, 300mM sodium chloride). Each consisted of 150µg of yeast particulate fractions and the following PLPC concentrations, 1, 0.5, 0.25, 0.125, 0.063 and 0.031mM. Reactions were started by addition of the yeast fraction and incubated at 37°C for 3min, after which the reaction was stopped by addition of 10µl of 1mM methyl arachidonyl fluorophosphonate (MAFP) in DMF. MAFP is a potent inhibitor of lysophospholipase (Wang *et al.*, 1999a) and the most potent known inhibitor of the PV hydrolase activity of NEST (van Tienhoven *et al.*, 2002). For each PLPC concentration, duplicate zero time reactions were also carried out by addition of MAFP prior to the yeast fraction, followed by a 3min incubation. For each PLPC concentration, zero time point values of liberated FFA (as determined below) were subtracted from that of the corresponding 3min incubation.

2.8.9 Determination of liberated free fatty acid

The half-micro free fatty acid determination kit (Roche diagnostics) was used in accordance with the manufacturers instructions. The assay relies on a three-step process where free fatty acid is converted, in the presence of adenosine-5'-triphosphate (ATP), coenzyme A

(CoA) and acyl-CoA synthetase, to acyl-CoA. This then reacts with oxygen in the presence of acyl-CoA oxidase to produce hydrogen peroxide. This reacts with 2,4,6-tribromo-3-hydroxy-benzoic acid (TBHB) and 4-aminoantipyrine in the presence of peroxidase to produce a red dye which can be measured at 546nm (Shimizu *et al.*, 1980).

Known quantities of oleic acid (50, 25, 12.5, 6.3 and 0nmol) were assayed to generate a standard curve, which was used to determine the FFA content of the test samples.

2.8.10 [^{3}H]cAMP binding filter assay

Assays for the binding of [^{3}H]cAMP to yeast particulate fractions were based on the methods of Doskeland and Ogreid (1988) modified to include ammonium sulphate in the binding reaction as suggested by Van Haastert (1985). The procedure was carried out as follows (preliminary experiments were set up as below, with the addition of 40µl of assay buffer in place of the ammonium sulphate):

For the single point assays of yeast particulate fractions and PKA-R1α, duplicate 50µl reactions were set up consisting of 20µl of sample (yeast particulate fractions at 5mg ml^{-1} and/or PKA-R1α) in assay buffer (2M sodium chloride, 1mg ml^{-1} BSA, 40µM IBMX, 0.3% w/v CHAPS, 0.05M sodium phosphate pH6.8) plus 20µl of 80% saturated ammonium sulphate and 1µl of 10mM cold cAMP or assay buffer. 10µl of [^{3}H]cAMP (specific activity 1.3KBq pmol^{-1}) was added to each tube, giving duplicate reactions with a final concentration of 0.4µM [^{3}H]cAMP with or without an excess of unlabelled cAMP. Tubes were incubated for 45min at 30°C after which the reaction was stopped by the addition of 3ml of ice-cold 80% $(NH_4)_2SO_4$. Pre-soaked HAWP filters were placed in a vacuum manifold and washed through with 65% saturated $(NH_4)_2SO_4$. Each reaction was drawn through a HAWP filter after which the reaction tube was rinsed with 2ml of 65% saturated $(NH_4)_2SO_4$ and drawn through again. The filter was then washed twice with 2ml of 65% saturated $(NH_4)_2SO_4$, after which the filters were transferred to scintillation vials containing 1.6ml of 2% w/v SDS and vortexed thoroughly. 10ml of scintillant was added and the tubes were vortexed and counted in a Wallac 1414 liquid scintillation counter for 1min; averaging the result from duplicate reactions.

Assays using a range of [^{3}H]cAMP concentrations were performed exactly as above except duplicate 100µl reactions were set up consisting of 40µl of yeast particulate fractions at 5mg ml^{-1} in assay buffer, plus 40µl of 80% saturated ammonium sulphate and 10µl of 10mM cold cAMP or assay buffer. 10µl of [^{3}H]cAMP (specific activity: 260Bq nmol^{-1}) was added to each tube at a range of dilutions, thereby producing duplicate reactions with a final

concentration of 5, 2.5, 1, 0.5 and 0.1μM [^{3}H]cAMP with or without an excess of unlabelled cAMP.

For each [^{3}H]cAMP concentration, the results in the presence of excess cold cAMP were subtracted from those without. The quantity of bound [^{3}H]cAMP was calculated based on its specific activity.

2.8.11 Reaction with [^{3}H]DFP

Each of the following were added to one of 5 tubes containing 200μl of yeast particulate fraction (adjusted to 2mg ml^{-1} in TE pH8), vortexed and incubated at 37°C for the indicated time: 40μl of 30μM [^{3}H]DFP (20 and 60min), 40μl TE (0, 20 and 60min). Following incubation, tubes were placed on ice and 2×40μl samples were removed from each for duplicate PV hydrolase assays. The inhibition by DFP (as a percentage of the activity of the corresponding TE control) was determined for each incubation. Loss of activity in the absence of an inhibitor was quantified by comparing the activity after 20 and 60min incubations with TE, to that of the zero time point.

40μl of 10% SDS-PAGE sample buffer (300mM Tris-HCl, pH6.8, 10% w/v SDS, 10% v/v glycerol, 10% w/v DTT, 0.01% w/v bromophenol blue) was added to those samples incubated with [^{3}H]DFP. After boiling for 5min, 20μl samples were separated on SDS-PAGE gels for scintillation counting and imaging.

In order to quantify [^{3}H]DFP binding by scintillation counting, duplicate samples were loaded into neighbouring lanes (57μg of sample in a pair of lanes). After coomassie staining the positions of the molecular weight markers were noted and lanes were cut into 3mm slices and placed in scintillation vials, pooling duplicate pairs of lanes. Samples were incubated overnight with 1ml of 0.5M sodium hydroxide to liberate protein-bound tritium, before adding 1ml glacial acetic acid and 10ml of scintillant. Including a blank to determine the background counts, vials were vortexed and counted over 1min using a Wallac 1414 liquid scintillation counter.

For imaging, gels were transferred to a PVDF membrane, the procedure for which was identical to that described for western blotting (see section 2.8.3) with the exception that PVDF required soaking for 1min in methanol prior to transfer. The blot was then stained with 0.25% Coomassie brilliant blue in 50% v/v methanol, 10% v/v acetic acid for 2min and destained briefly in 50% v/v methanol, 10% v/v acetic acid before washing with distilled water and drying between 2 pieces of Whatman 3MM. Imaging was performed by John

Lees (Department of Physics, University of Leicester) using a micro-channel plate detector (Lees and Richards, 1999).

2.9 Confocal and fluorescence microscopy

For confocal imaging of yeast, 5ml cultures were grown to mid log phase (approximately 1×10^7 cells ml^{-1}) using SDgal media, supplemented with the required amino acids and bases. Cultures were harvested by centrifugation at 3,500rpm for 7min and resuspended in 1ml of water. 1% w/v low gelling temperature (LGT) agarose was melted in water and then maintained at 42°C using a heated block. An equal volume of cells and LGT agarose was then combined and spotted onto warmed microscope slides, overlaid with a coverslip and allowed to set before viewing by confocal microscopy. Imaging was conducted by Kul Sikland.

Figure 2.1. PCR mediated gene disruption/tagging

The selectable marker (in this case the KanMX4 module conferring geneticin resistance) is PCR amplified using primers with overhangs homologous to 40bp regions up and downstream of the gene to be disrupted.

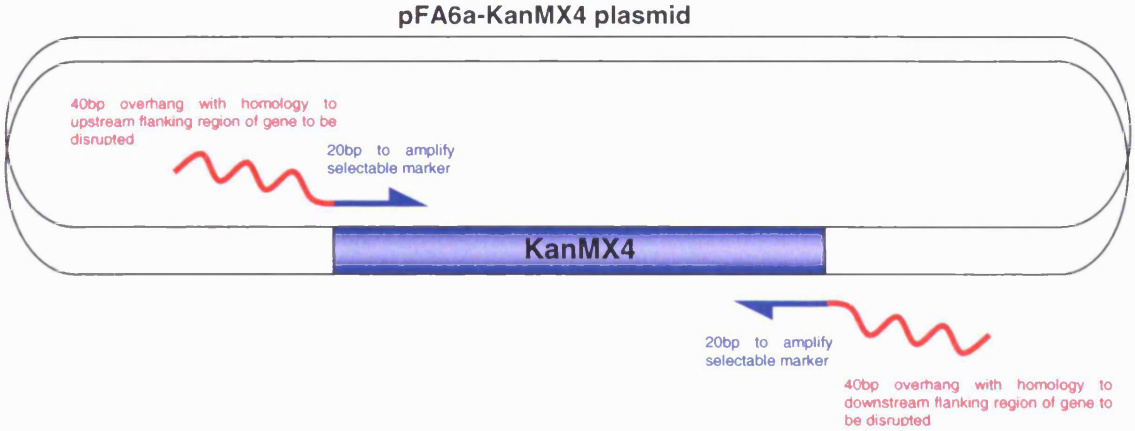

PCR generates a knockout cassette with ends homologous to the flanking regions of the gene to be disrupted.

When transformed into yeast and selected on geneticin containing media, only those cells in which homologous recombination has replaced the targeted gene with the selectable marker will form colonies.

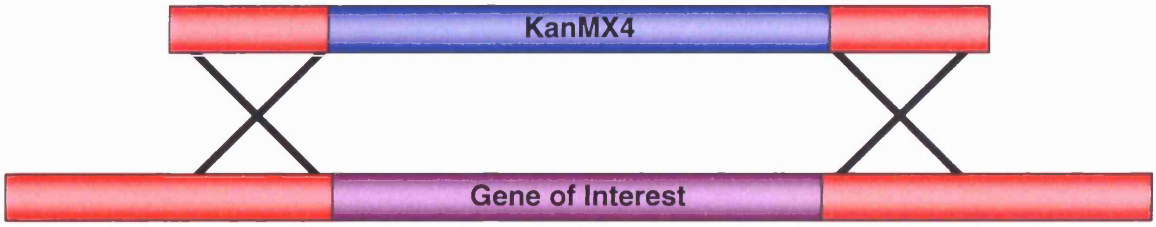

Alternatively nutritional markers can be used in place of the KanMX marker with tranformants being selected with the relevant selective media.

Chapter 3: Genetic Disruption, Overexpression and Fusion Constructs for the Study of *YML059c* and NTE

3.1 Introduction

This chapter describes the generation and confirmation of yeast knockout strains used during this study and the various strategies employed for the overexpression and GFP tagging of *YML059c* and NTE. As will be discussed in detail in Chapter 5, overexpression of Yml059c provided a means of investigating its biochemical properties, with the aim of making a comparison to NTE. GFP tagging also proved useful, not only as a method for subcellular visualisation but also as a convenient tool for determining successful overexpression, both by fluorescence microscopy and western blotting. With the aim of comparing the two proteins directly, attempts were also made to express *YML059c* in mammalian cells and to express NTE in *S.cerevisiae.* The construction of a *BCY1* overexpression plasmid is also described.

3.2 Confirmation of genetic disruption of *YML059c* from the Euroscarf yeast strains

PCR was used to determine that *YML059c* had been correctly disrupted in the MAT 'a', 'α' and 'a/α' diploid yeast strains obtained from Euroscarf. Oligonucleotide primers were designed that would anneal within the *YML059c* gene, within the KanMX4 knockout cassette and within the flanking region of *YML059c*. Reactions were performed using genomic template DNA and diagnostic pairs of primers that would produce amplification products of expected sizes that would indicate either the presence of the wild type *YML059c* gene, or the correctly integrated knockout cassette (see Figure 3.1, for annealing coordinates see Table 2.4).

When genomic DNA from the *yml059c* knockout strains (the haploids BY4741 *yml059cΔ*, BY4742 *yml059cΔ* and the diploid BY4743 *yml059cΔ/Δ*) was used as the template, primer pairs P7-P3 and P4-P16 amplified bands of the expected sizes (747bp and 1022bp respectively) to indicate the successful replacement of *YML059c* with the KanMX4 marker. For these three strains primer pairs P7-P8 and P15-P16 failed to amplify any product, consistent with *YML059c* being absent from this locus. Genomic DNA from the diploid parental strain, BY4743 was used as a control. When the control DNA was the template, primer pairs P7-P8 and P15-P16 produce bands of the expected size (1021bp and 951bp respectively) to show the presence of the wildtype gene. No product was seen when primer pairs P7-P3 and P14-P16 were used. This shows that all bands are specific amplification

products and that each band does confirm the presence of the gene/knockout cassette and the absence of a band confirms the absence of the gene/knockout cassette.

3.3 Genetic disruption of *YML059c* from pseudohyphal competent yeast

PCR mediated gene disruption (Wach *et al.*, 1994) was used to knockout *YML059c* from the pseudohyphal competent strain MW1076/7. Primers KOLYMF and KOYMLR (see Table 2.4) were used to PCR amplify *HIS3MX6* and *TRP1* knockout cassettes from pFA6a-*HIS3MX6* and pFA6a-*TRP1* plasmid DNA. Primers were designed such that each cassette had 40bp of flanking sequence homologous to the regions immediately up and downstream of the start and stop codons of the *YML059c* open reading frame (ORF), allowing exact gene replacement of the entire ORF by homologous recombination (see Figure 2.1). *YML059c* was replaced in the 'a' mating type MW1076 strain with the *HIS3MX6* cassette and replaced in the 'α' mating type strain MW1077 with the *TRP1* cassette, generating MW1076 *yml059cΔ* and MW1077 *yml059cΔ.* These haploid strains were crossed to form a diploid; MW1076/7 *yml059cΔ/Δ*, in which one allele of *YML059c* has been replaced by *HIS3MX6* and the other by *TRP1*.

PCR was used to determine that *YML059c* had been correctly disrupted in these strains. Oligonucleotide primers were used that would anneal within the *YML059c* gene, within the *HIS3MX6* cassette, within the *TRP1* cassette and within the flanking region of *YML059c*. Reactions were performed using genomic template DNA and diagnostic pairs of primers that would produce amplification products of expected sizes that would indicate either the presence of the wild type *YML059c* gene, or the correctly integrated knockout cassette (see Figure 3.2, for annealing coordinates see Table 2.4).

When genomic DNA from the candidate MW1076 *yml059cΔ* knockout strain was used as template, primer pairs P7-P3, P4-P16 and P7-TP1 amplified bands of expected sizes (747bp, 1019bp and 549bp respectively) to indicate the successful replacement of *YML059c* with the *HIS3MX6* cassette. When genomic DNA from the candidate MW1077 *yml059cΔ* knockout strain was used as template, primer pairs P7-TP1 and TP2-P16 amplified bands of expected sizes (549bp and 1512bp respectively) to indicate the successful replacement of *YML059c* with the *TRP1* cassette. Primers P3 and P4 are specific to the *HIS3MX6* cassette and primer TP2 is specific to *TRP1*, therefore the bands produced by P7-P3 and P4-P16 are specific to the *HIS3MX6* cassette and the band produced by TP2-P16 is specific to the *TRP1* cassette. The bands produced by P7-P3, P4-P16, P7-TP1 and TP2-P16 (747bp, 1019bp, 549bp and 1512bp respectively) when the

genomic DNA of the knockout diploid was used as template indicated that both copies of *YML059c* had been replaced; one with *HIS3MX6* and the other with *TRP1*. In the two haploids and the diploid knockout strains primer pairs P7-P8 and P15-P16 failed to amplify any product, consistent with *YML059c* being absent from this locus. Genomic DNA from the diploid parental strain, MW1076/7 was used as a control. When the control DNA was used as template, primer pairs P7-P8 and P15-P16 amplified bands of the expected sizes (1021bp and 951bp respectively) showing the presence of the wildtype gene. No other primer pair produced any specific amplification product, thereby validating those produced with template DNA from the disruption strains. The faint band amplified by primer pair P7-TP1 of approximately 1200bp can be assumed to be non-specific as it was not of the relevant size.

3.4 Cloning of the putative catalytic domain of *YML059c* into an *E.coli* expression vector

A region of *YML059c* (bases +2610 to +4920, relative to the ATG start codon) encompassing that encoding the putative catalytic domain was cloned into the *E.coli* expression vector pET21b such that the reading frame was conserved. When carried in the *E.coli* strain BL21(DE3)pLysS this vector allows high levels of IPTG inducible expression of a cloned gene via a T7 promoter, with the option of including N-terminal T7 and C-terminal 6His epitope tags. Cloning was achieved by amplifying the region of *YML059c* by PCR using BY4741 genomic DNA as template and primers YF2 and SC-R1 (see Table 2.4), incorporated into which were the restriction sites *Sac*I and *Xho*I respectively. These sites were used to clone the PCR product into the unique *Sac*I and *Xho*I sites of the expression vector, generating the plasmid pET-YNEST, encoding the fusion peptide YNEST, with N-terminal T7 and C-terminal 6His tags (see Figure 3.3 for plasmid map).

3.5 Chromosomal constructs for the overexpression and GFP-tagging of *YML059c*

For the overexpression and GFP tagging of Yml059c in yeast, *GAL1* promoter and GFP fusions to *YML059c* were generated in the yeast chromosome using a PCR mediated method (Wach *et al.*, 1997; Longtine *et al.*, 1998) (for an overview see section 2.3.1). The *GAL1* promoter allows inducible expression in yeast, through use of growth media containing galactose as the sole carbon source.

3.5.1 Generation of a C-terminal GFP fusion to Yml059c

A C-terminal GFP fusion to Yml059c was constructed in the chromosome of the diploid yeast strain BY4743 (Wach *et al.*, 1997). A GFP-tagging cassette with *HIS3MX6* selectable

marker was PCR amplified from pFA6a-GFP(S65T)-*HIS3MX6* plasmid DNA, using primers GFPL and GFPR (see Table 2.4). Primers were designed such that the cassette had 40bp of flanking sequence homologous to the region immediately up and downstream of the stop codon of *YML059c*. Homologous recombination would therefore replace the stop codon with the GFP tag and selectable marker, generating BY4743 *YML059c*-GFP/+, with heterozygous C-terminal GFP fusion. The tagging was performed in a diploid strain as their larger size would allow easier viewing under the microscope. With the fusion peptide being expressed using the native *YML059c* promoter the level of expression would indicate the endogenous expression level of *YML059c,* albeit from one allele.

PCR was used to determine that *YML059c* had been successfully GFP tagged. Oligonucleotide primers were used that would anneal within the *YML059c* gene, within the *HIS3MX6* marker and within the flanking region of *YML059c*. Reactions were performed using genomic template DNA and diagnostic pairs of primers that would produce amplification products of expected sizes that would indicate either the presence of the untagged gene, or the correctly integrated GFP fusion cassette (see Figure 3.4, for annealing coordinates see Table 2.4). When genomic DNA from the C-terminal tagged candidate BY4743 *YML059c*-GFP/+ was used as the template, primer pairs P15-P3 and P4-P16 amplified bands of the expected sizes (1233bp and 1019bp respectively) indicating the successful integration of the GFP tag and *HIS3MX6* selectable marker. Primer pair P15-P16 produced two bands (951bp and 3259bp respectively) consistent with the candidate being heterozygous for the GFP fusion; with the smaller fragment amplified from the wildtype allele and the larger product amplified from the successful chromosomal fusion construct. Genomic DNA from the diploid parental strain, BY4743 was used as a control. When the control DNA was the template, primer pairs P15-P16 amplified only the 951bp band and primer pairs P15-P3 and P4-P16 failed to amplify any product. Therefore all bands were specific amplification products indicating the presence or absence of the fusion.

Primer P15 was used to sequence the PCR product amplified from BY4743 *YML059c*-GFP/+ genomic DNA by primer pair P15-P3. This confirmed that the fusion junction was in-frame.

3.5.2 Generation of overexpression constructs of *YML059c* with or without a C-terminal GFP fusion

The *GAL1* promoter was integrated into the yeast chromosome upstream of both wildtype *YML059c* of the diploid strain BY4743 and the GFP fusion of BY4743 *YML059c*-GFP/+, thereby generating the heterozygous diploids BY4743 P_{gal1}-*YML059c*/+ and BY4743 P_{gal1}-*YML059c*-GFP/+, in which Yml059c can be overexpressed with or without a C-terminal GFP

fusion. Each was constructed by amplifying the *GAL1* cassette with KanMX6 selectable marker from pFA6a-KanMX6-P_{gal1} (Longtine *et al.*, 1998) using primers 5GFPL and GALR (see Table 2.4). The primers were designed such that the cassette would carry 40bp of flanking sequence homologous to the 40bp upstream of the *YML059c* ORF and the first 40bp of the coding region, including the ATG start codon. Homologous recombination would therefore introduce the cassette immediately before the ATG start codon of *YML059c* without any deletion of the native sequence (see Figure 2.1).

PCR was used to determine that the cassettes had been successfully inserted. Primers were used that would anneal within the *YML059c* gene, the selectable markers, the GFP tag, the *GAL1* promoter and the flanking region of *YML059c*. Reactions were performed using genomic template DNA and diagnostic pairs of primers that would produce amplification products of expected sizes that would indicate either the presence of the untagged gene, or the correctly integrated cassettes (see Figure 3.5, for annealing coordinates see Table 2.4).

Using genomic DNA from the *GAL1* promoter fusion candidate BY4743 P_{gal1}-*YML059c*/+ as the template, primer pair P3-P8 amplified a band of the expected size (1238bp) indicating the successful integration of the *GAL1* promoter and KanMX6 selectable marker upstream of the *YML059c* ORF. Primer pair P7-P8 produced two bands (1021bp and 3025bp) consistent with the candidate being heterozygous for the promoter fusion; with the smaller fragment amplified from the wildtype allele and the larger product amplified from the successful chromosomal fusion construct. When the template was DNA from the *GAL1* promoter fusion to the previously C-terminally GFP tagged gene, primer pairs P3-P8 and P3-P15 amplified bands to indicate the presence of an upstream *GAL1* promoter and C-terminal GFP tag (1238bp and 1233bp respectively). Primer pairs P7-P8 and P15-P16 each produced two bands (For P7-P8: 1021bp and 3025bp, and for P15-P16: 951bp and 3259bp) consistent with each fusion being heterozygous, with the smaller fragment in each case amplified from the wildtype allele and the larger from the successful fusion. The 5130bp fragment amplified by primer pair GALB-GFPA confirms that both fusions have integrated up and downstream of the same allele, therefore one copy of *YML059c* carries both *GAL1* and C-terminal GFP tag. Genomic DNA from the parental strain BY4743 was used as a control. When the control DNA was the template, only primer pairs P7-P8 and P15-P16 amplified specific products (1021bp and 951bp respectively). The faint band produced by P3-P8 of approximately 3kb can be considered non-specific as it was competed out in the presence of a specific product.

3.5.3 Generation of overexpression constructs of *YML059c* with an N-terminal GFP fusion

An overexpression N-terminal GFP fusion was constructed using the same principle, generating BY4743 P_{gal1}-GFP-*YML059c*/+. A cassette containing the *GAL1* promoter plus GFP tag and *HIS3MX6* marker was PCR amplified from pFA6a-*HIS3MX6*-P_{gal1}-GFP (Longtine *et al.*, 1998) plasmid DNA using primers 5GFPL and 5GFPR. Again the primers were designed so that the flanking sequence of the cassette would allow insertion by homologous recombination of the selectable marker, the *GAL1* promoter and the GFP tag upstream of *YML059c*. This would generate an in-frame N-terminal GFP fusion regulated by the *GAL1* promoter. The resultant heterozygous diploid was induced to undergo meiosis and sporulation. From the resultant haploid products, BY4741 P_{gal1}-GFP-*YML059c* and BY4742 P_{gal1}-GFP-*YML059c* were selected. These were then crossed to form BY4743 P_{gal1}-GFP-*YML059c*/P_{gal1}-GFP-*YML059c*. PCR was carried out using genomic DNA from each strain as template and diagnostic pairs of primers to confirm the constructs (see Figure 3.6, for annealing coordinates see Table 2.4)

Primer pairs P7-P8, P7-P4 and P8-GALB all produced bands of expected sizes (3665bp 667bp and 1263bp respectively) when PCR using genomic DNA from the haploid and homozygous diploid fusion strains was performed. These products confirm the correct insertion of the *GAL1* promoter and GFP tag upstream of *YML059c*. Primer pair P7-P8 failed to detect the successful fusion in genomic DNA from the heterozygote, amplifying only a single band (1021bp) of the size expected from the wildtype allele. However, the amplification products of primer pairs P7-P4 and P8-GALB did indicate a successful fusion (667bp and 1263bp respectively). This strain does therefore carry a heterozygous fusion and perhaps the conditions used allow only the amplification of the smaller product by P7-P8. As a control each reaction was performed using DNA from the diploid parental strain, BY4743. Only primer pair P7-P8 amplified any product (1021bp) confirming the diagnoses of the successful fusions.

3.5.4 Northern and western blots confirm overexpression of *YML059c*

In order to confirm overexpression of *YML059c* at the transcriptional level, northern blot analysis was carried out using RNA obtained from cultures of BY4743, BY4743 P_{gal1}-*YML059c*-GFP/+, BY4743 P_{gal1}-GFP-*YML059c*/+ and BY4743 P_{gal1}-*YML059c*/+ grown using either glucose or galactose as the sole carbon source (see Figure 3.7). As well as hybridising with a specific probe for *YML059c,* a second hybridisation probe for *ACT1* was included as a loading control. With galactose as the sole carbon source an abundant *YML059c* transcript was clearly visible from the overexpression strains after a 4 hour

exposure of the autoradiograph. The open reading frame of those constructs incorporating a GFP fusion is 732bp larger than the wildtype gene. This results in a small but visible increase in transcript size above that of the wildtype length. Since the *ACT1* control confirmed an equal loading, it appeared that the construct with the N-terminal GFP tag expressed *YML059c* at approximately double the level of that with a C-terminal or no GFP tag. Perhaps the inclusion of an N-terminal fusion stabilised the message? A 96 hour exposure was required to detect the endogenous transcript in the parental strain, confirming that this ORF is indeed expressed, albeit at a low level. A *YML059c* transcript of similar abundance was visible in the overexpression strains under the non-inducing glucose conditions. Being of wild type length these transcripts must be from the wild type allele present in these heterozygous strains rather than any leaky expression of the ORF under control of the *GAL1* promoter. This demonstrates the tight transcriptional regulation of this overexpression system.

Western blot analysis was used to confirm the presence of the Yml059c polypeptide in the overexpression strains. Particulate fractions of BY4743, BY4743 P_{gal1}-*YML059c*-GFP/+ and BY4743 P_{gal1}-GFP-*YML059c*/P_{gal1}-GFP-*YML059c* were subjected to western blot analysis using an anti-GFP antibody. A polypeptide of the predicted size of GFP-tagged Yml059c (214kDa) was detected in strains expressing either the C or N terminally tagged protein, with the homozygous N-terminal fusion expressed greater than 2-fold above the C-terminally tagged heterozygote (see Figure 3.8). This product was not detected in the parental strain. The GFP-antibody binds to a variety of smaller polypeptides in the extracts obtained from the homozygous N-terminally tagged strain, and to a lesser extent in the C-terminally tagged heterozygote. These smaller products were not detected in the parental strain and therefore must represent degradation of the full-length polypeptide. For the N-terminally tagged protein these smaller bands may also be the products of incomplete translation.

3.6 Plasmid constructs for the expression of *YML059c* and NTE

Various constructs for plasmid based overexpression of Yml059c and NTE were generated. These included strategies for expressing NTE in yeast and Yml059c in mammalian cells.

3.6.1 *YML059c* was cloned into the constitutive yeast expression vector pG3

pG3 is a 2-μm based yeast expression plasmid that allows the constitutive overexpression of a cloned gene via the glyceraldehyde-3-phosphate dehydrogenase (GDP) promoter (Bitter and Egan, 1984). Translation initiation is dependent upon the ATG start codon of the cloned ORF and termination either via the cloned gene's own stop codon or a cluster of

termination codons in all three reading frames immediately downstream of the polylinker. Using BY4741 genomic DNA as template, the whole *YML059c* open reading frame was amplified by PCR and cloned into pG3, generating pG3-*YML059c*. The PCR reaction was performed using primers YML5 and YML3, which incorporated the restriction sites *Bcl*I and *Xho*I respectively (see Table 2.4). These sites enabled *YML059c* to be inserted downstream of the GDP promoter, between *BamH*I and *Sal*I sites (see Figure 3.9 for plasmid map).

3.6.2 NTE and *YML059c* were cloned into the yeast expression vector pEMBLyex4

Both *YML059c* and NTE were cloned into pEMBLyex4 generating pEMBL-*YML059c* and pEMBL-NTE. pEMBLyex4 is a 2-μm based yeast expression plasmid that allows the inducible expression of a cloned gene via a galactose regulated promoter. The promoter is a hybrid consisting of 365bp of the intergenic region between the yeast genes *GAL1* and *GAL10*, and 250bp of the 5' untranslated region of the yeast gene *CYC1* (Baldari and Cesareni, 1985). As with pG3 no translation start codon is present and must be included in the cloned gene.

For pEMBL-*YML059c* the complete ORF was again amplified using primers YML5 and YML3 from BY4741 genomic DNA and cloned between *BamH*I and *Sal*I sites, inserting the ORF downstream of the promoter. pEMBL-NTE was constructed by excising NTE from pTARGET-NTE with *BamH*I, ligating into the *BamH*I site of pEMBLyex4 and restriction mapping to ensure the correct orientation (see Figure 3.10 for plasmid maps).

Northern blot analysis was used to determine whether *YML059c* was successfully transcribed using this system. A northern blot was performed using RNA recovered from cultures of BY4743, BY4743 P_{gal1}-GFP-*YML059c*/+, BY4743 + pEMBLyex4 and BY4743 + pEMBL-*YML059c* grown in media containing galactose as the sole carbon source. This would allow a comparison between the pEMBLyex4 plasmid based system and an overexpressing chromosomal construct. After a 5 hour exposure both the chromosomal and pEMBLyex4 based overexpression system are shown to express an abundant *YML059c* transcript that is not detected in the parental strain or vector only control. The inclusion of a GFP tag in the BY4743 P_{gal1}-GFP-*YML059c*/+ can be seen to confer a slight increase in the *YML059c* transcript size. Allowing for an unequal loading, as represented by the intensity of *ACT1* transcript, each system produces approximately equal levels of *YML059c* transcript (see Figure 3.11).

3.6.3 NTE was cloned into the yeast expression vectors pYES2/CT and pYC2/CT

NTE carrying a C-terminal GFP tag was cloned into the yeast 2-μm based expression vector pYES2/CT and the centromeric pYC2/CT. Both pYES2/CT and pYC2/CT allow overexpression of a cloned gene via the galactose inducible *GAL1* promoter. Each carries tags allowing a C-terminal V5 epitope and concomitant 6His fusion. Again the cloned gene must possess its own ATG start codon.

The NTE-GFP fusion was excised from pEGFP-NTE with *EcoR*I and *Not*I and cloned into the unique *EcoR*I and *Not*I sites of pYC2/CT and pYES2/CT, generating pYC2/CT-NTE-GFP and pYES2/CT-NTE-GFP. In each case a stop codon was introduced so that the resultant polypeptide would carry a GFP fusion but not the V5 or 6His tags (see Figure 3.12 for plasmid map).

No fluorescence could be detected in yeast cultures carrying one of three independent clones of pYC2/CT-NTE-GFP or pYES2/CT-NTE-GFP constructs (data not shown) and western blot analysis using an anti-GFP antibody failed to detect any polypeptide (see Figure 3.13). These constructs therefore failed to translate a stable protein product.

3.6.4 Plasmid based overexpression systems generated by transfer of chromosomal *YML059c* overexpression constructs to a yeast cloning vector

As an alternative method of producing plasmid based overexpression systems, chromosomal *YML059c* constructs were amplified by PCR and cloned into the centromeric yeast cloning vector pRS416 (Brachmann *et al.*, 1998). PCR amplification of the chromosomal constructs was performed using primers GALYMLF and GALYMLR (see Table 2.4) and genomic DNA from BY4743 P_{gal1}-*YML059c*/+ and BY4743 P_{gal1}-GFP-*YML059c*/+ as template. The forward primer, GALYMLF, amplifies from 2bp upstream of the *Bgl*II site that marks the start of the *GAL1* promoter. The reverse primer, GALYMLF, anneals immediately after the stop codon of *OGG1* (the next downstream ORF on the opposite strand) thereby including the 219bp region between *YML059c* and *OGG1*. This ensured inclusion of the entire transcriptional terminator. Incorporated into the primers were the restriction sites *Sac*I and *Xho*I respectively. This allowed the PCR products to be ligated into the *Sac*I and *Xho*I sites of pRS416, generating pRS416-P_{gal1}-*YML059c* and pRS416-P_{gal1}-GFP-*YML059c* (see Figure 3.14 for plasmid maps).

3.7 The putative active site serine was disrupted by site directed mutagenesis

The putative active site serine of *YML059c* in the plasmid pRS416-P_{gal1}-GFP-*YML059c* was mutated using the QuikChange site directed mutagenesis strategy (Stratagene). The principle was to design complementary oligonucleotide primers that spanned the region encoding the active site serine. The primers used, S1406AF and S1406AR (see Table 2.4) were identical to the native plasmid sequence of this region except for a single base alteration that would make a T to G transversion of base 4216 of the *YML059c* ORF. Thermal cycling with a proof-reading polymerase was used to generate mutated plasmid DNA with staggered single-stranded nicks. As non-mutated plasmids would be methylated they were removed by treating with the endonuclease *Dpn*I that specifically cleaves methylated and hemimethylated DNA. Finally the successfully mutated plasmid DNA was transformed into *E.coli* XL-1 Blue in which the single-stranded nicks are repaired (see Figure 3.15). The resultant point mutation altered codon 1406 from TCG to GCG causing a serine to alanine point mutation generating pRS416-P_{gal1}-GFP-*YML059c*(S1406A). Successful mutagenesis was confirmed by sequencing across the relevant region using the sequencing primer SERSEQ (see Table 2.4).

Yeast containing either the S1406A mutation or the wildtype overexpression construct possess equivalent levels of Yml059c polypeptide, as determined by GFP fluorescence levels in live cells (see Figure 5.10) and anti-GFP western blotting of particulate fractions (see Figure 3.16).

3.8 Expressing Yml059c in mammalian cells using pEGFP-N1

NTE has been overexpressed in mammalian cells in a functional form using pEGFP-NTE; NTE cloned into the mammalian expression vector pEGFP-N1 (Li *et al.*, 2003). This vector allows the expression of a cloned gene with a C-terminal GFP fusion, driven from the cytomegolovirus immediate early promoter (P_{CMVIE}). The GFP tag encoded by this vector carries various mutations for efficient expression and enhanced fluorescence in mammalian cells.

YML059c was cloned into the mammalian expression vector pEGFP-N1. The *YML059c* ORF was amplified by PCR using BY4741 genomic DNA as template and primers YML3.3 and YML5.3 (see Table 2.4). Incorporated into these primers were the restriction sites *Kpn*I and *Sac*I respectively. These sites were used to clone the PCR product into the unique *Kpn*I and *Sac*I sites of pEGFP-N1, generating pEGFP-*YML059c.* The PCR primers were designed so as to produce a peptide with an in-frame C-terminal GFP fusion (see Figure

3.17 for plasmid map). No fluorescence was detectable in COS-7 or Hela cells transiently transfected with pEGFP-*YML059c* (see Figure 3.19). Western blot analysis using an anti-GFP antibody failed to detect any Yml059c polypeptide in microsomes of COS-7 or Hela cells carrying pEGFP-*YML059c*. This indicates that Yml059c was not successfully expressed in this system.

3.9 Overexpression of *BCY1* in yeast

Overexpression of the yeast gene *BCY1* was achieved by cloning into the galactose inducible centromeric yeast expression vector pYC2/CT. *BCY1* was amplified using BY4741 genomic DNA as template and primers BCYF and BCYR, incorporated into which were the restriction sites *Hind*III and *Eco*RI respectively (see Table 2.4). This allowed cloning of the PCR product into the unique *Hind*III and *Eco*RI sites of pYC2/CT, generating pYC2/CT-*BCY1* with C-terminal V5 epitope and 6His fusion (see Figure 3.20 for plasmid map).

The expression level of *BCY1* using this system was determined by northern blot analysis of RNA obtained from BY4743 + pYC2/CT and BY4743 carrying one of 3 independent clones of pYC2/CT-*BCY1* (see Figure 3.21). Although the endogenous level is just detectable after a 2 hour exposure of the autoradiograph, each of the 3 clones clearly confer a significant increase in *BCY1* transcription. The increase in transcript size due to the inclusion of epitope tags is also visible. As a control *ACT1* was also probed, confirming approximately equal loading in each lane.

3.10 Discussion

In this chapter, the successful genetic knockout of *YML059c* from a BY yeast strain and the pseudohyphal competent strain MW1076/7 has been described. Although Southern blot analysis (Southern, 1975) would have further confirmed the gene disruption, the PCR methods used have been sufficiently rigorous to leave no doubt as to the success of the knockouts.

All chromosomal *YML059c* fusions were initially constructed in diploid yeast, creating heterozygotes. The exceptionally poor sporulation efficiency of the BY yeast strain series hampered the generation of haploid fusion strains by sporulation. This was only achieved for the N-terminal P_{gal1}-GFP fusion, for which haploid fusion strains were produced and mated to generate a homozygous diploid. If other haploid or homozygous diploid fusions were needed, further rounds of PCR mediated manipulation would have proved less time consuming.

Fusion of the *GAL1* promoter to *YML059c* in the chromosome clearly allowed induction of increased expression levels, both in terms of its transcript and polypeptide. This increase in polypeptide is maintained in plasmid-based systems generated by transfer of a chromosomal construct to a centromeric yeast cloning vector. Expression of Yml059c from the galactose inducible promoter of pEMBlyex4 also effectively raised the transcriptional level of Yml059c. However, without epitope tags or antibodies raised to the protein no information as to polypeptide level could be gained.

Attempts to express NTE in yeast using pYES2/CT and pYC2/CT failed to produce a detectable polypeptide, as did attempts to express Yml059c in COS-7 and Hela cells. Although no expression data were obtained, NTE was not expressed in a functional form using the pEMBLyex4 vector (see section 5.3.2). Despite a high degree of sequence similarity the two proteins appear to be insufficiently homologous to allow stable expression in such evolutionarily diverse systems. Northern blot analysis could be used to determine whether the failure in expression was before or after transcription.

As described in Chapter 5, only overexpression of Yml059c from the chromosomal constructs and constructs generated by the transfer of chromosomal fusions to plasmids, resulted in the production of an enzyme with any detectable biochemical activity. It is unclear as to why no enzymatic activity was detected when Yml059c was expressed using pG3 or pEMBLyex4, particularly as yeast carrying pEMBL-*YML059c* could be induced to transcribe an abundant *YML059c* mRNA. It may be possible that the high copy number of these 2-μm based plasmids led to excessively high protein expression that forms inactive aggregates. However, the level of transcription from pEMBlyex4 was approximately equal to that of the chromosomal systems, making this seem unlikely.

An alternative method of disrupting the putative active site serine of Yml059c would have been to alter the chromosomal overexpression constructs using the deleto perfeto method of *in vivo* site directed mutagenesis (Storici *et al.*, 2001)

Figure 3.1. PCR confirmation of replacement of *YML059c* with KanMX4 knockout cassette

PCR was performed using genomic DNA from the parental strain and the strains in which *yml059c* has been disrupted with the KanMX cassette. Primer pairs were designed that would indicate the successful replacement of *YML059c*. **A.** Predicted annealing positions of diagnostic primers are indicated with arrows. For a given outcome the expected sizes of amplification products are shown for each primer pair. **B.** Products were visualised by agarose gel electrophoresis. Each lane shows the PCR products amplified by the indicated primer pair, using template genomic DNA from the strain marked above the group of lanes. In this case '*yml059cΔ*' denotes an allele in which *YML059c* has been replaced by the KanMX4 cassette. The sizes (in bp) of DNA markers are indicated.

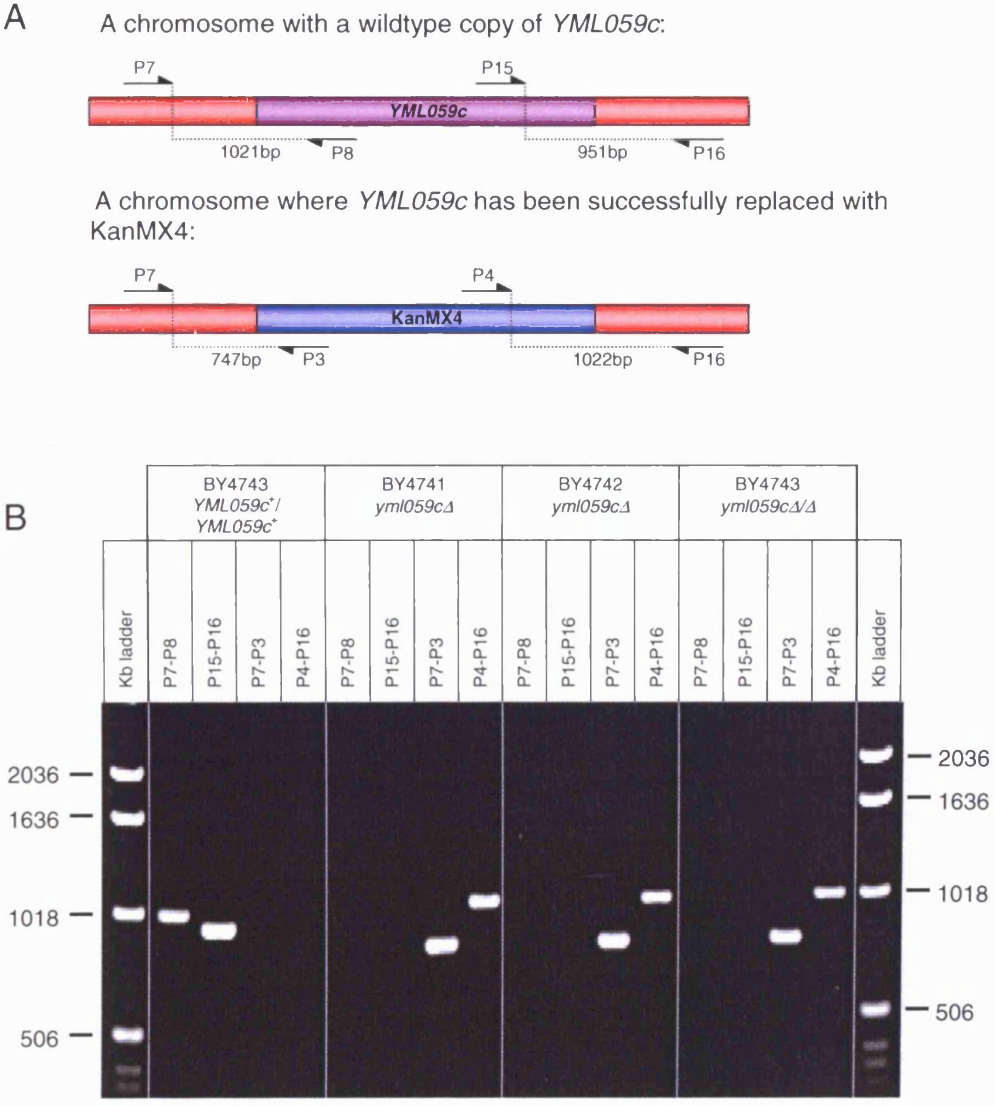

Figure 3.2. Annealing of diagnostic primers and predicted PCR product sizes for confirmation of replacement of *YML059c* with *HIS3MX6* and *TRP1* knockout cassettes

PCR was performed using genomic DNA from parental and potential *yml059c* disrupted strains as template. Primer pairs were designed that would indicate the successful replacement of *YML059c*. **A.** Predicted annealing positions of diagnostic primers are indicated with arrows. For a given outcome the expected sizes of amplification products are shown for each primer pair. **B.** Products were visualised by agarose gel electrophoresis. Each lane shows the PCR products amplified by the indicated primer pair, using template genomic DNA from the strain marked above the group of lanes. The knockout cassette used to generate the disruptant is indicated in parentheses. The sizes (in bp) of DNA markers are indicated.

A

A chromosome with a wildtype copy of *YML059c*:

A chromosome where *YML059c* has been successfully replaced with *HIS3MX6*:

A chromosome where *YML059c* has been successfully replaced with *TRP1*:

B

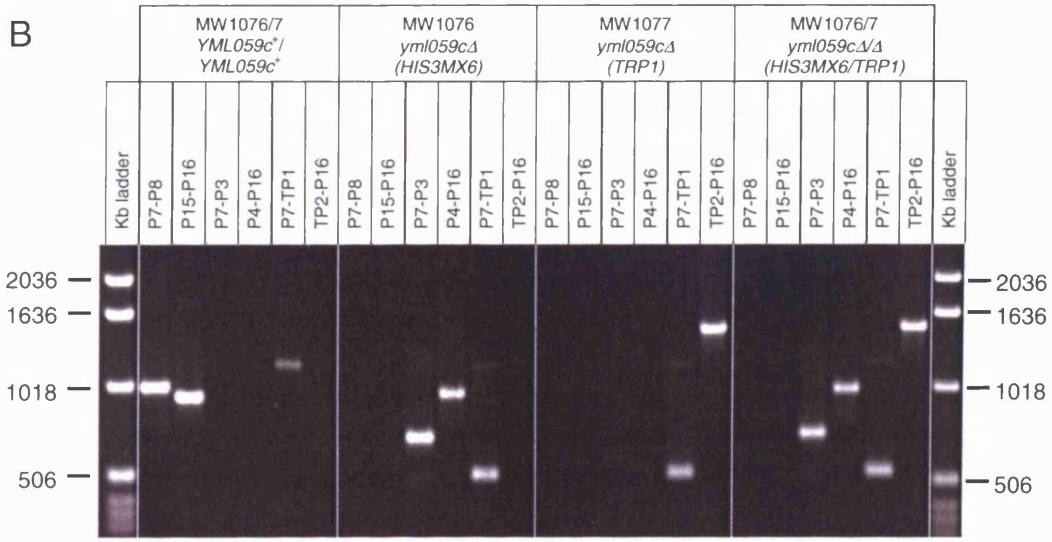

Figure 3.3. Plasmid map of pET-YNEST

Plasmid map showing the features of the *E.coli* expression plasmid pET-YNEST. The in frame N-terminal T7 tag and C-Terminal 6His tag have not been shown. Base pair coordinates are shown in parentheses.

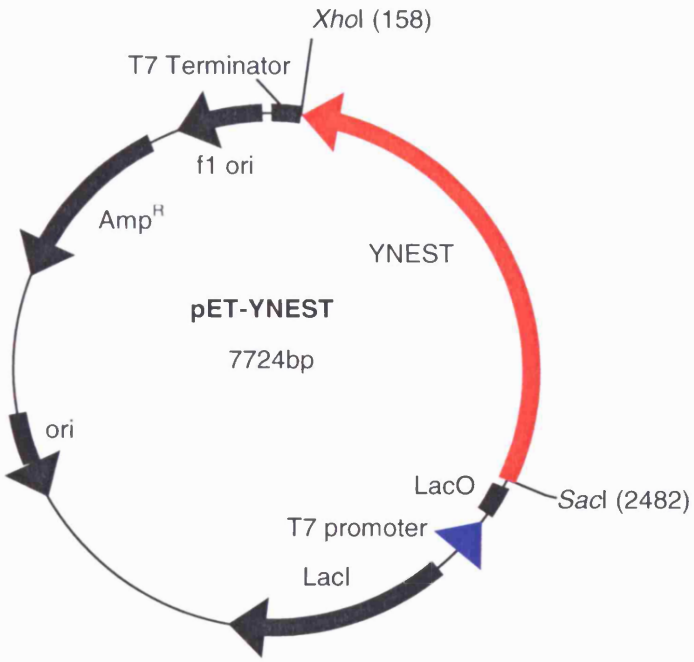

Figure 3.4. PCR confirmation of GFP fusion to 3' end of *YML059c*

PCR was performed using genomic DNA from parental and potential C-terminal *YML059c* GFP fusion strains. Primer pairs were designed that would indicate the successful tagging of *YML059c*. **A.** Predicted annealing positions of diagnostic primers are indicated with arrows. For a given outcome the expected sizes of amplification products are shown for each primer pair. **B.** Products were visualised by agarose gel electrophoresis. Each lane shows the PCR products amplified by the indicated primer pair, using template genomic DNA from the strain marked above the group of lanes. The sizes (in bp) of DNA markers are indicated.

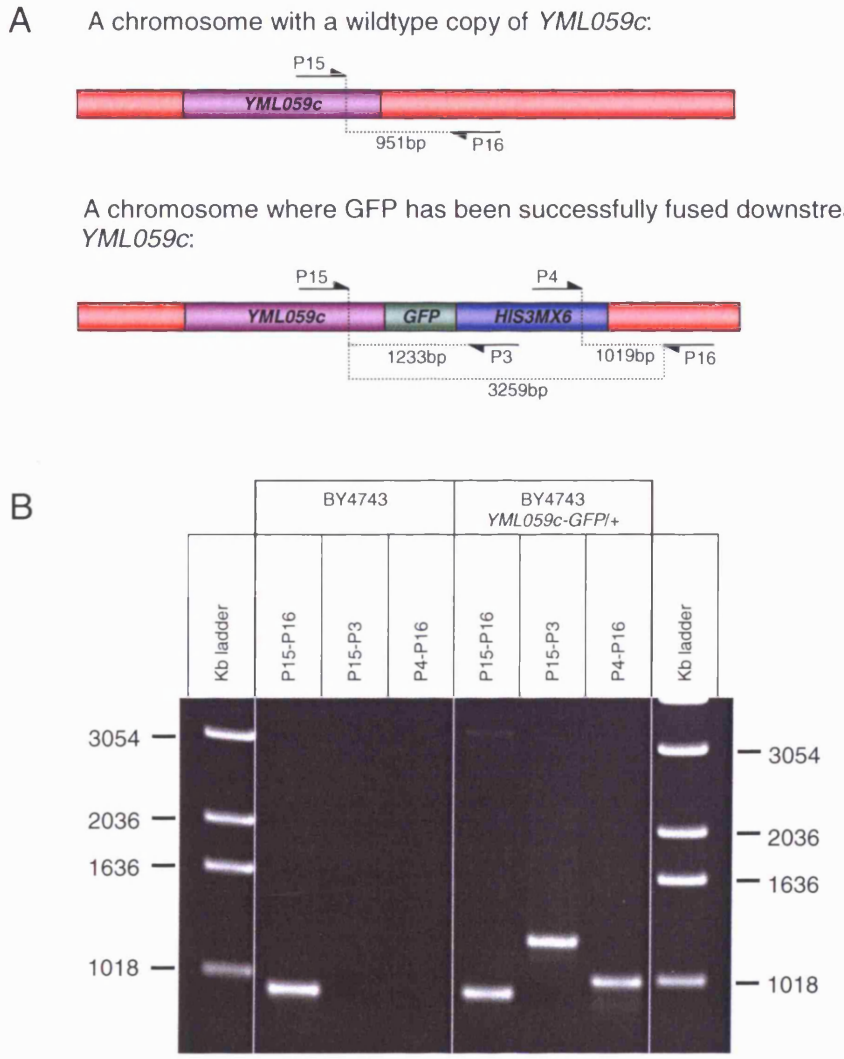

Figure 3.5. PCR Confirmation of insertion of *GAL1* promoter upstream of *YML059c* with or without C-terminal GFP tag

PCR was performed using genomic DNA from parental and potential *GAL1* promoter fusion strains. Primer pairs were designed that would indicate the successful promoter insertion upstream of *YML059c*. **A.** Predicted annealing positions of diagnostic primers are indicated with arrows. For a given outcome the expected sizes of amplification products are shown for each primer pair. **B.** Products were visualised by agarose gel electrophoresis. Each lane shows the PCR products amplified by the indicated primer pair, using template genomic DNA from the strain marked above the group of lanes. Part of the image has been overexposed so as to make faint bands more visible. The sizes (in bp) of DNA markers are indicated.

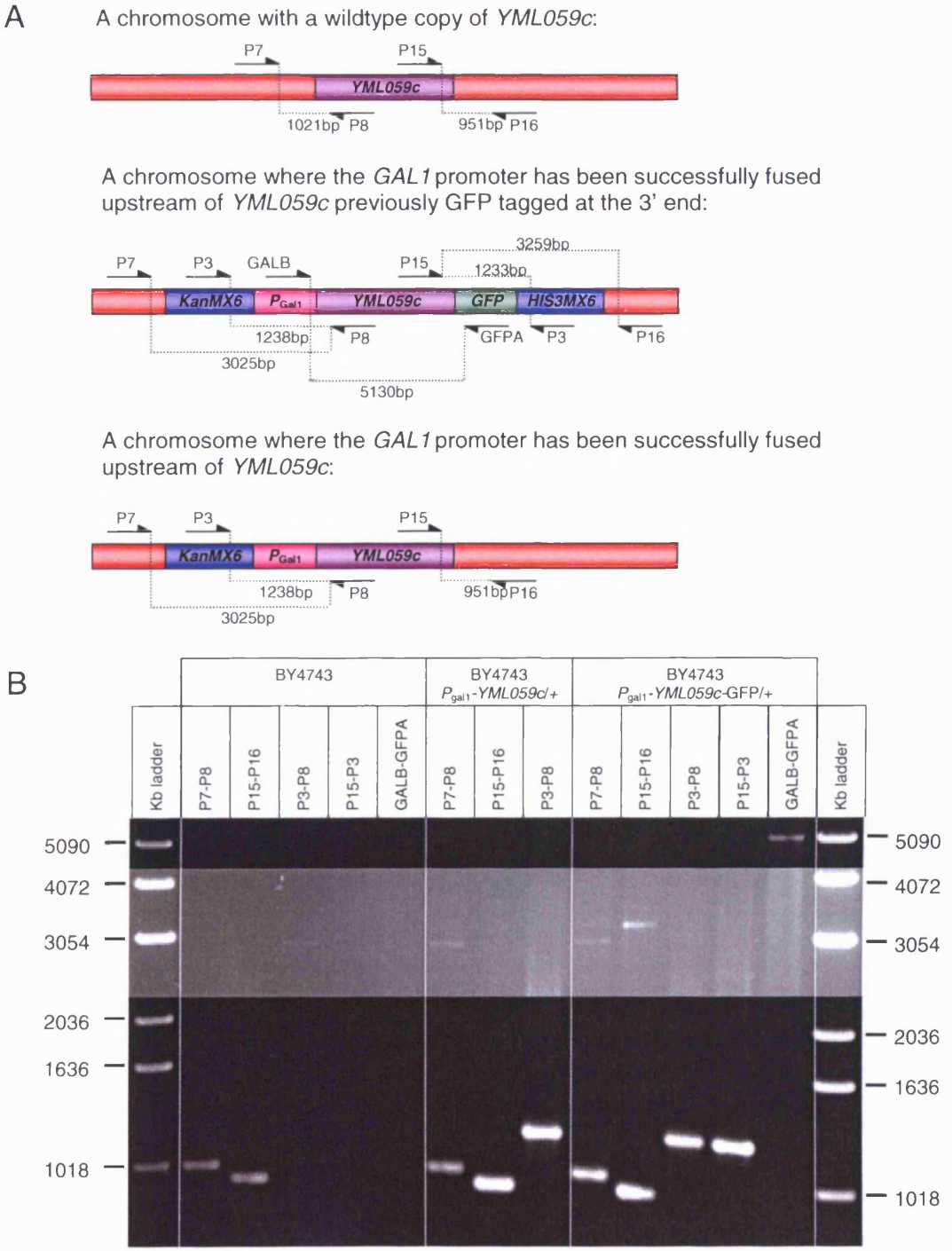

Figure 3.6. Annealing of diagnostic primers and predicted PCR product sizes for confirmation of insertion of *GAL1* promoter and concomitant GFP tag upstream of *YML059c*

PCR was performed using genomic DNA from parental and potential *GAL1* promoter plus GFP tag fusion strains. Primer pairs were designed that would indicate the successful insertion upstream of *YML059c*. **A.** Predicted annealing positions of diagnostic primers are indicated with arrows. For a given outcome the expected sizes of amplification products are shown for each primer pair. **B.** Products were visualised by agarose gel electrophoresis. Each lane shows the PCR products amplified by the indicated primer pair, using template genomic DNA from the strain marked above the group of lanes. The sizes (in bp) of DNA markers are indicated.

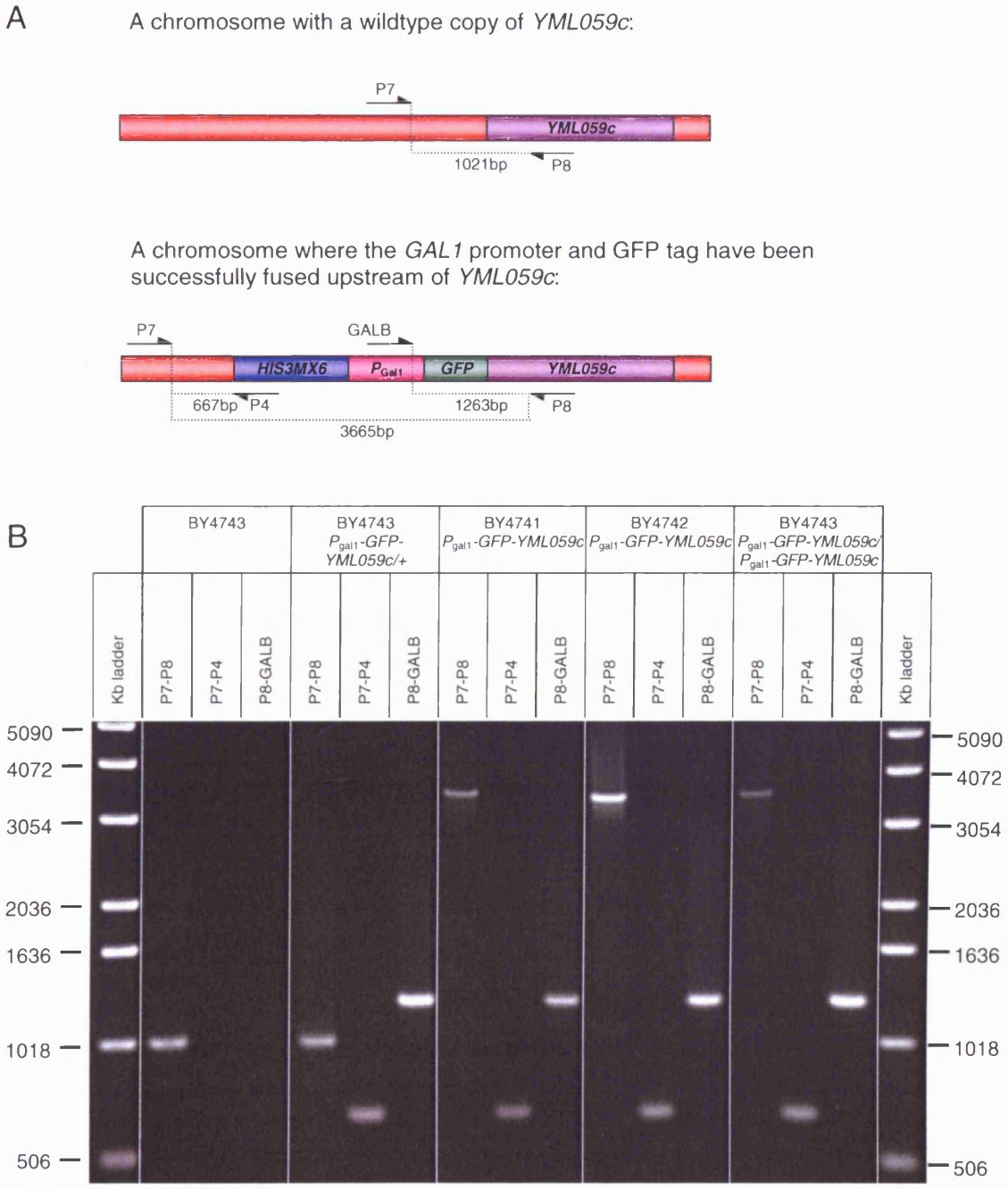

Figure 3.7. Northern blot showing high levels of *YML059c* transcript in chromosomal overexpression constructs

Northern blot analysis was carried out using RNA obtained from the strains indicated above each lane, with cultures having been grown using either glucose or galactose as carbon source. Two probes were used, one for *YML059c* and a second for *ACT1* to be used as a loading control. The size (in kilobases) and position of RNA markers is indicated.

The boxed area shows a 96 hour exposure; the remaining autoradiograph shows a 4 hour exposure after which time no transcript was visible within the boxed section.

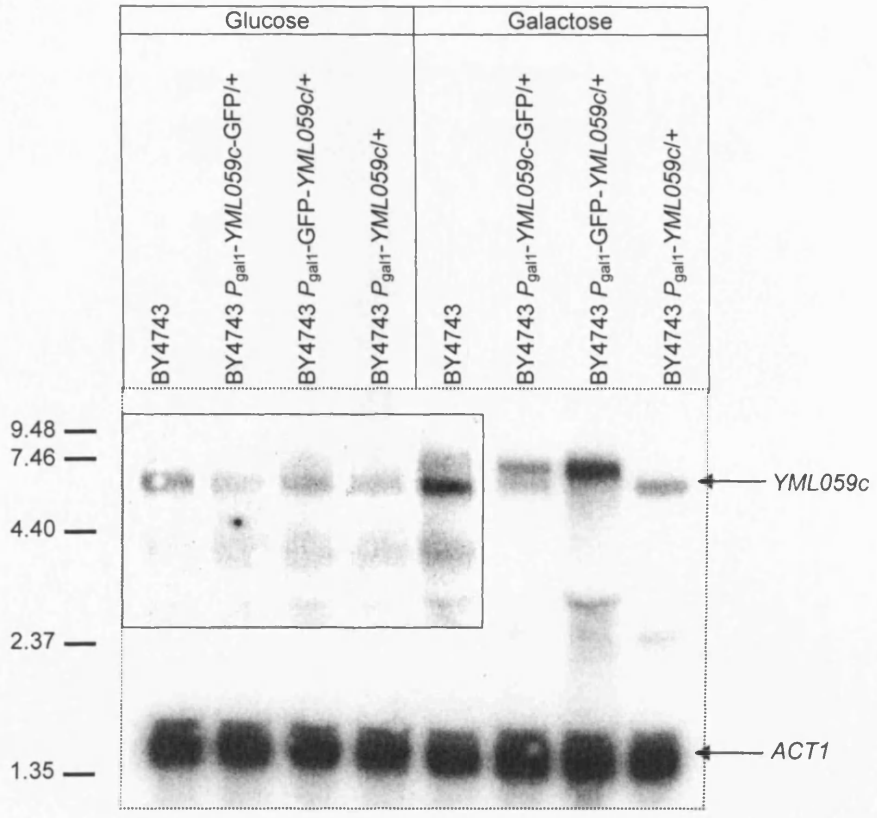

Figure 3.8. Western blot showing overexpression of GFP-tagged Yml059c

Western blot analysis using an anti-GFP antibody shows the presence of a full length (214kDa) in both N and C terminally tagged Yml059c overexpression strains. In each case a number of smaller products are also present.

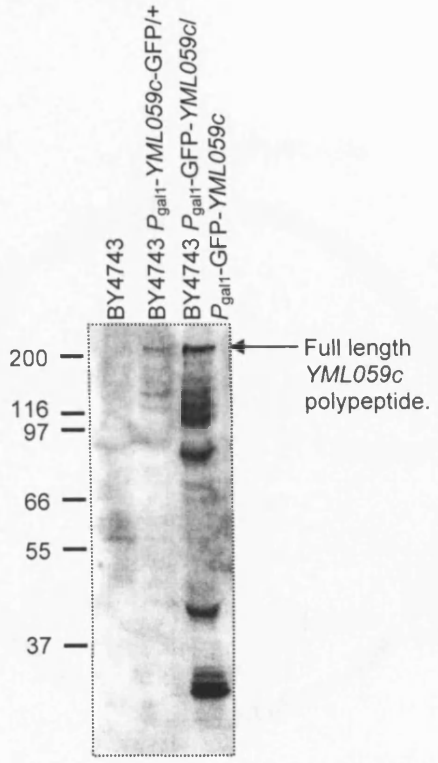

Figure 3.9. Plasmid map of pG3-*YML059c*

A plasmid map showing the features of the 2µm based constitutive yeast expression construct pG3-*YML059c*. Base pair coordinates (in parentheses) and total plasmid size are only approximate. Note that *Bam*HI and *Sal*I sites have been lost due to ligation with *Bcl*I and *Xho*I ends respectively.

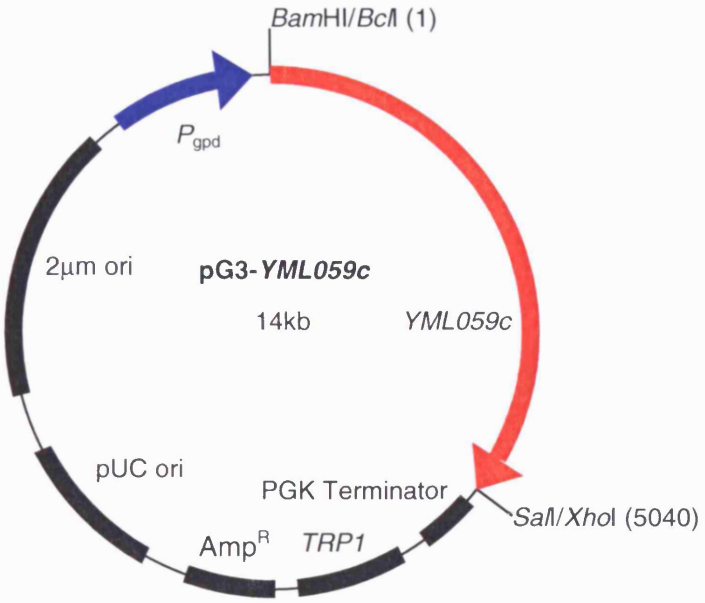

Figure 3.10. Plasmid maps of pEMBL-*YML059c* and pEMBL-NTE

Plasmid maps showing the features of the galactose regulatable 2µm base yeast expression constructs pEMBL-*YML059c* and pEMBL-NTE. Base pair coordinates (in parentheses) and total plasmid size are only approximate.

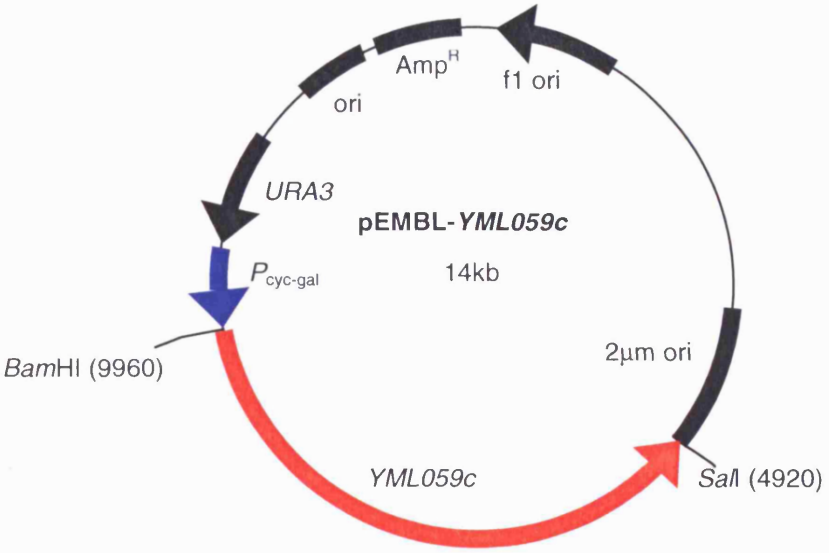

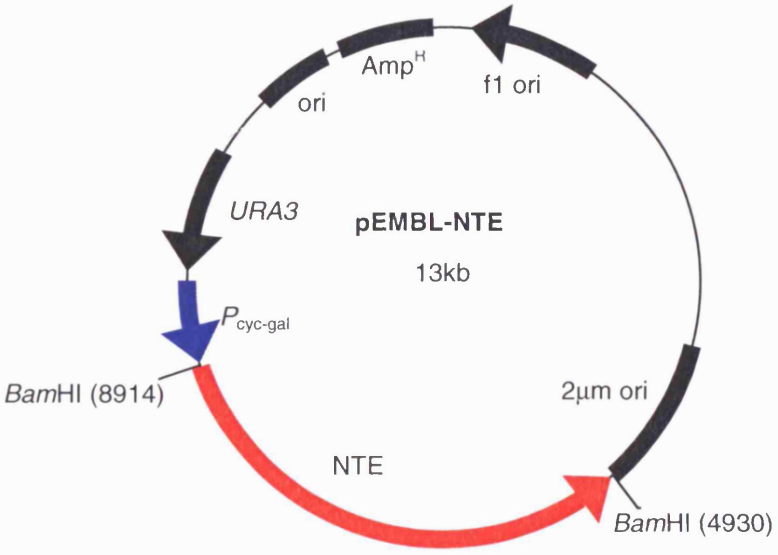

Figure 3.11. Northern blot comparing *YML059c* transcript levels from yeast carrying pEMBL-*YML059c* and the chromosomal overexpression strain BY4743 P_{gal1}-GFP-YML059c/+

Northern blot analysis of RNA obtained from the strains indicated above each lane, probing for the *YML059c* and *ACT1* transcripts. The size (in nucleotides) and position of RNA markers is indicated. The transcripts attributable to *YML059c* and *ACT1* after a 5 hour exposure are indicated.

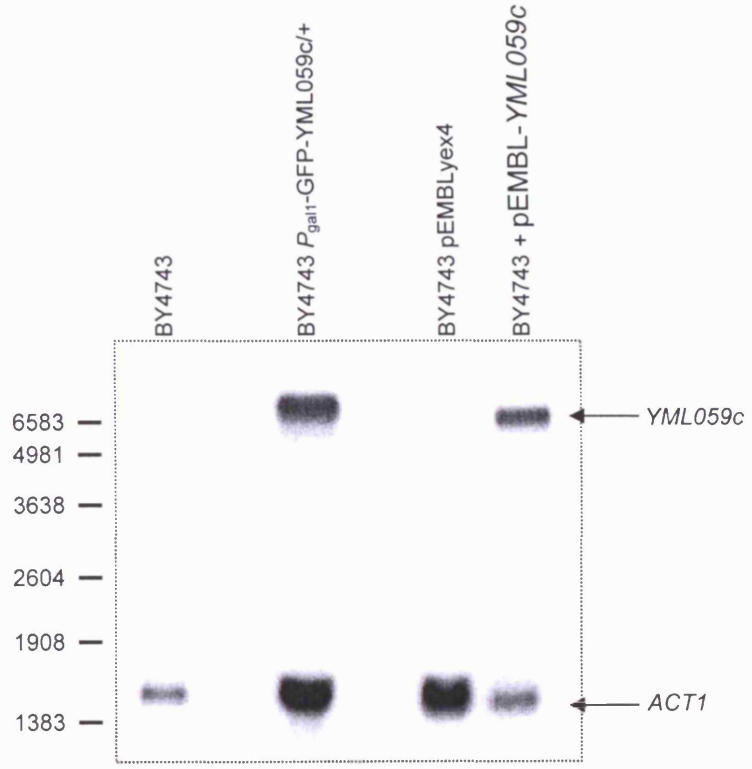

Figure 3.12. Plasmid maps of pYC2/CT-NTE-GFP and pYES2/CT-NTE-GFP

Plasmid maps showing the features of the centromeric yeast expression construct pYC2/CT-NTE-GFP and the 2µm based yeast expression construct pYES2/CT-NTE-GFP for the regulatable expression of GFP-tagged NTE. Base pair coordinates are shown in parentheses.

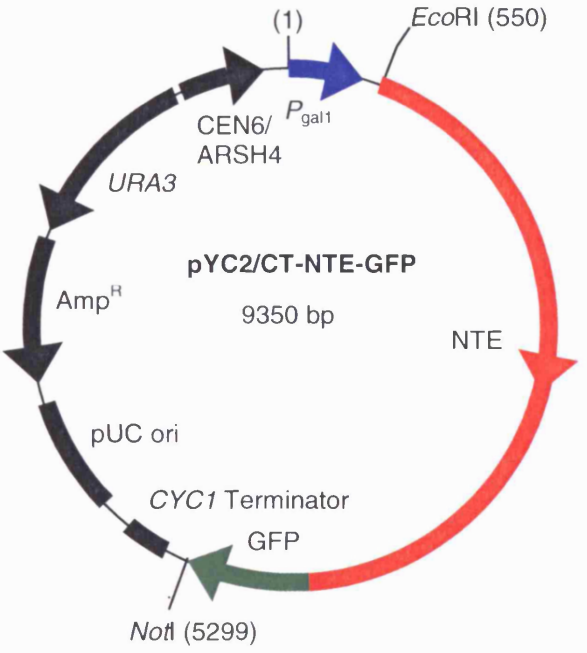

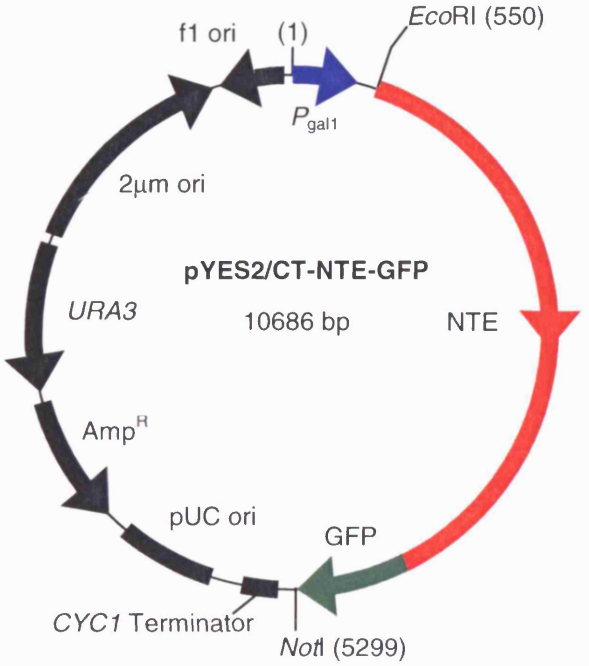

Figure 3.13. Western of NTE expressed in yeast

Western blot analysis using an anti-GFP antibody fails to detect an NTE polypeptide in particulate fractions of yeast carrying pYC2/CT-NTE-GFP or pYC/CT-NTE-GFP clones. Yeast overexpressing GFP-Yml059c was included as a positive control. The positions and sizes (kDa) of molecular weight markers are indicated.

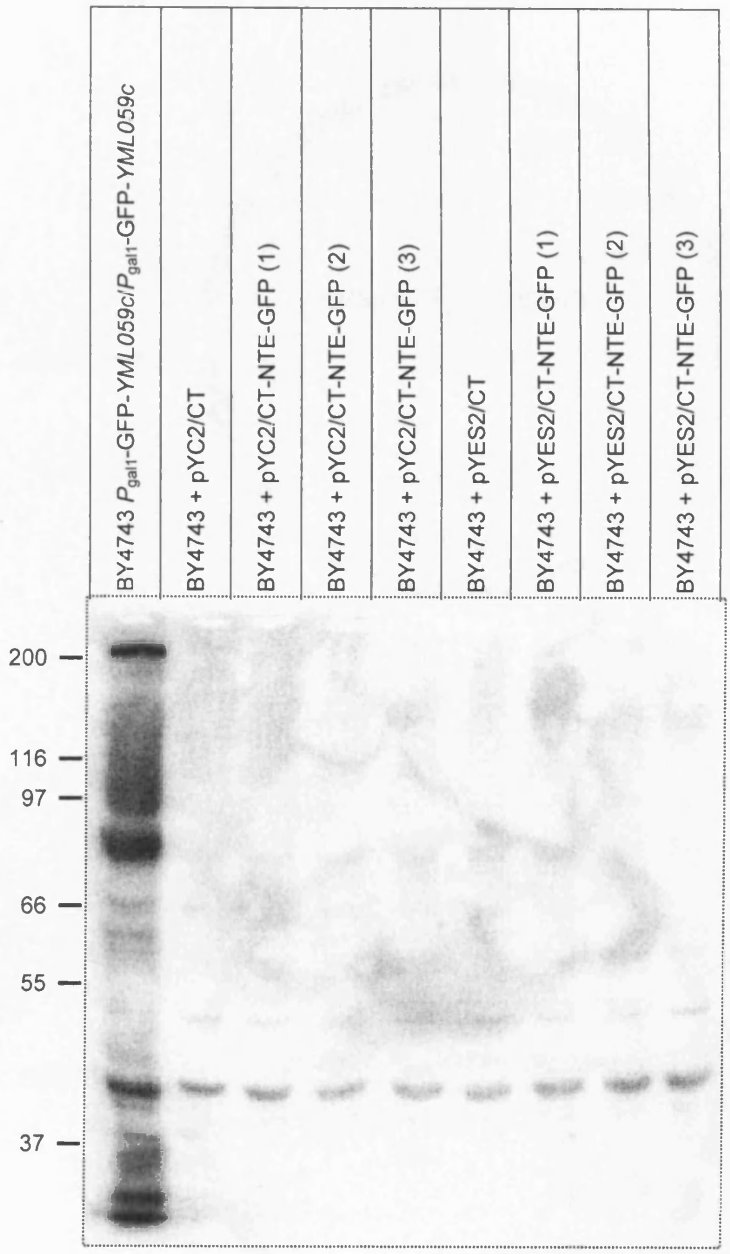

Figure 3.14. Plasmid maps of pRS416-P_{gal1}-*YML059c* and pRS416-P_{gal1}-GFP-*YML059c*

Plasmid maps showing the features of the galactose regulated centromeric yeast expression vectors pRS416-P_{gal1}-*YML059c* and pRS416-P_{gal1}-GFP-*YML059c*. 'Terminator' denotes the downstream region of *YML059c* presumed to contain the transcriptional terminator. Base pair coordinates are shown in parentheses.

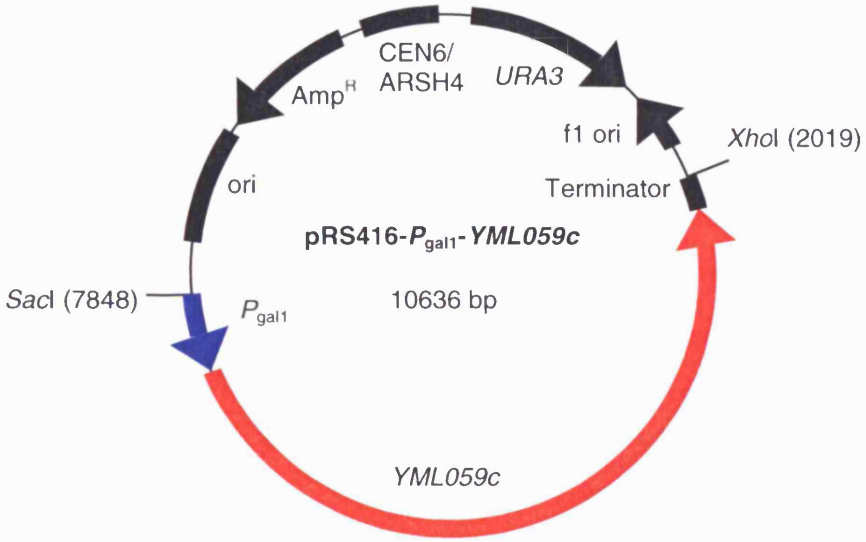

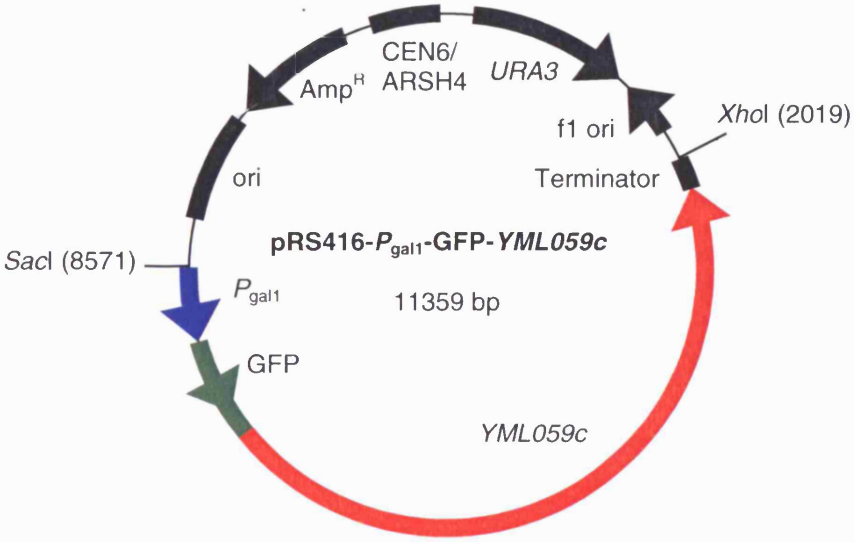

Figure 3.15. Site directed mutagenesis

Schematic showing the QuikChange strategy for site directed mutagenesis.

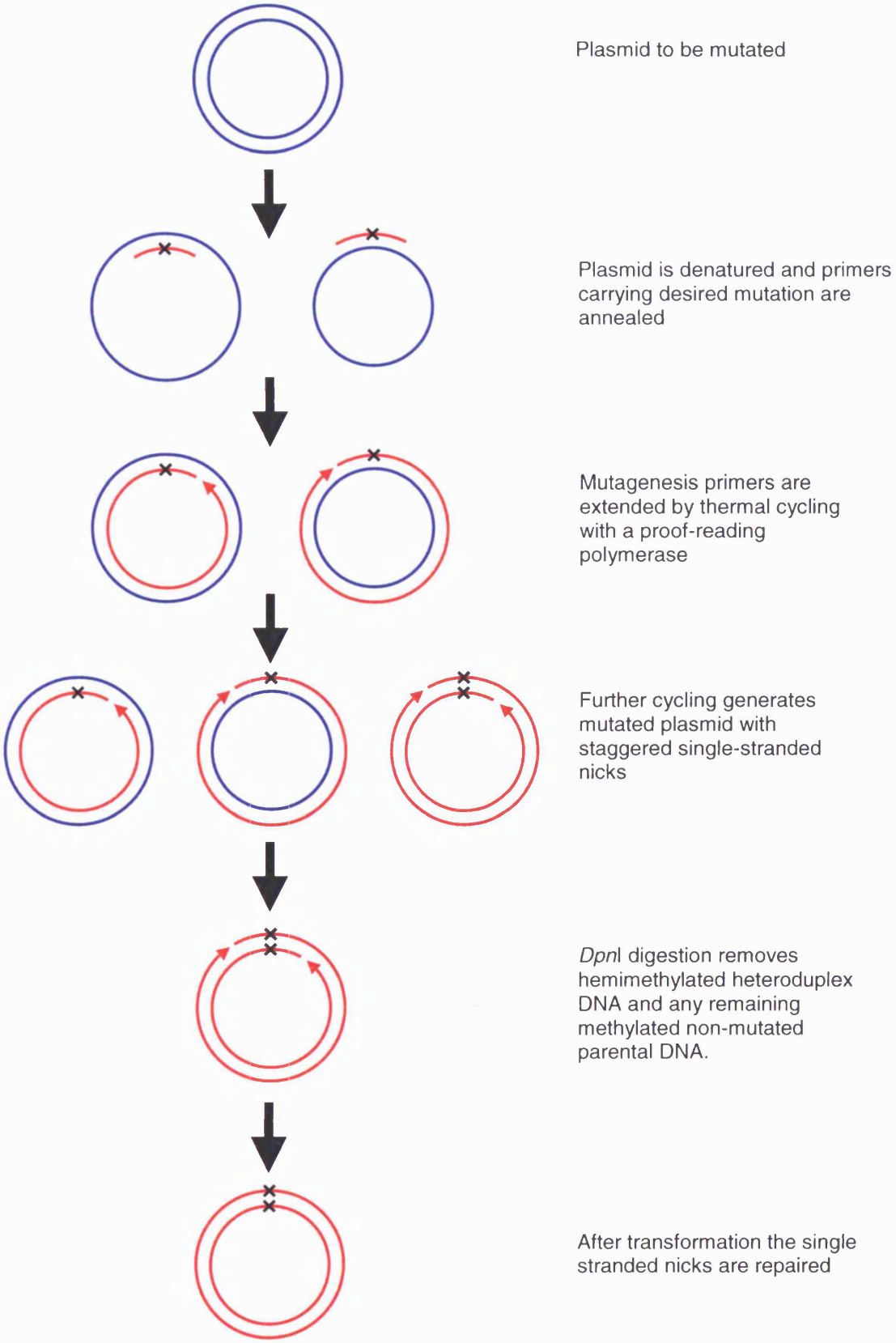

Figure 3.16. Western blot showing expression levels of Yml059c

Western blotting using an anti-GFP antibody shows that particulate fractions of yeast carrying pRS416-P_{gal1}-GFP-*YML059c* or pRS416-P_{gal1}-GFP-*YML059c*(S1406A) each possess similar levels of Yml059c polypeptide. BY4743 P_{gal1}-GFP-*YML059c*/P_{gal1}-GFP-*YML059c* was included as a positive control. No Yml059c polypeptide can be detected in either BY4743 or BY4743 + pRS416. The positions and sizes of molecular weight markers (kDa) are indicated.

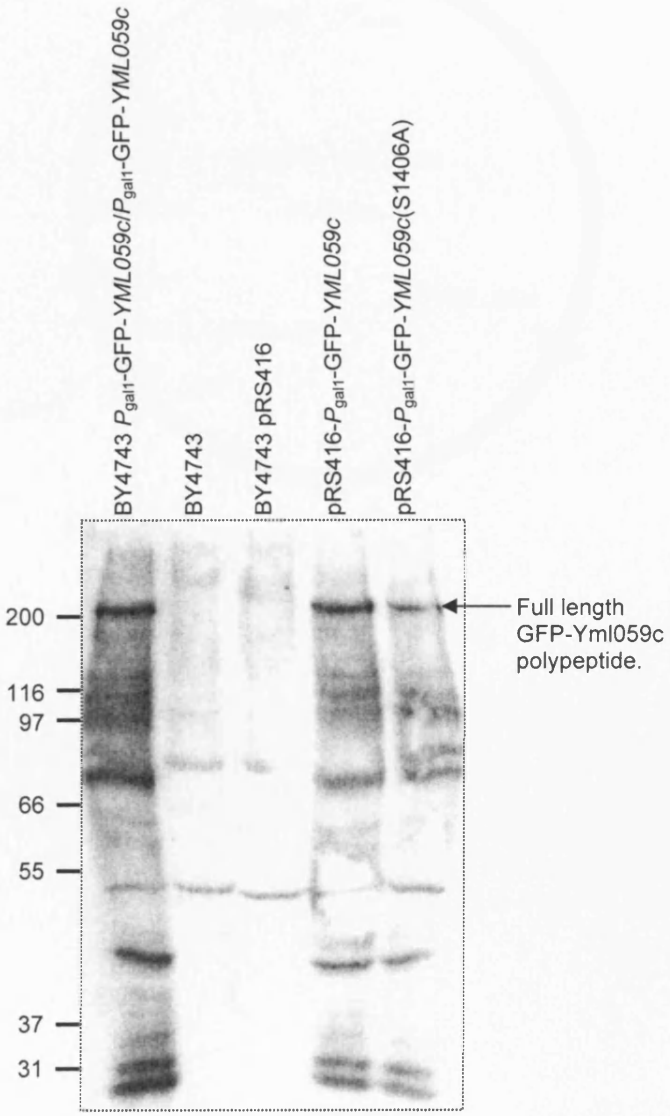

Figure 3.17. Plasmid map of pEGFP-*YML059c*

Plasmid map showing the features of the mammalian expression construct pEGFP-*YML059c*. Base pair coordinates are shown in parentheses.

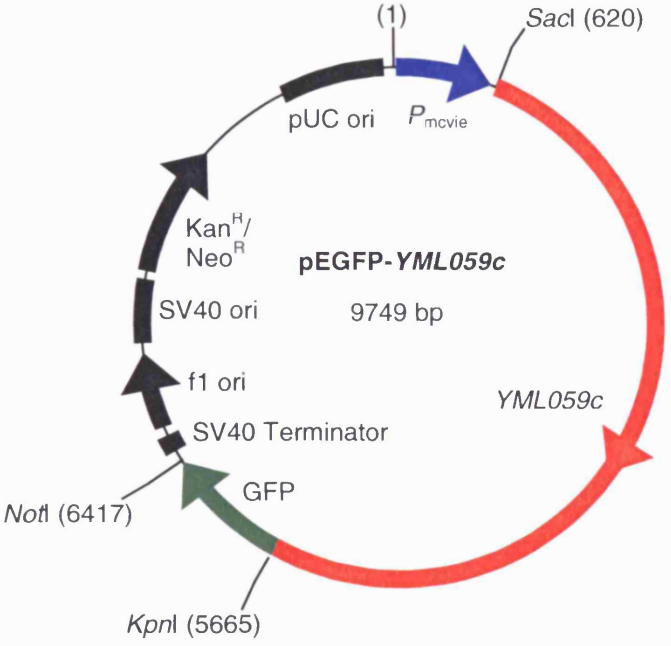

Figure 3.18. Western blot of *YML059c* expressed in COS-7 and Hela cells

Western blot analysis using an anti-GFP antibody confirms the expression of GFP and NTE in COS-7 and Hela cells transiently transfected with pEGFP and pEGFP-NTE respectively. No Yml059c polypeptide is detectable in either COS-7 or Hela cells transfected with pEGFP-*YML059c*. The positions and sizes of molecular weight markers (kDa) are indicated.

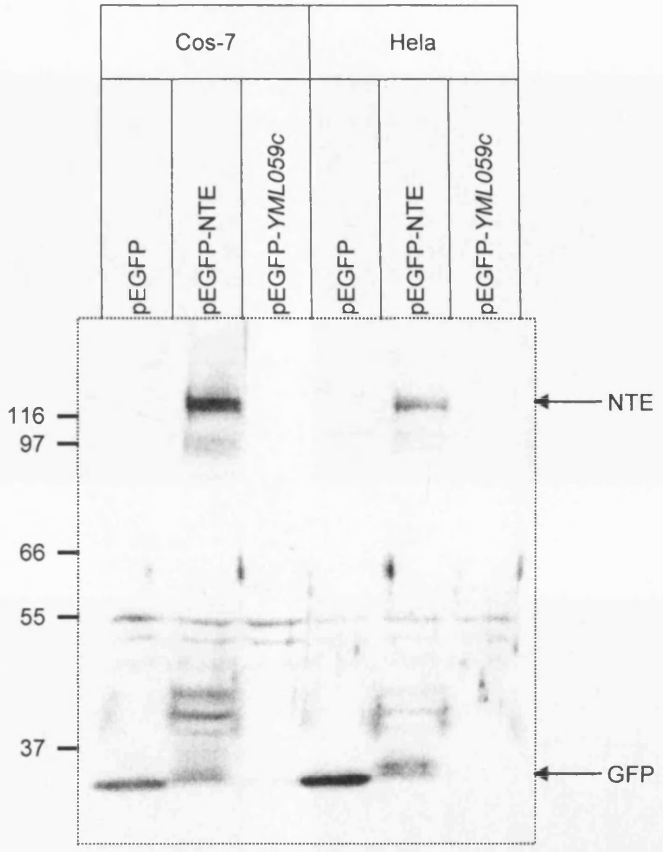

Figure 3.19. GFP-tagged Yml059c fails to display any fluorescence when expressed in COS-7 cells

Low-power images of COS-7 cells transiently transfected with pEGFP, pEGFP-NTE and pEGFP-*YML059c*. Images were taken under phase contrast (left) and by fluorescence microscopy (right). No fluorescence was detectable from COS-7 cells carrying pEGFP-*YML059c*.

pEGFP

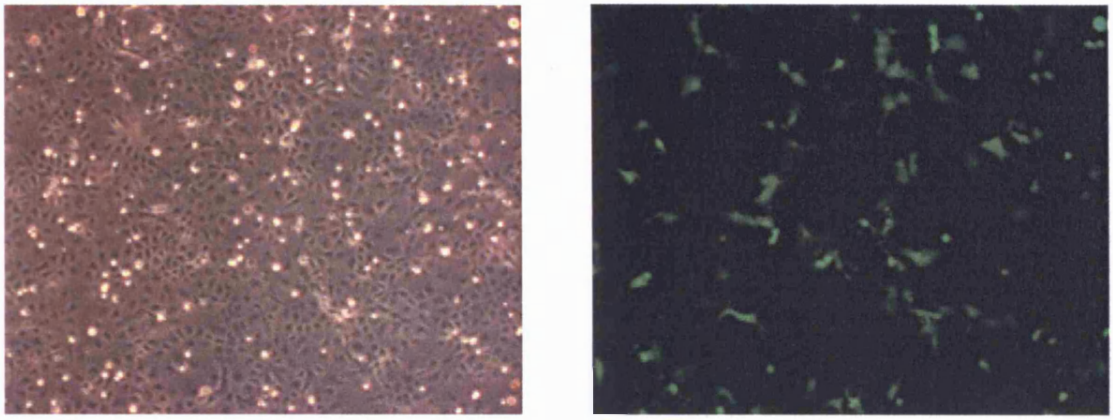

pEGFP-NTE

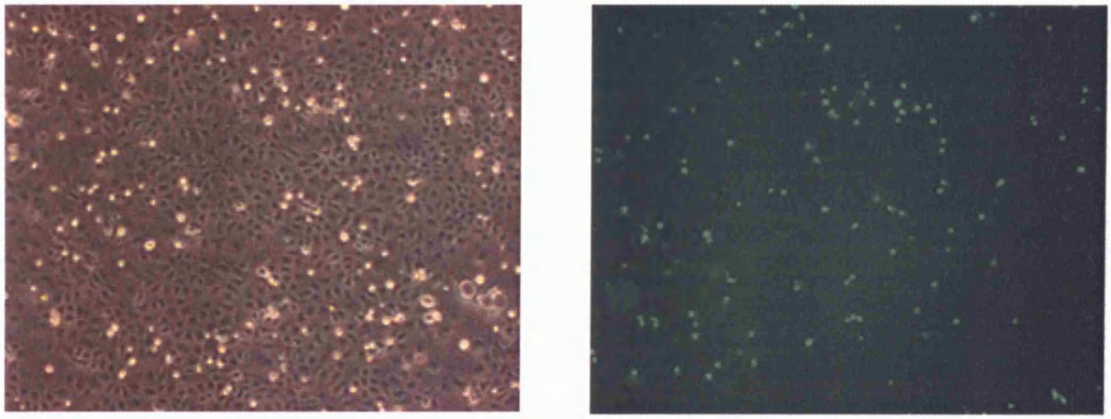

pEGFP-*YML059c*

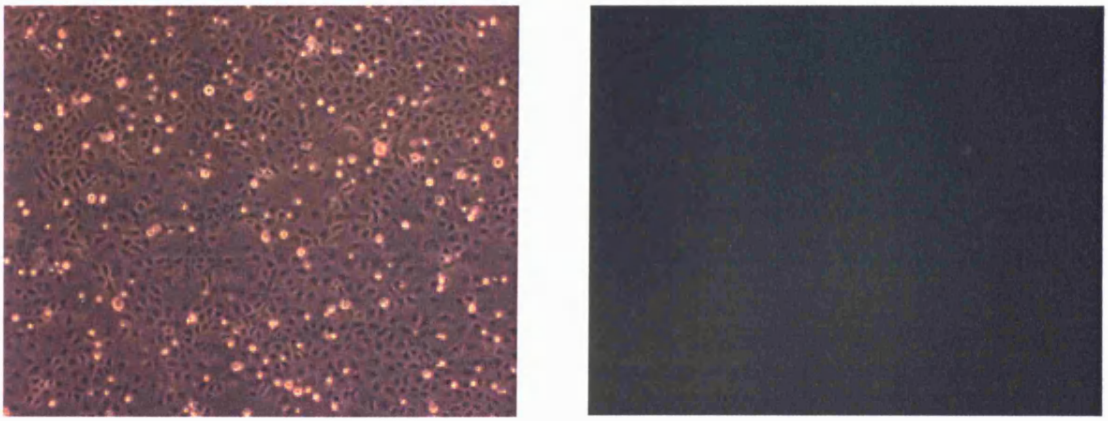

Figure 3.20. Plasmid map of pYC2/CT-*BCY1*

Plasmid map showing the features of the centromeric galactose regulatable yeast expression construct pYC2/CT-*BCY1*. The in-frame C-terminal V5 epitope and 6His tags are not shown. Base pair coordinates are shown in parentheses.

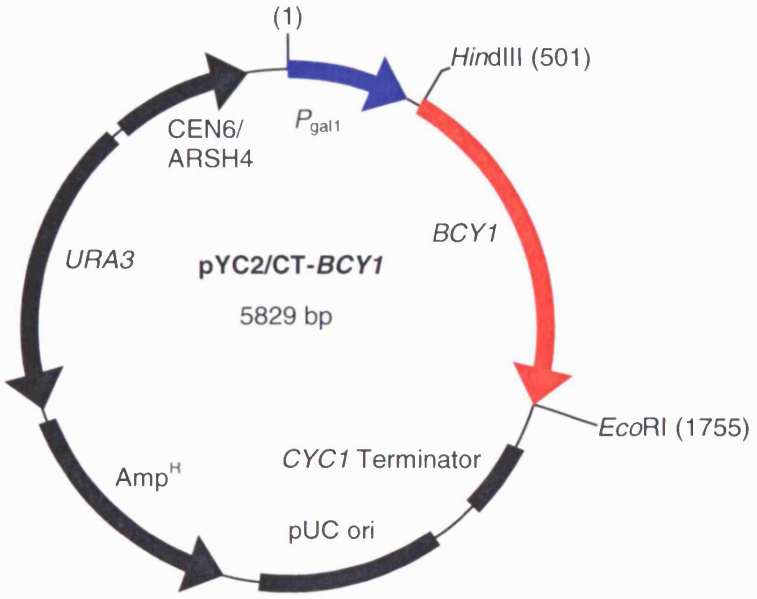

Figure 3.21. Northern showing overexpression of *BCY1*

Northern blot analysis was used to determine the level of *BCY1* transcript in yeast carrying one of 3 independent clones of pYC2/CT-*BCY1* compared to the endogenous expression of BY4743 + pYC2/CT. For each panel, the size (in nucleotides) and position of RNA markers is indicated. **A.** Each of the 3 clones clearly confers a dramatic increase in *BCY1* transcription above that of the empty vector level. **B.** Probing of *ACT1* as a loading control confirms approximately equal loading in each lane. Probing of *ACT1* was performed on a separate identical blot due to the similarity of transcript size to *BCY1*.

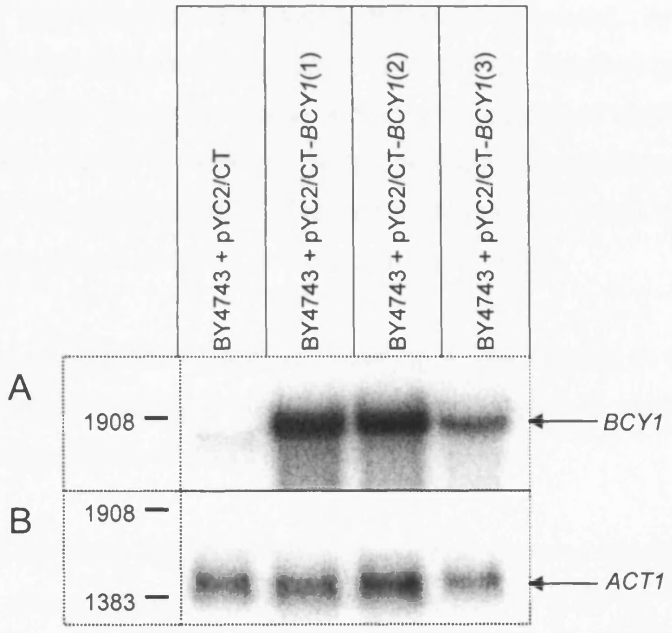

Chapter 4: Phenotypic Analysis of *yml059c* mutants

4.1 Introduction

With no prior knowledge of a gene's function the most logical starting point in the functional analysis of any yeast gene is genetic knockout of the gene of interest. The ease by which PCR mediated gene disruption (Wach *et al.*, 1994) allows the exact replacement of any non-essential ORF provides a powerful tool to the yeast geneticist. Analysis of a mutant's phenotype may provide important clues as to the wildtype function of the mutated gene; whether the phenotype is obvious such as a dramatic loss of cell viability or a more subtle effect, such as a reduction of growth rate under very specific conditions when compared to the parental strain. Complementation of a mutant phenotype could also provide a useful tool for dissecting the role of domains or individual amino acids.

Initial investigations of *YML059c* involved obtaining a yeast strain in which *YML059c* had been deleted and then assessing if the mutant had a decrease in viability or displayed any phenotype when subjected to an array of growth conditions.

Sequencing of the complete *Saccharomyces cerevisiae* genome (Goffeau *et al.*, 1996) has shown there to be approximately 6,200 open reading frames (ORFs). The *Saccharomyces* Genome Deletion Project has since individually deleted all non-essential genes (Giaever *et al.*, 2002) from the BY yeast strain series (Brachmann *et al.*, 1998). Each deletion involved the complete removal of a single ORF from start to stop codon by PCR mediated gene disruption using the geneticin (G418) resistance module KanMX4 (Wach *et al.*, 1994), the general procedure for which is described in Figure 2.1. This strain collection has been made publicly available through Euroscarf.

4.2 The *YML059c* gene is not essential for viability

Mating type 'a' and 'α' haploids lacking *YML059c* (BY4741 *yml059cΔ* and BY4742 *yml059cΔ* respectively) and a homozygous mutant diploid lacking *YML059c* (BY4743 *yml059cΔ/Δ*) were obtained from the Euroscarf collection (see Table 2.1 for details of genotypes). PCR was used to determine that *YML059c* had been correctly disrupted in these strains (see section 3.2), thus it can be concluded that *YML059c* is not an essential gene for cell viability and that mutation of this gene confers no obvious phenotype.

4.3 Phenotypic analysis of the *yml059cΔ* mutant

As the *yml059cΔ* mutant has no obvious phenotype it is possible that the yeast cell requires this gene product only under very specific conditions. In order to conserve the cell's resources many genes are regulated in such a fashion as to be expressed only when the yeast is in an environment where that protein is required. Examples of this are those genes required for nutrient utilisation or those that encode proteins conferring resistance to an environmental stress, such as the heat shock proteins or those required to survive oxidative stress.

Tests were carried out to compare the parental, BY4741, and the BY4741 *yml059cΔ* mutant's response to a wide variety of nutrients, stress conditions and inhibitors, seeking to determine if any condition will cause the mutant to display a phenotype (for a summary of all conditions tested see Table 4.1). Many of these were taken from Hampsey (1997).

4.3.1 Carbon sources

Although glucose is the preferred carbon source for *S. cerevisiae*, this yeast is able to utilise a wide variety of other carbon sources. In the presence of glucose those genes that are required for the utilisation of other carbon sources are repressed by a system known as carbon catabolite repression (Johnston and Carlson, 1992). Yml059c is not essential for growth on glucose, as the strain has been maintained on YPD. Tests were performed in order to determine whether Yml059c has any role in carbon source utilisation, whether in sugar uptake or metabolism, or in derepression or activation of those genes required for these processes.

Serial dilutions of BY4741 and BY4741 *yml059cΔ* were spotted on YP agar plates containing one of the following as the sole carbon source; glucose (0.02g ml^{-1}) galactose (0.02g ml^{-1}), sucrose (0.02g ml^{-1}), maltose, (0.02g ml^{-1}), glycerol (3% v/v) or potassium acetate (0.03g ml^{-1}). Reduced growth of the mutant compared to the parental strain on any of these carbon sources would imply a role for Yml059c in carbon source utilisation. A further test was carried out where both 2-deoxyglucose (0.2mg ml^{-1}) and sucrose (0.02g ml^{-1}) were used as carbon sources. 2-deoxyglucose is a glucose analogue that will cause the yeast to maintain carbon catabolite repression but cannot be metabolised. Strains that are able to utilise sucrose in the presence of 2-deoxyglucose are defective in this regulatory mechanism. Plates were incubated for 4 days, after which their growth was scored (Table 4.2). The two strains grew equally well on any of the carbon sources, with both growing equally poorly where the test plate contained both 2-deoxyglucose and sucrose.

4.3.2 Nitrogen sources

Glutamate, asparagine and ammonia are the preferred nitrogen sources for yeast (Cooper, 1982). In the absence of these, yeast can utilise a number of alternative sources including arginine, proline, allantoin, γ-aminobutyrate and urea. Experiments were performed in order to determine if Yml059c had a role in the utilisation of ammonia or proline.

Serial dilutions of BY4741 and BY4741 *yml059cΔ* were spotted on a YNB with ammonium sulphate agar plate and a YNB without ammonium sulphate agar plate supplemented with 0.1% proline. The strains were also spotted onto a standard YPD plate as a control. Plates were incubated for 3 days and growth was scored (Table 4.3). Both grew equally well on the control plate and on each nitrogen source test plate.

4.3.3 Stress conditions

Tests were performed in order to compare the *yml059c* mutant's response to that of the parental strain when exposed to conditions of stress.

4.3.3.1 Heat shock

To test for response to heat shock, serial dilutions of BY4741 and BY4741 *yml059cΔ* were spotted on YPD plates and sealed with parafilm. Plates were then floated in a 55°C waterbath for 30min, 60min or 90min; a control plate that had received no heat shock was included. Plates were then incubated at 30°C for 2 days and growth was scored (Table 4.4). The strains grew equally well on the control plate and each displayed an equal level of growth restriction after the varying heat shocks.

4.3.3.2 Oxidative stress

Sensitivity to H_2O_2 was used to test for response to oxidative stress. 50μl of mid-log cultures of BY4741 and BY4741 *yml059cΔ* were radially streaked from the centre of a YPD plate. At the centre a filter paper disc impregnated with 5μl of 30% v/v H_2O_2 was placed. The plate was incubated for 3 days and the distance from the centre over which no growth was observed was measured. Neither strain exhibited any growth within 15mm of the centre of the filter disc and each had grown equally well outside of this region.

4.3.3.3 Osmotic stress

Sensitivity to sorbitol or glycerol was used to test for response to osmotic stress. Serial dilutions of BY4741 and BY4741 *yml059cΔ* were spotted on YPD plates containing 0.2M, 1M and 2M concentrations of sorbitol or 4% 8% 10% and 20% v/v glycerol. In each case a standard YPD plate was included as a control. Plates were incubated for 2 days and

growth was scored (Table 4.5). The strains grew equally well on the control plates and each displayed equal growth on the varying sorbitol and glycerol concentrations.

4.3.3.4 Acidic pH

To test for response to low pH levels. Serial dilutions of BY4741 and BY4741 *yml059cΔ* were spotted on YPD plates of varying pH (7, 5, 4, 3 and 1). The plates were then incubated for 4 days. Following incubation the pH of the plates was verified using pH indicator strips and growth of the strains was scored (Table 4.6). All plates had maintained their initial pH level except the plate at pH7 which had reduced to pH6 over the course of the incubation. The strains showed no significant difference in growth at any pH.

4.3.3.5 Alcohol stress

Yeast can utilise ethanol as a carbon source but high concentrations will inhibit growth (Gray, 1941). Serial dilutions of BY4741 and BY4741 *yml059cΔ* were spotted on to YPD containing 0%, 3%, 8% and 10% v/v ethanol. 0% represents a standard YPD plate included as a control. Plates were incubated for 4 days after which growth was scored (Table 4.7). No significant difference in growth of either strain was observed on the control plate or at any ethanol concentration.

4.3.4 Inhibitors

Tests were performed in order to compare the *yml059c* mutant's response to that of the parental strain when exposed to a range of inhibitors. Tests to determine any difference in response to calcofluor, caffeine, 6-azauracil, EDTA and formamide were performed by spotting serial dilutions of BY4741 and BY4741 *yml059cΔ* onto YPD plates containing 0, 12, 100 and 500mg ml^{-1} calcofluor, 0, 1, 10 and 20mM caffeine, 0, 60, 120 and 240μg ml^{-1} 6-azauracil, 0, 0.2, 2 and 20mM EDTA and 0, 1, 3 and 6% v/v formamide. In each case 0 represents a standard YPD plate as a control.

Calcofluor is an anti-fungal agent with a high affinity for the yeast cell wall chitin and has been used to identify mutants defective in cell wall biogenesis (Roncero *et al.*, 1988). Caffeine is a purine analogue that affects many cellular processes and 6-azauracil inhibits the UTP and GTP biosynthetic pathways (Hampsey, 1997). Aguilera (1994) has identified formamide sensitive mutants and the chelating agent EDTA has been demonstrated to have antifungal properties towards the pathogenic yeast *Candida albicans* (Sen *et al.*, 2000).

Plates were incubated for 2 days (or 4 days in the case of the formamide plates) and growth was scored (Table 4.8). No significant difference in growth of each strain was observed for either control plate or any of the inhibitor concentrations.

Other inhibitors were tested using filter discs impregnated with aqueous solutions of one of the following; 20μl sodium orthovanadate (50μM), 10μl Actinomycin D (1mg ml^{-1}), 20μl phenanthroline (10mg ml^{-1}), 20μl PMSF (0.1M), 20μl cycloheximide (0.1mg ml^{-1}), 5μl staurosporine (1mM) and 20μl phenyl saligenin phosphate (10mM). With the exception of PSP, these were then placed onto YPD plates covered with top agar seeded with either BY4741 or BY4741 *yml059cΔ*. The PSP impregnated filter discs were placed onto YPgal plates seeded with either BY4743, BY4743 *yml059cΔ/Δ,* or BY4743 P_{gal1}-*GFP-YML059c*/P_{gal1}-*GFP-YML059c*.

Vanadate resistance has been associated with mutants that are defective in protein glycosylation (Ballou *et al.*, 1991). Phenanthroline is a metal chelating agent to which resistant phenotypes have been previously described (Schnell and Entian, 1991). Cycloheximide is a potent inhibitor of protein synthesis. Resistance to cycloheximide has been attributed to mutations in a number of genes (McCusker and Haber, 1988). PMSF is a serine hydrolase inhibitor and poor non-neuropathic inhibitor of NTE, whereas the organophosphate PSP is a potent neuropathic NTE inhibitor (Atkins and Glynn, 2000). Actinomycin D is a DNA intercalating agent and staurosporine is a protein kinase inhibitor (Hampsey, 1997)

Plates were incubated overnight (2 days for the PSP plates) and the diameter of the zone of inhibition around each paper disc was measured (Table 4.9). Each inhibitor produced a zone of inhibition of equal size with each strain; PMSF, staurosporine and actinomycin D failed to produce any zone of inhibition for any strain.

4.3.5 Metal ions

A number of phenotypes associated with resistance or sensitivity to various metal ions have been previously described (Hampsey, 1997). Tests were performed to assess the mutant's response to high levels of various metal ions in the growth media. Tests to determine any response to high levels of calcium chloride or cadmium chloride were performed by spotting serial dilutions of BY4741 and BY4741 *yml059cΔ* onto YPD plates containing 0, 0.1, 0.5, and 1M $CaCl_2$, and 0, 10, 50 and 100μM $CdCl_2$. In each case 0M represents a standard YPD plate as a control. Plates were incubated for 2 days and growth was scored (Table 4.10). Each strain grew equally well on the control plate and each displayed equal growth on the varying $CaCl_2$ and $CdCl_2$ concentrations.

Other metal ions were tested using filter discs impregnated with 20μl of aqueous solutions of one of the following; caesium chloride (3M), cobaltous chloride (0.3M), cupric sulphate

(0.5M), manganese chloride (0.1M), sodium fluoride (1M) and zinc chloride (0.1M). These were then placed onto YPD plates covered with top agar seeded with either BY4741 or BY4741 *yml059cΔ*. Plates were incubated overnight and the diameter of the zone of inhibition around each paper disc was measured (Table 4.11). Each metal ion tested produced a zone of inhibition of equal size on both BY4741 and BY4741 *yml059c,* with CsCl, $MnCl_2$ and $ZnCl_2$ failing to produce any zone of inhibition for either strain.

4.3.6 Other growth conditions

Under anaerobic conditions *S.cerevisiae* can grow via fermentation. To determine whether Yml059c has any role in those metabolic pathways required for anaerobic growth serial dilutions of BY4741 and BY4741 *yml059cΔ* were spotted onto 2 YPD plates. One was incubated in standard aerobic conditions, the other under anaerobic conditions. After 3 days the growth was scored (Table 4.12). Both strains grew equally well under aerobic and anaerobic conditions.

Tests were performed to assess the mutant's response to growth at various temperatures. Serial dilutions of BY4741 and BY4741 *yml059cΔ* were spotted onto 4 YPD plates, one of which was incubated at each of the following temperatures: 22°C, 30°C, 37°C for 4 days and 4°C for 25 days. Growth was then scored (Table 4.13). No significant difference in growth of each strain was observed at any of the tested growth temperatures.

4.4 Does *YML059c* have any role in pseudohyphal development?

As stated earlier, diploid yeast can be induced to form pseudohyphae in conditions of nitrogen limitation, growing as filamentous chains rather than discrete round cells. I observed that BY4743 overexpressing *YML059c* appeared to flocculate slightly and occasionally formed elongated cells (data not shown). With cAMP known to have a role in pseudohyphal development and Yml059c possessing a putative cAMP-binding site it is conceivable that Yml059 might function in pseudohyphal growth and that these elongated cells may be an attempt to form pseudohyphae. The BY yeast strain series cannot normally undergo pseudohyphal differentiation as it is descended from S288C which is known to carry a mutation in *FLO8,* an essential gene for this morphological transition (Liu *et al.*, 1996). Phenotypic changes in a pseudohyphal competent strain caused by genetic knockout or overexpression of *YML059c* would point towards Yml059c having a role in pseudohyphal growth.

4.4.1 The effect of genetic disruption or overexpression of *YML059c* on pseudohyphal growth

PCR mediated gene disruption (Wach *et al.*, 1994) was used to knockout *YML059c* from the pseudohyphal competent strain MW1076/7, in order to determine whether this gene is necessary for pseudohyphal development (see section 3.3).

MW1076/7, MW1076/6 *yml059cΔ/Δ* and BY4743 were incubated on low ammonium SLAD agar (containing 50μM ammonium sulphate as the sole nitrogen source; Gimeno *et al.*, 1992). As predicted, the BY4743 diploid failed to develop any of the characteristic structures of pseudohyphal development retaining a typical smooth round colony morphology (see Figure 4.1). At areas of high colony density both MW1076/7 and MW1076/6 *yml059cΔ/Δ* were induced to form pseudohyphae equally readily, indicating that Yml059c does not have an essential role in pseudohyphal growth.

In order to investigate the effect of overexpression of *YML059c* on pseudohyphal growth MW1076/7 + pRS416, MW1076/7 + pRS416-P_{gal1}-*YML059c* and MW1076/7 + pRS416-P_{gal1}-GFP-*YML059c* were incubated on SLAG medium (low ammonium media containing 2% galactose as the carbon source) as galactose is required for the induction of overexpression. Under these conditions none of the above strains formed pseudohyphae and no difference in colony morphology could be observed between them. From this observation it would seem that galactose is an inappropriate carbon source for pseudohyphal growth. Although this failure of even the parental strain to undergo pseudohyphal differentiation on galactose-containing media does hamper the study of any possible subtle affect, we can conclude that overexpression of Yml059c does not cause a radical induction of pseudohyphae under these conditions.

4.5 Discussion

From the tests performed, disruption of *YML059c* appears to confer no mutant phenotype. However, the list of conditions tested is by no means exhaustive and it is still possible that an appropriate condition has not been discovered that would elicit a phenotypic change, or that the methods used might lack the sensitivity to distinguish a subtle growth defect. With the exception of the nitrogen source tests and the 6-azauracil sensitivity tests, all were carried out using rich media; it has been reported that use of SC media in place of YPD can enhance subtle, perhaps otherwise undetectable phenotypes (Hampsey, 1997). In a number of experiments (e.g. metal ions $ZnCl_2$, $MnCl_2$, $CsCl_2$ and inhibitors PMSF, staurosporine and actimoymcin D) the growth of neither the parental nor mutant strain was perturbed. In these cases it is not possible to determine whether the compound has been

taken up by the cell or whether the concentration was insufficient to inhibit growth of either strain. Ideally, each experiment would have included a strain known to be sensitive to the test condition, as a positive control. Nitiss and Wang (1988) identified a drug-permeable yeast strain for use in the study of topoisomerase-targeting anti-tumour drugs. Such a strain's increased permeability to test compounds might uncover an inhibitor sensitivity associated with disruption of *yml059c* that might have otherwise remained undetected. The use of radiolabelled inhibitors could also provide a means of assessing uptake.

It is interesting to note that the potently neuropathic OP, phenyl saligenin phosphate failed to significantly affect the parental, knockout or overexpression strain; although again it is not certain that the inhibitor has entered the cell. Inhibition of the overexpresser's catalytic activity (see Chapter 5) after incubation with PSP could be used to assess PSP uptake, but culturing yeast in the presence of sufficient quantities of toxic OP would not be practically possible.

A number of groups have attempted global phenotypic analysis by individually disrupting large numbers of ORFs within the yeast genome and subjecting the mutant strains to arrays of phenotypic tests. Many of these have included *YML059c*. One ongoing study has used transposon mutagenesis as a means of generating mutant strains for phenotypic tests (Ross-Macdonald *et al.*, 1999; Kumar *et al.*, 2000) while others have analysed the mutants generated by the Saccharomyces Genome Deletion Project (Winzeler *et al.*, 1999; Deutschbauer *et al.*, 2002; Giaever *et al.*, 2002; Steinmetz *et al.*, 2002). None of these studies have uncovered any phenotype for yeast lacking *YML059c*.

A recent study has suggested that approximately a quarter of gene deletions in yeast that cause no phenotype are compensated for by a duplicate gene (Gu *et al.*, 2003). Although a standard BLAST search, using the full length Yml059c peptide sequence as the query, failed to detect any possible homologues within the yeast genome, the more sensitive PSI-BLAST program (Altschul *et al.*, 1997) found 3 translated ORFs with regions of similarity spanning the active site serine of the catalytic domain (see Figure 4.2). These are Ymr313c, Yor081c and Ykr089c with *E* scores of 0.042, 0.12 and 0.48 respectively; the latter two of which display a high level of homology to each other (61% identity and 77% similarity over a 509 amino acid region). With no significant similarity over any other region, these three cannot be considered duplications of *YML059c* but they do possess some of the essential features of NTE's active site. Each has a GXSXG motif in an equivalent location to that of NTE's active site and some degree of similarity to the region immediately up and downstream.

As well as the active site serine, residues His^{860}, His^{885}, Asp^{960} and Asp^{1086} have all been shown to be essential for NTE's catalytic activity (Atkins and Glynn, 2000). Although Yml059c has an identical residue to NTE at the equivalent location to each of these, only some can be found in the other possible yeast homologues. None possess either of the essential histidines but all three have an aspartate equivalent to Asp^{960} of NTE (albeit offset by 4 residues to that of NTE or Yml059c) and both Yor081c and Ykr089c have an aspartate at a corresponding location to Asp^{1086} of NTE. As all three have some of the features of NTE and Yml059c they are likely to be serine hydrolases, possibly with similar natural substrates. Although no functional information is available for Yor081c and Ykr089c, Ymr313c has been shown to be localised to lipid particles and possibly to have a role in lipid metabolism, as yeast lacking *ymr313c* accumulate triacylglycerols (Athenstaedt *et al.*, 1999). However, it is doubtful that any of these proteins are sufficiently similar to Yml059c to fully complement its cellular function.

Many groups have published micro-array expression data for all of the yeast ORFs under a variety of conditions. Analysis of the data available via the "Expression Connection" on the Saccharomyces Genome Database (http://genome-www.stanford.edu/Saccharomyces/) (DeRisi *et al.*, 1997; Cho *et al.*, 1998; Chu *et al.*, 1998; Spellman *et al.*, 1998; Ferea *et al.*, 1999; Wyrick *et al.*, 1999; Gasch *et al.*, 2000; Lyons *et al.*, 2000; Ogawa *et al.*, 2000; Roberts *et al.*, 2000; Gasch *et al.*, 2001) also fails to shed any light on a possible role for *YML059c*.

Yeast two-hybrid analysis has suggested an interaction between Yml059c and the non-essential protein Yfr021w (Georgakopoulos *et al.*, 2001). Although the function of this protein has yet to be established, yeast lacking *yfr021w* have impaired respiratory function, as determined by a reduced ability to grow on the non-fermentable carbon source glycerol. No such phenotype was observed for the *yml059cΔ* mutant (see section 4.3.1) discounting the possibility that Yml059c is required for the function of Yfr021w.

Yml059c is not essential for pseudohyphal differentiation, as determined by genetic knockout. Overexpression of Yml059c also failed to have any obvious affect. However the overexpression strategy required the use of galactose as the sole carbon source, under which conditions the parental strain was unable to form pseudohyphae, a phenomenon previously identified by Lorenz *et al.* (2000). The expression vectors described by Gari *et al.* (1997) employ a tetracycline regulated promoter, providing an inducible system that can achieve expression levels comparable to that of *GAL1* but do not require alteration of the growth media. Such a system could be used to study the effect of overexpression of Yml059c under conditions that allow the parental strain to form pseudohyphae.

Table 4.1. Summary of all phenotypic tests performed

Condition Under Test	Phenotypic Test Method (1 or 2)	Comments
Carbon Sources		
Galactose	1	0.02g ml^{-1} in YP agar
Sucrose	1	0.02g ml^{-1} in YP agar
Maltose	1	0.02g ml^{-1} in YP agar
Glycerol	1	3% in YP agar
Acetate	1	0.03g of potassium acetate ml^{-1} of YP agar
2-Deoxyglucose and sucrose	1	0.2mg ml^{-1} 2-deoxyglucose and 0.02g ml^{-1} sucrose in YP agar
Nitrogen Sources		
Ammonium	1	YNB with ammonium sulphate
Proline	1	YNB without ammonium sulphate, supplemented with 0.1% proline
Stress Conditions		
Heat Shock	1	Strains spotted onto YPD agar plates. Floated in 55°C water-bath for 30, 60 and 90 minutes prior to incubation
Oxidative Stress	2	5µl of 30% H_2O_2 on paper disc
Osmotic stress	1	0.2,1 and2M sorbitol or 4, 8, 10 and 20% v/v glycerol in YPD agar
Low pH	1	pH 7, 5, 4, 3 and 1 by addition of 6M HCl to YPD agar
Ethanol	1	0, 3, 8 and 10% v/v in YPD agar
Inhibitors		
Formamide	1	6, 3, 1 and 0.1% in YPD agar
Calcofluor	1	500, 100, 12, 1 and 0.1µg ml^{-1} in YPD agar
Caffeine	1	50, 20, 10 and 1mM in YPD agar
6-azauracil	1	60, 30 and 10 µg ml^{-1} in SD agar with 5µg ml^{-1} of uracil
EDTA	1	40, 20, 2 and 0.2 mM in YPD
Sodium Orthovanadate	2	20µl of 50µM on paper disc
Actinomycin D	2	10µl of 1mg ml^{-1} on paper disc
Phenanthroline	2	20µl of 10mg ml^{-1} on paper disc
Phenylmethylsulfonylfluoride	2	20µl of 0.1M on paper disc
Cycloheximide	2	20µl of 0.1mg ml^{-1} on paper disc
Staurosporine	2	5µl of 1mM on paper disc
Phenyl saligenin phosphate	2	20µl of 10mM on paper disc
Metal Ions		
$CaCl_2$	1	0, 0.1, 0.5, 1M in YPD agar
$CdCl_2$	1	0, 10, 50 and 100µM in YPD agar
$Cu(SO)_4$	2	20µl of 0.5M on paper disc
$CoCl_2$	2	20µl of 0.3M on paper disc
CsCl	2	20µl of 3M on paper disc
$ZnCl_2$	2	20µl of 0.1M on paper disc
MnCl	2	20µl of 0.1M on paper disc
NaF	2	20µl of 1M on paper disc
Miscellaneous Growth Conditions		
Aerobic versus anaerobic growth	1	Anaerobic conditions achieved in BBL GasPak chamber containing oxoid gas-generating sachet. Growth was on YPD agar containing Tween 80 (0.9ml l^{-1}) and ergosterol (30mg l^{-1}).
Growth temperatures	1	4, 22, 30 and 37°C on YPD agar

Table 4.2. Affect of various carbon sources on growth rate of *yml059c* mutant

		Level of growth at dilution			
Carbon Source	**Strain**	1	1/10	1/100	1/1000
Glucose	BY4741	5	5	5	4
	BY4741 *yml059cΔ*	5	5	5	4
Galactose	BY4741	5	5	5	2
	BY4741 *yml059cΔ*	5	5	4	2
Sucrose	BY4741	5	5	5	4
	BY4741 *yml059cΔ*	5	5	5	4
Maltose	BY4741	5	5	3	1
	BY4741 *yml059cΔ*	5	5	2	1
Glycerol	BY4741	4	3	2	1
	BY4741 *yml059cΔ*	4	3	2	1
Acetate	BY4741	3	2	1	0
	BY4741 *yml059cΔ*	3	2	1	0
2-deoxyglucose and Sucrose	BY4741	4	1	0	0
	BY4741 *yml059cΔ*	4	1	0	0

Table 4.3. Affect of nitrogen sources ammonium and proline on growth rate of *yml059c* mutant

		Level of growth at dilution			
Nitrogen Source	**Strain**	1	1/10	1/100	1/1000
Ammonium	BY4741	5	5	4	2
	BY4741 *yml059cΔ*	5	5	4	2
Proline	BY4741	5	5	4	3
	BY4741 *yml059cΔ*	5	5	4	3
YPD control	BY4741	5	5	4	3
	BY4741 *yml059cΔ*	5	5	4	3

Table 4.4. Response to transient heat shock

		Level of growth at dilution			
Duration of 55°C heat shock (min)	**Strain**	1	1/10	1/100	1/1000
0	BY4741	5	5	3	2
	BY4741 *yml059cΔ*	5	5	3	2
30	BY4741	2	1	0	0
	BY4741 *yml059cΔ*	2	1	0	0
60	BY4741	1	0	0	0
	BY4741 *yml059cΔ*	1	0	0	0
90	BY4741	1	0	0	0
	BY4741 *yml059cΔ*	1	0	0	0

Table 4.5. Response to osmotic stress

Concentration of sorbitol (M)	Strain	Level of growth at dilution			
		1	1/10	1/100	1/1000
0	BY4741	5	5	4	3
	BY4741 *yml059cΔ*	5	5	4	3
0.2	BY4741	5	5	4	3
	BY4741 *yml059cΔ*	5	5	4	3
1	BY4741	5	4	3	2
	BY4741 *yml059cΔ*	5	4	3	2
2	BY4741	1	0	0	0
	BY4741 *yml059cΔ*	1	0	0	0
Concentration of Glycerol (% v/v)	**Strain**	1	1/10	1/100	1/1000
0	BY4741	5	5	5	4
	BY4741 *yml059cΔ*	5	5	5	4
4	BY4741	5	5	5	4
	BY4741 *yml059cΔ*	5	5	5	4
8	BY4741	5	5	5	4
	BY4741 *yml059cΔ*	5	5	5	4
10	BY4741	5	5	4	3
	BY4741 *yml059cΔ*	5	5	4	3
20	BY4741	2	1	0	0
	BY4741 *yml059cΔ*	2	1	0	0

Table 4.6. Response to low pH

Initial pH	Strain	Level of growth at dilution			
		1	1/10	1/100	1/1000
7	BY4741	5	5	5	4
	BY4741 *yml059cΔ*	5	5	4	4
5	BY4741	5	5	5	4
	BY4741 *yml059cΔ*	5	5	4	4
4	BY4741	5	5	5	4
	BY4741 *yml059cΔ*	5	5	4	4
3	BY4741	5	5	5	4
	BY4741 *yml059cΔ*	5	5	4	4
1	BY4741	5	5	3	1
	BY4741 *yml059cΔ*	5	5	3	1

Table 4.7. Response to high levels of ethanol

Concentration of Ethanol (% v/v)	Strain	Level of growth at dilution			
		1	1/10	1/100	1/1000
0	BY4741	5	5	5	4
	BY4741 *yml059cΔ*	5	5	4	4
3	BY4741	5	5	5	4
	BY4741 *yml059cΔ*	5	5	4	4
8	BY4741	5	5	2	1
	BY4741 *yml059cΔ*	5	5	2	1
10	BY4741	5	4	1	0
	BY4741 *yml059cΔ*	5	4	1	0

Table 4.8. Response to calcofluor, caffeine, 6-azauracil, EDTA and formamide

		Level of growth at dilution			
Concentration of calcofluor (μg ml^{-1})	**Strain**	1	1/10	1/100	1/1000
0	BY4741	5	5	4	3
	BY4741 *yml059cΔ*	5	5	4	3
12	BY4741	5	5	4	3
	BY4741 *yml059cΔ*	5	5	4	3
100	BY4741	5	4	2	1
	BY4741 *yml059cΔ*	5	4	2	1
500	BY4741	5	4	1	0
	BY4741 *yml059cΔ*	5	4	1	0
Concentration of caffeine (mM)	**Strain**	1	1/10	1/100	1/1000
0	BY4741	5	5	4	3
	BY4741 *yml059cΔ*	5	5	4	3
1	BY4741	5	5	4	3
	BY4741 *yml059cΔ*	5	5	4	3
10	BY4741	5	2	1	0
	BY4741 *yml059cΔ*	5	2	1	0
20	BY4741	1	0	0	0
	BY4741 *yml059cΔ*	1	0	0	0
Concentration of 6-azauracil (μg ml^{-1})	**Strain**	1	1/10	1/100	1/1000
0	BY4741	5	5	4	3
	BY4741 *yml059cΔ*	5	5	4	3
60	BY4741	5	5	4	3
	BY4741 *yml059cΔ*	5	5	4	3
120	BY4741	5	5	4	2
	BY4741 *yml059cΔ*	5	5	4	2
240	BY4741	5	5	4	2
	BY4741 *yml059cΔ*	5	5	4	2
Concentration of EDTA (mM)	**Strain**	1	1/10	1/100	1/1000
0	BY4741	5	5	5	5
	BY4741 *yml059cΔ*	5	5	5	5
0.2	BY4741	5	5	5	5
	BY4741 *yml059cΔ*	5	5	5	5
2	BY4741	5	1	0	0
	BY4741 *yml059cΔ*	5	1	0	0
20	BY4741	0	0	0	0
	BY4741 *yml059cΔ*	0	0	0	0
Concentration of formamide (% v/v)	**Strain**	1	1/10	1/100	1/1000
0	BY4741	5	5	5	4
	BY4741 *yml059cΔ*	5	5	4	4
1	BY4741	5	5	5	4
	BY4741 *yml059cΔ*	5	5	4	4
3	BY4741	5	5	4	1
	BY4741 *yml059cΔ*	5	5	3	1
6	BY4741	0	0	0	0
	BY4741 *yml059cΔ*	0	0	0	0

Table 4.9. Response to sodium orthovanadate, actinomycin D, phenanthroline, PMSF, cycloheximide, staurosporine and phenyl saligenin phosphate

Inhibitor	Strain	Diameter of Zone of Inhibition (mm)
Sodium Orthovanadate	BY4741	8
	BY4741 *yml059cΔ*	8
Actinomycin D	BY4741	0
	BY4741 *yml059cΔ*	0
Phenanthroline	BY4741	30
	BY4741 *yml059cΔ*	31
PMSF	BY4741	0
	BY4741 *yml059cΔ*	0
Cycloheximide	BY4741	15
	BY4741 *yml059cΔ*	16
Staurosporine	BY4741	0
	BY4741 *yml059cΔ*	0
Phenyl saligenin phosphate	BY4743	1
	BY4743 *yml059cΔ*/yml059cΔ	1
	BY4743 P_{gal1}-*GFP-YML059c*/ P_{gal1}-*GFP-YML059c*	1

Table 4.10. Response to calcium chloride and cadmium chloride

		Level of growth at dilution			
Concentration of $CaCl_2$ (M)	**Strain**	1	1/10	1/100	1/1000
0	BY4741	5	5	4	3
	BY4741 *yml059cΔ*	5	5	4	3
0.1	BY4741	5	5	4	3
	BY4741 *yml059cΔ*	5	5	4	3
0.5	BY4741	4	2	1	0
	BY4741 *yml059cΔ*	4	2	1	0
1	BY4741	0	0	0	0
	BY4741 *yml059cΔ*	0	0	0	0
Concentration of $CdCl_2$ (μM)	**Strain**	1	1/10	1/100	1/1000
0	BY4741	5	5	4	3
	BY4741 *yml059cΔ*	5	5	4	3
10	BY4741	5	4	3	1
	BY4741 *yml059cΔ*	5	4	3	1
50	BY4741	2	1	0	0
	BY4741 *yml059cΔ*	2	1	0	0
100	BY4741	1	0	0	0
	BY4741 *yml059cΔ*	1	0	0	0

Table 4.11. Response to CsCl, $CoCl_2$, $CuSO_4$, $MnCl_2$, NaF, $ZnCl_2$

Metal Ion	Strain	Diameter of Zone of Inhibition (mm)
CsCl	BY4741	0
	BY4741 *yml059cΔ*	0
$CoCl_2$	BY4741	29
	BY4741 *yml059cΔ*	29
$CuSO_4$	BY4741	8
	BY4741 *yml059cΔ*	8
$MnCl_2$	BY4741	0
	BY4741 *yml059cΔ*	0
NaF	BY4741	8
	BY4741 *yml059cΔ*	8
$ZnCl_2$	BY4741	0
	BY4741 *yml059cΔ*	0

Table 4.12. Response to anaerobic conditions

		Level of growth at dilution				
Conditions	**Strain**	1	1/5	1/25	1/125	1/625
Aerobic	BY4741	5	5	5	5	4
	BY4741 *yml059cΔ*	5	5	5	5	4
Anaerobic	BY4741	5	5	5	5	4
	BY4741 *yml059cΔ*	5	5	5	5	4

Table 4.13. Response to various growth temperatures

		Level of growth at dilution			
Growth Temperature (°C)	**Strain**	1	1/10	1/100	1/1000
4	BY4741	5	5	4	1
	BY4741 *yml059cΔ*	5	5	3	1
22	BY4741	5	5	4	1
	BY4741 *yml059cΔ*	5	5	3	1
30	BY4741	5	5	5	4
	BY4741 *yml059cΔ*	5	5	5	4
37	BY4741	5	5	4	1
	BY4741 *yml059cΔ*	5	5	3	1

Figure 4.1. Images of yeast forming pseudohyphae

Images of yeast colonies after growth on SLAD media. **A.** shows the characteristic pseudohyphal colony morphology of the MW1076/7 strain **B.** shows a higher magnification image of the pseudohyphal structures. **C.** shows the contrasting smooth round colony morphology of the BY4743 yeast strain.

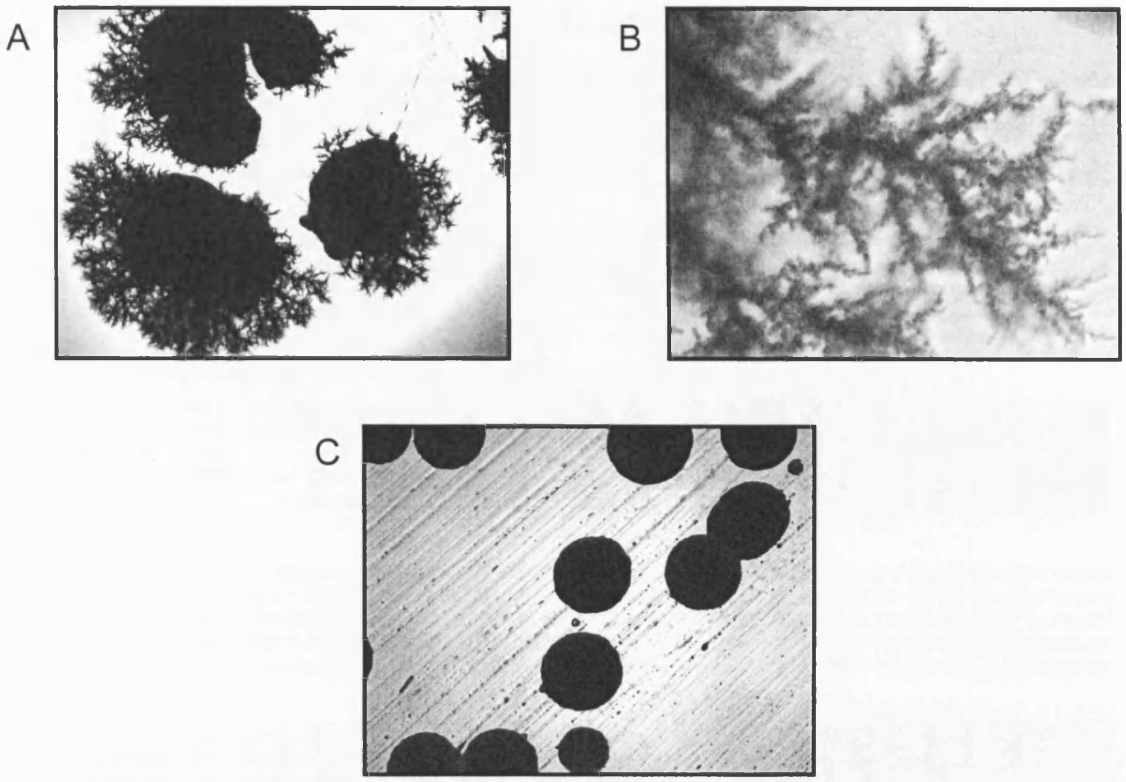

Figure 4.2. Three other yeast proteins with similarity to NTE and Yml059c

Clustal W alignment (Thompson *et al.*, 1994) of a 281 residue region of NTE with its possible homologues in yeast. Shading indicates related amino acids in 4 out of 5 sequences (white-on-black for identical residues, white-on-grey for similar). Those residues shown to be essential to the catalytic activity of NEST are numbered (with 4 denoting the active site serine). The arrow indicates the position of an aspartate residue found in Ymr313c, Yor081c and Ykr089c that might be equivalent to Asp[960] of NTE (3) offset by 4 amino acids.

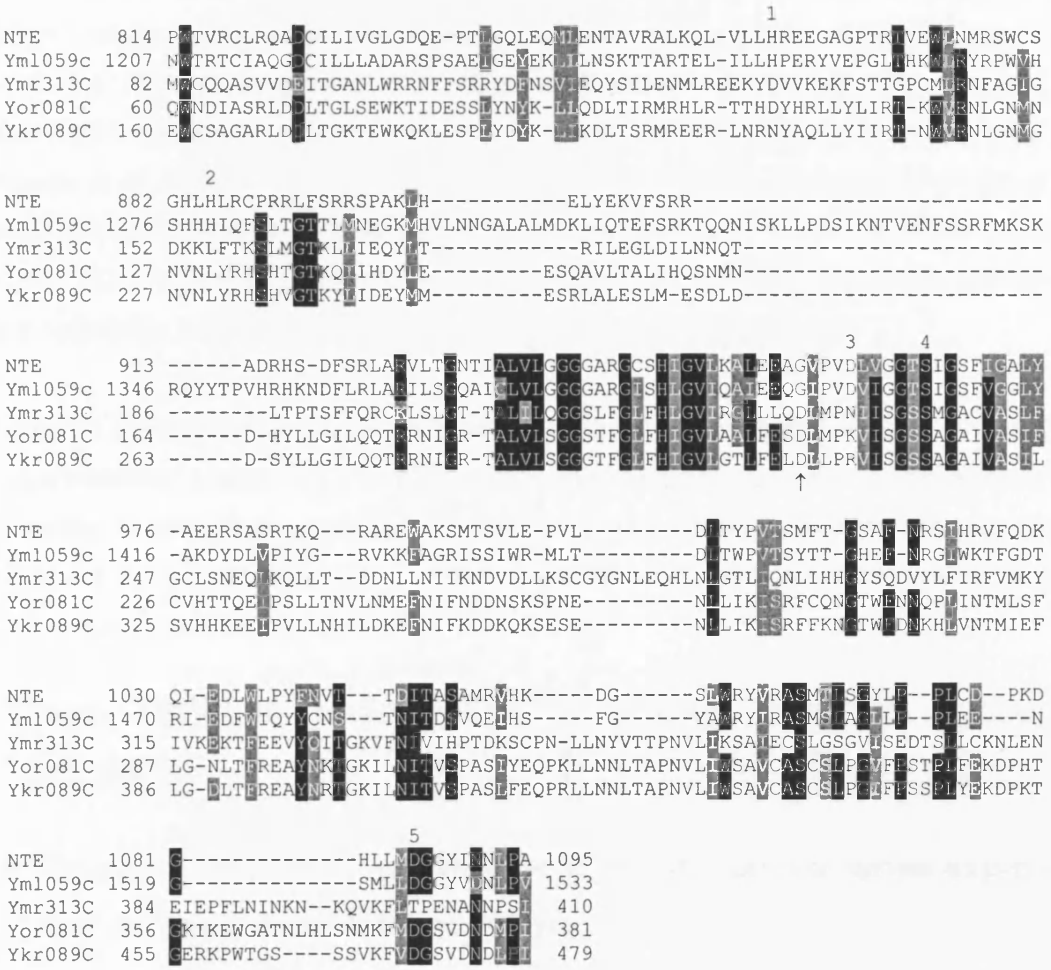

Chapter 5: Characterisation of the Yml059c protein

5.1 Introduction

As described in Chapter 1, NTE acts as a serine esterase capable of hydrolysing the artificial substrate phenyl valerate. Covalent modification of the enzyme's active site by OPs inhibits this activity and provides a means of labelling the protein using [^{3}H]DFP (Johnson, 1969a; Johnson, 1969b). Lysates of *E.coli* expressing the NEST domain of NTE maintain the catalytic properties of the full-length protein (Atkins and Glynn, 2000) and purified NEST has been used to determine that NTE can hydrolyse membrane lipids (van Tienhoven *et al.*, 2002). The major NTE-like region of Yml059c (residues 797-1646) is 32% identical and 51% similar to NTE and spans both the catalytic and putative regulatory domains. This level of similarity suggests that they might conceivably catalyse the same or related substrates and have their activity modulated in a similar fashion.

This chapter attempts to characterise Yml059c, with the aim of establishing to what extent it can be considered a homologue of NTE, with emphasis placed on determining whether both have similar biochemical properties. Steps were also taken to explore the potential for cAMP to act as a regulatory ligand to Yml059c and to visualise Yml059c within the yeast cell by confocal microscopy using GFP tags.

5.2 Does Yml059c have NTE-like phenyl valerate hydrolase activity?

5.2.1 The catalytic domain of Yml059c is non-functional when expressed in *E.coli* as a recombinant polypeptide

A previous attempt to express the putative catalytic domain of Yml059c in *E.coli* involved cloning the region encoding amino acid residues 1111-1640 into an *E.coli* expression vector. This encompasses the NEST-like segment including transmembrane helix 7 at the N-terminus of this region. However, the resultant polypeptide proved insoluble and inactive (Yong Li unpublished work). In this study, a further attempt was made to express the putative catalytic domain in a functional form by expressing amino acids 870-1640 using pET21b-YNEST (see section 3.4). This plasmid was designed such that a further 241 amino acids towards the N-terminus would be incorporated, thereby including TM domain 6 into the recombinant polypeptide (see Figure 5.1). TMpred analysis scores TM6 significantly more highly that TM7 (see Figure 1.5) and with membrane association known

to be essential for the catalytic activity of NEST (Atkins and Glynn, 2000) the inclusion of TM6 might be required to obtain functional YNEST.

Crude homogenates of *E.coli* BL21(DE3)pLysS carrying either the empty pET21b vector or pET-YNEST were obtained from induced mid-log cultures and assayed for phenyl valerate hydrolase activity. No increase in activity was detected in crude homogenates of *E.coli* expressing YNEST above that of *E.coli* containing the empty vector. This would indicate that either the polypeptide was not expressed in a functional form or that this portion of Yml059c is unable to hydrolyse this substrate.

Western blot analysis was performed on crude cellular extracts of *E.coli,* using an antibody directed to the N-terminal T7 tag of the recombinant protein. A polypeptide of the predicted size of YNEST (89kDa) could be detected in extracts of *E.coli* carrying the pET-YNEST plasmid but not in extracts of *E.coli* carrying the empty pET vector (see Figure 5.2). Therefore the YNEST peptide can be expressed in this system.

Western blot analysis using the anti-T7 antibody was used to determine that the peptide was soluble in 1% w/v of the denaturing detergent SDS but insoluble in 1% Triton (see Figure 5.2 and section 2.8.4). It has been shown for constructs of the catalytic domain of NTE expressed in *E.coli* that polypeptides soluble under non-denaturing conditions had PV hydrolase activity while those soluble only under denaturing conditions lacked this activity (Atkins and Glynn, 2000). By analogy this suggests that YNEST was not expressed in an active form but possibly as inactive inclusion bodies.

5.2.2 Yml059c has NTE-like phenyl valerate hydrolase activity

Crude yeast homogenates of the strains BY4743, BY4743 *yml059cΔ/Δ* and the chromosomal overexpression strains BY4743 P_{gal1}-*YML059c*/+, BY4743 P_{gal1}-*YML059c*-GFP/+, BY4743 P_{gal1}-GFP-*YML059c*/+ and BY4743 P_{gal1}-GFP-*YML059c*/P_{gal1}-GFP-*YML059c* (see Chapter 3 for generation of these strains) were assayed for PV hydrolase activity. Extracts obtained from either the BY4743 parental, or the BY4743 *yml059cΔ/Δ* null mutant strains displayed a background esterase activity of approximately 5 nmol of phenol $min^{-1}mg^{-1}$ with no significant difference between them. Extracts obtained from the chromosomal overexpression strains all showed significant increases in PV hydrolase activity above that of the parental level (see Table 5.1). Thus Yml059c shows similarity to NTE in its ability to hydrolyse the same artificial substrate, but natural expression levels of Yml059c are too low to allow the direct detection of this activity in crude homogenates of wild type yeast.

Assays were performed using particulate fractions of the same strains (see section 2.3.6). Using this method the mean activity of the BY4743 parental strain was marginally higher than that of the null mutant. Although an insufficient number of experiments were performed for this difference in mean activity to be considered significant, the activity of the parental strain was consistently higher (average 20%) than that of the null mutant in any single experiment. This repeatable difference was shown to be significant at the $p<0.01$ level using a Wilcoxon signed-rank test. This statistical test ranks the results of pairs of assays based on the magnitude of the difference in the results. Next the ranks are assigned a positive or negative sign based on which sample produced the higher result. The sum of the positive and negative ranks would be expected to be equal if there were no difference between the two samples. In this case, over seven repeated assays the difference was significant as determined from a Wilcoxon probability table.

The increase in the parental strain represents the PV hydrolase activity of Yml059c at endogenous expression levels. The activity directly attributable to Yml059c in the parental and overexpression strains was calculated by subtracting the background level of activity detected in the null mutant (see Table 5.1). Overexpression by introducing the *GAL1* promoter, with no GFP tag, to one allele of Yml059c caused a 20-fold increase in activity above the parental level. With the introduction of both the *GAL1* promoter and a C-terminal GFP tag the increase was only 8.5 times that of the parental strain; it is conceivable that the close proximity of the GFP tag to the catalytic domain inhibits the activity of the protein. The heterozygous overexpression strain with N-terminal GFP tag displayed activity nearly 30 times that of the parental strain and the equivalent homozygote possessed nearly double this figure. The activity of this homozygous N-terminally GFP tagged overexpression construct is approximately ¼ of that determined for particulate fractions of COS-7 cells overexpressing full length NTE (≈400 nmol of phenol $min^{-1}mg^{-1}$; Li *et al*, 2003).

The dramatic increases in functional enzyme levels achieved by overexpression of Yml059c enabled further study of the protein's biochemical activity.

5.2.3 The activity of Yml059c is enriched in the particulate fraction

Particulate and soluble fractions of BY4743, BY4743 *yml059cΔ/Δ* and the chromosomal overexpresser BY4743 P_{gal1}-*GFP-YML059c*/P_{gal1}-*GFP-YML059c* were assayed for their ability to hydrolyse PV. Overexpression of Yml059c resulted in only a minor increase in PV hydrolase activity in the soluble fraction but a marked increase in activity was detectable in the particulate fraction (see Table 5.2). 96% of the total PV hydrolase activity of the overexpression strain was in the particulate fraction. This enrichment of activity in the

particulate fraction indicates that Yml059c is likely to be associated with cellular membranes.

5.2.4 Conditions used for assaying NTE activity are appropriate for Yml059c

Historically, assays of NTE's activity have been conducted at pH8 and 37°C (Johnson, 1977). As the preferred growth temperature of yeast is 28-30°C experiments were performed to determine how appropriate the standard conditions for the NTE assay are for use with the yeast protein Yml059c. The high level of activity of the overexpresser BY4743 *P_{gal1}-GFP-YML059c*/*P_{gal1}-GFP-YML059c* compared to the parental strain provides a means of determining the optimal reaction conditions for assaying Yml059c. PV hydrolase assays were carried out using particulate fractions of BY4743, BY4743 *yml059cΔ/Δ* and BY4743 *P_{gal1}-GFP-YML059c*/*P_{gal1}-GFP-YML059c* at 37°C and pH3, 4, 5, 6, 7 and 8 (see section 2.3.6). Experiments were also conducted at 30°C and 37°C with a fixed pH of 8 (see Figure 5.3).

When the reaction temperature was fixed at 37°C and the pH varied, Yml059c displayed maximal activity at pH7. The pH8 conditions routinely used for the analysis of NTE, reduced the PV hydrolase activity of Yml059c to 91% of this maximal value. Therefore although pH7 is optimal, pH8 conditions are still appropriate. Performing the reactions at pH6 or lower caused a radical reduction in the activity of Yml059c. With a fixed pH of 8 and varied reaction temperatures activity at 30°C was marginally higher than at 37°C. However, from this experiment 37°C was still an appropriate reaction temperature as activity was 84% of that at 30°C.

5.3 Attempts to make a direct biochemical comparison of Yml059c and NTE

A fair biochemical comparison of the activities of NTE and Yml059c cannot be made unless both proteins are being expressed in the same system. If a comparison were made of NTE expressed in mammalian cells with Yml059c expressed in yeast, any difference in biochemistry could be attributable to the system in which the protein is being expressed rather than any specific difference in activity. By using appropriate plasmid expression systems, attempts were made to express each in both yeast and mammalian cells.

5.3.1 *YML059c* could not be functionally expressed in yeast using the constitutive expression vector pG3

PV hydrolase assays were carried out on crude homogenates of BY4733 carrying pG3-*YML059c* or the empty pG3 vector. The plasmid pG3-*YML059c* conferred no significant increase in PV hydrolase activity above that of the empty vector (approximately 7.6 nmol of phenol $min^{-1}mg^{-1}$). This plasmid system is therefore failing to overexpress the recombinant polypeptide sufficiently to allow the detection of an increase in activity, or failing to express the product in a functional form.

5.3.2 Neither *YML059c* or NTE were functionally expressed in yeast using the galactose-regulatable vector pEMBLyex4

Crude homogenates of the yeast strain BY4743 carrying the overexpression plasmids pEMBL-*YML059c* or pEMBL-NTE or the vector control pEMBLyex4 were assayed for PV hydrolase activity. Neither *YML059c* nor NTE overexpression constructs conferred a significant increase in activity above that of the empty vector (approximately 5 nmol of phenol $min^{-1}mg^{-1}$).

Northern blot analysis demonstrated that this expression system transcribed *YML059c* at a similar level to the biochemically active chromosomal expression system BY4743 P_{gal1}-GFP-*YML059c*/+ (see Figure 3.11). Despite this successful overexpression at the transcriptional level the pEMBLyex4 based system failed to express a polypeptide with detectable esterase activity.

5.3.3 NTE could not be functionally expressed in yeast using the expression vectors pYC2/CT or pYES2/CT

Western blot analysis was used to show that the constructs pYC2/CT-NTE-GFP and pYES2/CT-NTE-GFP, for the expression of NTE in yeast, failed to produce a stable polypeptide (see section 3.6.3).

5.3.4 *YML059c* could not be functionally expressed in mammalian cells using the expression vector pEGFP-N1

Expressing a functional NTE polypeptide in yeast had not proved possible, precluding a direct biochemical comparison of NTE and Yml059c in this system. As NTE has been successfully overexpressed in mammalian cells (Li *et al.*, 2003), expressing *YML059c* in COS-7 and Hela cells was attempted as an alternative method for comparing each in the same system. For this pEGFP-*YML059c* was used, but no stable Yml059c polypeptide was produced by this strategy (see section 3.8).

5.4 Serine 1406 of Yml059c is essential for catalysis

Transfer of chromosomal expression constructs by PCR to the yeast cloning vector pRS416 was used to generate the *YML059c* overexpression plasmids pRS416-P_{gal1}-*YML059c* and pRS416-P_{gal1}-GFP-*YML059c* (see section 3.6.4). Particulate fractions of the yeast strain BY4743 carrying the plasmids pRS416, pRS416-P_{gal1}-*YML059c* and pRS416-P_{gal1}-GFP-*YML059c* were assayed for PV hydrolase activity. Yeast containing the overexpression constructs displayed significantly higher levels of activity than yeast carrying the empty vector (see Table 5.3).

Site directed mutagenesis was used to replace serine 1406 of Yml059c (the putative active site serine) in pRS416-P_{gal1}-GFP-*YML059c* with an alanine residue, generating pRS416-P_{gal1}-GFP-*YML059c*(S1406A) (see section 3.7). This construct was used to determine whether this serine residue is essential for catalysis.

Particulate fractions of BY4743 carrying the plasmids pRS416, pRS416-P_{gal1}-GFP-*YML059c* or pRS416-P_{gal1}-GFP-*YML059c*(S1406A) were assayed for PV hydrolase activity. The wildtype overexpression plasmid conferred approximately 5 times the PV hydrolase activity of the vector control, whereas the serine mutant conferred no significant increase in activity (see Table 5.3). Yeast containing either the serine mutant or wildtype overexpression construct possessed equivalent levels of Yml059c polypeptide, as determined by GFP fluorescence levels in live cells (see Figure 5.10) and anti-GFP western blotting of particulate fractions (see Figure 3.16). Serine 1406 of Yml059c is therefore the essential active site serine.

5.5 Yml059c is inhibited by OPs in a similar fashion to NTE

Experiments were performed to determine if Yml059c was sensitive to compounds known to inhibit the activity of NTE. Particulate fractions of BY4743, BY4743 *yml059cΔ/Δ,* and BY4743 P_{gal1}-*GFP-YML059c*/P_{gal1}-*GFP-YML059c* were assayed for PV hydrolase activity after preincubation with varying concentrations of mipafox, PMSF, DFP and PSP. The inhibitors had only a negligible affect on the activities of the null and parental strains, and no significant difference could be observed between them. The activity of Yml059c in the particulate fraction of BY4743 P_{gal1}-*GFP-YML059c*/P_{gal1}-*GFP-YML059c* displayed the same rank order to inhibition by these compounds as had been previously determined for NTE (Atkins and Glynn, 2000), with PSP being the most potent followed by DFP, then mipafox and PMSF being the least (Figure 5.4).

5.6 Yml059c reacts with the radiolabelled OP, [^{3}H]Di-isopropyl fluorophosphate

Experiments were conducted to determine whether Yml059c can react with the radiolabelled OP [^{3}H]DFP. Reaction with a radiolabelled inhibitor could provide a means of quantifying the Yml059c protein. Particulate fractions of BY4743, BY4743 *yml059cΔ/Δ,* and BY4743 P_{gal1}-*GFP-YML059c*/P_{gal1}-*GFP-YML059c* were incubated with 5μM [^{3}H]DFP at 37°C for 20 and 60min. Each was also incubated without [^{3}H]DFP over 0, 20 and 60min. PV hydrolase assays found the activities of the parental and null mutant strains to be unaffected by DFP but that 20 and 60min incubation reduced the activity of the overexpresser by 65% and 85% respectively, compared to samples incubated over the same time in the absence of [^{3}H]DFP. A decrease in activity over time (7% after 20min, 14% after 60min) was also observed in the absence of any inhibitor, suggesting degradation of the active enzyme was occurring. Western blot analysis of samples after 0, 20 and 60min incubations confirmed a visible decrease of full length Yml059c polypeptide over time (see Figure 5.5).

After [^{3}H]DFP labelling, the samples were separated by SDS-PAGE. Labelled proteins were then imaged using a micro-channel plate detector (Lees and Richards, 1999) and quantified by cutting the gel into 3mm slices before measuring in a scintillation counter.

From the imaging, it is clear that more radiolabel has been incorporated into the overexpresser than the parental or null mutant strain, therefore Yml059c has been successfully labelled with [^{3}H]DFP (see Figure 5.6). The 60min incubation results in marginally greater incorporation than the 20min incubation. In agreement with the western blot analysis, only a fraction of the full-length polypeptide remains, with the majority of the labelled protein forming a smear of varying intensity. Therefore, despite a degree of degradation, much of the enzyme remains catalytically active and able to react with the radiolabelled inhibitor. At least one other protein present in yeast can react with [^{3}H]DFP, as shown by a distinct labelled product of approximately 60kDa present in all three samples.

The results of scintillation counting agree with the imaging in that the areas of intense labelling correspond, greater overall activity is evident in the overexpression strain and that increased incubation time results in a greater incorporation (see Figure 5.6). Using the following calculation, scintillation counting of the [^{3}H]DFP labelled samples provides a means of roughly estimating the quantity of catalytically active Yml059c that is present in the particulate fraction of BY4743 P_{gal1}-*GFP-YML059c*/P_{gal1}-*GFP-YML059c*:

$$\text{pmol of Yml059c per mg of particulate fraction} = \frac{100 \times (o - n)}{s \times p \times i}$$

Where: o = total disintegrations per minute (dpm) for the overexpression strain
n = total dpm for the null mutant strain
s = the specific activity of [^{3}H]DFP (18648 dpm pmol^{-1})
p = mg of particulate fraction loaded (in this case 0.057)
i = percentage inhibition of PV hydrolase activity

Using the above calculation with the results of both the 20min and 60min incubation, the particulate fraction of the overexpression strain contained approximately 5pmol of Yml059c per mg of total protein.

5.7 Yml059c has phospholipase activity

Recent investigations assessing the activity of recombinant NEST towards a variety of membrane lipids have pointed to the physiological substrate of NTE being a lysophospholipid (van Tienhoven *et al.*, 2002). Experiments were performed in order to determine whether Yml059c was also able to act as a lysophospholipase.

Particulate fractions of BY4743, BY4743 *yml059cΔ/Δ,* and BY4743 P_{gal1}-GFP-*YML059c*/P_{gal1}-GFP-*YML059c* were assessed for their ability to hydrolyse 1-palmitoyl-lysophosphatidylcholine, previously shown to be a substrate of NEST. Extracts were incubated for 0 and 3min with varying concentrations of PLPC, after which the free fatty acid content of each sample was measured (see sections 2.8.8 and 2.8.9). Liberated FFA was determined by subtracting the 0 time point result for each concentration from that produced over 3min. No significant PLPC hydrolase activity was detectable in the null mutant or wildtype extracts. The particulate fraction obtained from the *YML059c* overexpression strain clearly possessed lysophospholipase activity, liberating increasing FFA dependent upon PLPC concentration. Lineweaver-Burk transformations (1/v versus 1/s) of these data fit to a straight line, allowing the determination of kinetic values for the catalysis of FFA liberation from PLPC by Yml059c (see Figure 5.7). For this reaction K_m = 0.2mM compared to the value previously determined for NEST of 0.054mM (van Tienhoven *et al.*, 2002). For this reaction, using Yml059c in a heterogeneous preparation V_{max} = 71nmol min^{-1}mg^{-1}.

5.8 Yml059c: cAMP binding assays

Experiments were performed to determine whether the putative regulatory domain of Yml059c is able to bind cAMP and might therefore provide a possible regulatory mechanism. For this a [^{3}H]cAMP-binding filter assay was used to assess whether

overexpressing Yml059c would confer an increased capacity for cAMP-binding in yeast extracts. The basis of this assay is to determine whether radioactivity remains associated with filter membranes through which samples incubated with [^{3}H]cAMP have been passed. Retention of the radioactivity on the filter implies that the sample has cAMP binding properties.

To validate the method, two proteins known to bind cAMP were employed as controls; human PKA-R1α, the regulatory subunit of human protein kinase A (PKA)(reviewed in Amieux and McKnight, 2002) and *BCY1*, the regulatory subunit of yeast PKA (Hixson and Krebs, 1980; Johnson *et al.*, 1987). Purified recombinant PKA-R1α (a gift from Yong Li) was used to ensure the assay could detect binding to cAMP. Bcy1 was overexpressed in yeast to determine whether overexpression of a cAMP binding protein was a valid method of assessing a functional binding domain, using this assay (see section 3.9).

An initial experiment confirmed the binding of [^{3}H]cAMP to PKA-R1α and overexpressed Bcy1 in particulate yeast fractions, but failed to detect any increase in [^{3}H]cAMP-binding to extracts of yeast overexpressing Yml059c, above that of the parental or *yml059c* null mutant (data not shown). Further experiments were performed with the inclusion of saturated ammonium sulphate (32% v/v) in the binding reaction; a modification suggested to stabilise any [^{3}H]cAMP-protein interaction (Van Haastert, 1985).

The following binding reactions were performed with ammonium sulphate, and each containing 0.4μM [^{3}H]cAMP: particulate fractions of BY4743, BY4743 *yml059cΔ/Δ,* BY4743 P_{gal1}-GFP-*YML059c*/P_{gal1}-GFP-*YML059c,* BY4743 + pYC2/CT and BY4743 + pYC2/CT-*BCY1*. Again particulate fractions of BY4743 + pYC2/CT-*BCY1* bound significantly more [^{3}H]cAMP than the vector control. With the addition of ammonium sulphate to the binding reaction, BY4743 P_{gal1}-GFP-*YML059c*/P_{gal1}-GFP-*YML059c* appears to bind marginally more than the parental or null mutant strains (see Table 5.4).

To assess the sensitivity of the assay and any inhibitory affect of the presence of yeast extracts, the following samples were also included in the above experiment: 3.2pmol of PKA-R1α and 3.2, 1.6, 0.8, 0.4 and 0.2 pmol of PKA-R1α in the presence of 0.1mg of BY4743 particulate fraction.

The quantity of [^{3}H]cAMP binding to 3.2pmol PKA-R1α in the presence of BY4743 particulate fraction (1.20pmol) was compared to that for PKA-R1α alone (0.80pmol) and that of the yeast extract alone (0.12pmol). Clearly the inclusion of yeast extract does not inhibit the binding reaction; in this case, the effect of combining the purified protein and the yeast

preparation is slightly more than additive. The sensitivity of the assay was determined by subtracting the result for the yeast extract alone from the results obtained using a range of PKA-R1α concentrations in the presence of the particulate yeast fraction. Under these conditions as little as 0.2pmol of PKA-R1α could be detected (see Figure 5.8). By labelling with [^{3}H]DFP the particulate fraction of the overexpression strain was calculated to contain approximately 5pmol of catalytically active Yml059c per mg (see section 5.6). With each assay containing 0.1mg of yeast particulate fraction, approximately 0.5pmol of active Yml059c is present. Assuming that the number of catalytically active molecules present is indicative of the number of cAMP binding sites and that Yml059c binds with an affinity similar to PKA-R1α, then detection of cAMP-binding using this assay should be feasible.

Binding of [^{3}H]cAMP to Yml059c was further investigated by performing the assay using a range of [^{3}H]cAMP concentrations. Particulate fractions of BY4743 *yml059cΔ/Δ,* BY4743 P_{gal1}-GFP-*YML059c*/P_{gal1}-GFP-*YML059c,* BY4743 + pYC2/CT and BY4743 + pYC2/CT-*BCY1* were assayed for binding in the presence of 0.1, 0.5, 1, 2.5, and 5 μM [^{3}H]cAMP. These results were in agreement with the previous experiment; the *BCY1* overexpresser displayed the greatest binding to [^{3}H]cAMP, the *YML059c* overexpresser bound less and the null mutant and vector control both displayed an almost identical low level of binding.

Binding of [^{3}H]cAMP to Yml059c and Bcy1 was calculated by subtracting the results for the null mutant strain and vector control from those of the Yml059c and Bcy1 overexpression strains respectively. Scatchard transformations of these data (bound cAMP/free cAMP versus bound cAMP) were used to assess the binding affinity of both Yml059c and Bcy1 (see Figure 5.9). The transformation for Bcy1 approximately fits to a straight line, and from the negative reciprocal gradient the K_d was calculated as 650nM; compared to the figure of 76nM determined for purified Bcy1 (Johnson *et al.*, 1987). The transformation for Yml059c fit to a straight line rather less well but indicated the K_d to be approximately 850nM. From the x-intercept, the number of binding sites and therefore molecules of Yml059c was calculated to be approximately 0.8pmol. This is in close agreement with the result from the [^{3}H]DFP labelling experiment, that the 0.2mg of extract used in each assay should contain 1pmol of Yml059c. From these preliminary investigations it would appear that Yml059c does bind cAMP, with an affinity marginally lower than that of Bcy1.

5.9 Visualisation of GFP-tagged Yml059c in yeast

In order to visualise the GFP-tagged protein constructs within the yeast cell confocal microscopy images were taken of yeast cultures bearing the following chromosomal and plasmid based GFP constructs:

BY4743
BY4743 *YML059c*-GFP/+
BY4743 P_{gal1}-YML059c-GFP/+
BY4743 P_{gal1}-GFP-*YML059c*/+
BY4743 P_{gal1}-GFP-*YML059c*/P_{gal1}-GFP-*YML059c*
BY4743 + pRS416
BY4743 + pRS416-P_{gal1}-GFP-*YML059c*
BY4743 + pRS416-P_{gal1}-GFP-*YML059c*(S1406A)

As no fluorescence would be expected from BY4743 and BY4743 + pRS416 these were included as negative controls (see Figure 5.10).

No fluorescence was detectable from the parental strain (BY4743) or that carrying the vector control (BY4743 + pRS416). There was also none detectable in the BY4743 *YML059c*-GFP/+ strain, where the GFP fusion is driven by the native *YML059c* promoter. Those carrying chromosomal overexpression constructs (BY4743 P_{gal1}-*YML059c*-GFP/+, BY4743 P_{gal1}-GFP-*YML059c*/+ and BY4743 P_{gal1}-GFP-*YML059c*/P_{gal1}-GFP-*YML059c*) displayed levels of fluorescence significantly above that of the background.

As overexpression via the *GAL1* promoter was necessary to visualise the GFP-fusion protein, it would seem that the endogenous Yml059c expression level is insufficient for detection by this means. This would seem to be corroborated by the northern blot data (see Figure 3.7) showing that the endogenous transcriptional level of Yml059c is at least 20-fold lower than that achieved with one allele overexpressed via the *GAL1* promoter. Western blot analysis was also unable to detect the GFP fusion driven by the native promoter (data not shown).

Although the fluorescence pattern for the P_{gal1} driven heterozygotes carrying either an N or C terminal GFP tag is similar, the pattern for the C terminal fusion appears more localised and punctate. With the PV assay data showing that the heterozygote N terminal fusion possesses more than double the activity of the heterozygote C terminal fusion, then perhaps the more punctate localisation represents inactive aggregates.

Although bleaching of the fluorescence during the image capture reduces the apparent difference in intensity, the homozygotic overexpression strain, with N terminal fusion, displayed approximately double the fluorescence of the corresponding heterozygote. This is in agreement with the PV assay data (see Table 5.1), in that two copies of the overexpressing locus doubles the expression level and doubles the amount of functional enzyme.

Both native and S1406A plasmid-based overexpression constructs appear to display an identical localisation pattern, indicating that the catalytic activity of Yml059c is not essential for its normal subcellular localisation. One interesting observation is that while the fluorescence levels of individual cells appeared uniform for the chromosomal based overexpressers, it varied dramatically between cells carrying the plasmid overexpression system; ranging from some cells displaying no fluorescence, to others appearing brighter than the homozygotic chromosomal expression strain. The accepted copy number for centromeric yeast plasmids is 1-2 copies per cell (Guthrie and Fink, 1991). This variation alone could not account for the observed diversity.

Without co-localising with known stains or antibodies it is difficult to definitively determine the subcellular localisation of Yml059c. From these images it is clear that the tagged protein is not diffuse among the cytoplasm or confined to the nucleus, and therefore appears to accumulate in some intracellular organelle. A study in which a large number of yeast proteins were individually localised using an epitope tagged transposon also reported a punctate cytoplasmic staining for Yml059c (Kumar *et al.*, 2002).

5.10 Discussion

Through overexpression of the full-length protein in yeast, Yml059c has been shown to hydrolyse the same artificial substrate as NTE. This activity is enriched in the particulate fraction suggesting that, like NTE, Yml059c is associated with cellular membranes. This evidence for the membrane association of Yml059c could be further supported by phase partitioning experiments using the detergent Triton X-114. This detergent is soluble in aqueous buffers at 0°C but separates into a distinct detergent and aqueous phase at 20°C. In such conditions integral membrane proteins will typically partition into the detergent rich phase.

Similarities are evident between the catalytic activities of NTE and Yml059c in that both react with [^{3}H]DFP, both can hydrolyse the same artificial substrate and both display the same rank order to inhibition by DFP, PSP, PMSF and mipafox. However no direct biochemical comparison was possible due to the failure to express each in the same

system. In this study the catalytic domain of Yml059c could not be expressed in *E.coli* but it is possible that further attempts to express differing regions of Yml059c might yield a functional recombinant polypeptide. Expression of either NTE in yeast or Yml059c in mammalian cells also proved impossible, with each strategy failing to translate a stable polypeptide. However it is worth noting that achieving overexpression of Yml059c in yeast was not trivial when using a plasmid system (see sections 5.3.1and 5.3.2); so it may be the strategy employed that hampered the expression of NTE in yeast rather than any fundamental incompatibility.

Both western blot analysis and [^{3}H]DFP labelling of particulate fractions of yeast overexpressing GFP-tagged Yml059c showed that only a fraction of the extracted polypeptide was of the expected size (see Figure 5.5 and Figure 5.6). This suggests degradation had occurred either within the yeast cell or during or after the extraction process. Experiments conducted using older samples, extracted without protease inhibitors, showed that further degradation results in a complete loss of the full-length polypeptide. However, much of the catalytic activity remains, indicating that only a portion of the protein is required for catalysis (data not shown). [^{3}H]DFP labelling of samples prepared without protease inhibitors, showed a discrete labelled product of approximately 80kDa present in the overexpression strain but not the parental or null, rather than the smearing seen in Figure 5.6 (data not shown). Perhaps the catalytic site is located within a region that is resistant to proteolytic cleavage, possibly indicating its incorporation in to a cellular membrane.

Recently, NEST has been shown to possess lipase activity, hydrolysing phospholipids, monoacylglycerols and lysophospholipids (van Tienhoven *et al.*, 2002), with lysophospholipids being by far the preferred substrate ($Km \approx 0.05$mM). Like NEST, Yml059c can also hydrolyse the lysophospholipid PLPC at a somewhat reduced rate (Km = 0.2mM from one experiment), indicating a conserved activity towards this naturally occurring substrate. Further experiments using a variety of lipid substrates would need to be conducted in order to confirm that lysophospholipid was also its preferred substrate. From the PLPC hydrolase experiment, the negligible activity of the BY4743 parental strain did show some increase with increasing substrate concentration; this was not evident for the null mutant (data not shown). If further experiments could support this, then Yml059c may be the major lysophospholipase found in the particulate yeast fraction under these conditions. In collaboration with Günther Daum (Institut für Biochemie und Lebensmittelchemie, Technische Universität, Petergrasse, Austria) the various phospholipid constituents of BY4741 and BY4741 *yml059cΔ* were quantified and compared by the methods described by Daum *et al.* (1999). From this initial experiment lysophospholipid

represented 0.2% of the total phospholipid content of the *yml059cΔ* mutant, whereas no lysophospholipid was detectable in the parental strain. Also, overexpression of Yml059c has since been shown to confer a reduction in [^{14}C]-palmitate labelled lysophospholipid compared to that detected in the parental or *yml059cΔ* null mutant strain (Paul Glynn unpublished work). Although an indirect affect of Yml059c cannot be excluded, these data suggest that the cellular function of Yml059c involves hydrolysis of lysophospholipid.

The [^{3}H]cAMP-binding filter assay was able to show binding to overexpressed Bcy1 in yeast particulate fractions. Although the same method did seem to show some binding of [^{3}H]cAMP to Yml059c, it was far from robust. As stated previously, purified Bcy1 binds cAMP with an affinity of 76nM (Johnson *et al.*, 1987). Epac1, the recently identified Rap1-activating guanine exchange factor of higher eukaryotes that is directly activated by cAMP (de Rooij *et al.*, 1998), has a considerably lower affinity for cAMP, approximately 4μM (de Rooij *et al.*, 2000). If Yml059c were to bind cAMP with a similar affinity to that of Epac, detection of this binding by the methods used in this study might not be possible. Assays have shown that the PV hydrolase activity of chromosomal overexpression strains is increased when they also carry a Yml059c overexpression plasmid (data not shown). With the increase being additive, this method can be used to almost double the activity of the expression strain used for the [^{3}H]cAMP-binding experiments. Assuming that this is accompanied by a doubling in quantity of the regulatory domain, then this may improve the robustness of the Yml059 [^{3}H]cAMP-binding data. However, compelling evidence for the binding of the regulatory domain of Yml059c to [^{3}H]cAMP will remain difficult to achieve in such a heterogeneous preparation. If possible, the regulatory domain should be expressed as a recombinant protein in *E.coli* and the purified protein used to assess cAMP binding.

By overexpressing GFP-tagged constructs in COS-7 cells and using a combination of fluorescence microscopy and immunogold electron microscopy, NTE has been localised to the cytoplasmic surface of the endoplasmic reticulum (ER) membrane (Li *et al.*, 2003). However overexpression of full-length NTE in COS-7, HeLa or N2a cells caused fragmentation of the ER in the majority of cells. As no co-localising markers were used when visualising GFP-tagged Yml059c by fluorescence microscopy it is not possible to accurately ascertain its subcellular localisation, and with no ER specific marker any disruption to the ER morphology could not be determined.

Immunofluorescence of the ER-localised tSNARE Ufe1 could potentially provide an appropriate marker to test whether Yml059c is localised to the ER and to determine any affect that overexpression of Yml059c might have on the ER morphology. Alternative strategies for sub-cellular localisation include sub-cellular fractionation by centrifugation on

sucrose-density gradients using a method such as that used by Ossipov *et al*. (1999) or immunogold electron microscopy.

Table 5.1. PV hydrolase assay results using homogenates and particulate fractions of chromosomal overexpression strains

The results of PV hydrolase assays performed using crude homogenates and particulate membrane fractions of various yeast strains. The background activity detected in the null mutant was subtracted from each to determine the activity attributable to Yml059c. Results are the mean obtained from n separate assays and standard deviations are indicated in parentheses.

Strain	Activity (nmol phenol $min^{-1}mg^{-1}$)		
	Homogenate	Particulate Fraction	Yml059c activity
BY4743 *yml059cΔ/yml059cΔ*	4.71 n=1	6.96 (+/- 1.59) n=7	-
BY4743	5.16 (+/- 2.42) n=6	8.48 (+/- 1.91) n=8	1.52
BY4743 P_{gal1}-*YML059c*/+	12.29 n=1	36.40 (+/- 4.31) n=3	29.44
BY4743 P_{gal1}-*YML059c*-GFP/+	7.86 (+/- 1.25) n=2	19.63 (+/- 8.06) n=3	12.67
BY4743 P_{gal1}-GFP-*YML059c*/+	25.00 (+/- 5.52) n=6	48.75 (+/- 11.41) n=2	41.79
BY4743 P_{gal1}-GFP-*YML059c*/P_{gal1}-GFP-*YML059c*	41.55 n=1	105.44 (+/- 25.39) n=9	98.48

Table 5.2. PV hydrolase activity is enriched in the particulate fraction

The results of PV hydrolase assays performed using soluble and particulate membrane fractions of the *yml059cΔ* null mutant, the BY4743 parental strain and the BY4743 P_{gal1}-GFP-*YML059c*/P_{gal1}-GFP-*YML059c* overexpression strain. Data taken from a single assay.

	Activity (nmol phenol $min^{-1}mg^{-1}$)	
Strain	Soluble Fraction	Particulate Fraction
BY4743 *yml059cΔ/yml059cΔ*	3.5	7.6
BY4743	3.3	10.2
BY4743 P_{gal1}-GFP-*YML059c*/P_{gal1}-GFP-*YML059c*	5.8	140.5

Table 5.3. Phenyl valerate hydrolase activity conferred by plasmid-based Yml059c overexpression constructs: activity abolished by mutation of serine 1406

PV hydrolase assays were performed using particulate fractions of yeast carrying plasmid *YML059c* expression constructs. Results are the mean obtained from n separate assays and standard deviations are indicated in parentheses.

Strain	Activity (nmol phenol $min^{-1}mg^{-1}$)
BY4743 pRS416	8.53 (+/- 1.09) n=4
BY4743 pRS416-P_{gal1}-*YML059c*	86.11 (+/- 14.98) n=2
BY4743 pRS416-P_{gal1}-GFP-*YML059c*	45.88 (+/- 9.65) n=4
BY4743 pRS416-P_{gal1}-GFP-*YML059c*(S1406A)	9.09 (+/- 1.24) n=2

Table 5.4. Binding of [^{3}H]cAMP to yeast particulate fractions

Results of [^{3}H]cAMP-binding assays of particulate yeast fractions of the indicated strains. Results are taken from a single assay and represent means of duplicate determinations.

Strain	Bound [^{3}H]cAMP (pmol mg^{-1})
BY4743 *yml059cΔ/yml059cΔ*	1.2
BY4743	1.2
BY4743 P_{gal1}-GFP-*YML059c*/P_{gal1}-GFP-*YML059c*	1.7
BY4743 pYC2/CT	1.0
BY4743 pYC2/CT-*BCY1*	18.0

Figure 5.1. The region of Yml059c expressed in *E.coli*

The region of *YML059c* encoding the putative catalytic domain (residues 870-1640) was expressed in *E.coli* using the pET21b vector. The areas of Yml059c with similarity to NTE and NEST are indicated.

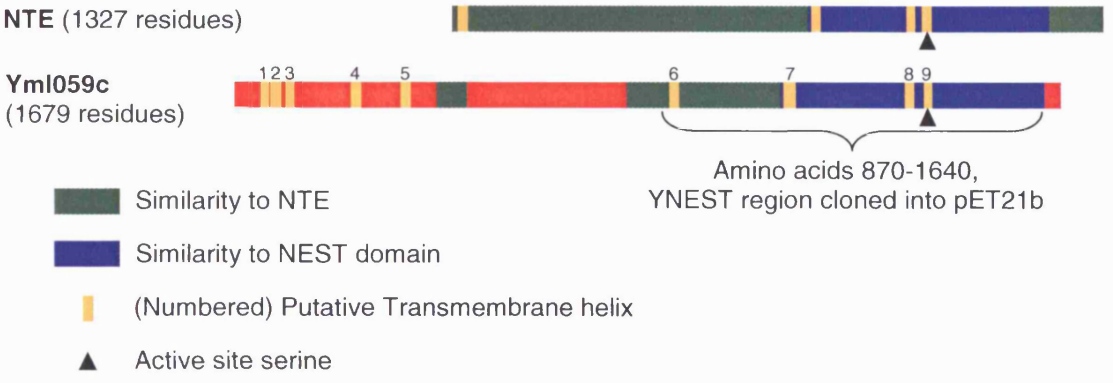

Figure 5.2. YNEST peptide expressed in *E.coli* is soluble in SDS but not Triton

Immunological detection of YNEST in extracts of *E.coli*, using Anti T7 antibody for the detection of T7 tag. The position and size (in kDa) of molecular weight markers are indicated.
A. Crude extracts of *E.coli* carrying the plasmid indicated above each lane.
B. Analysis of products solubilised by the indicated detergent after incubation with crude homogenates of *E.coli* carrying pET-YNEST.

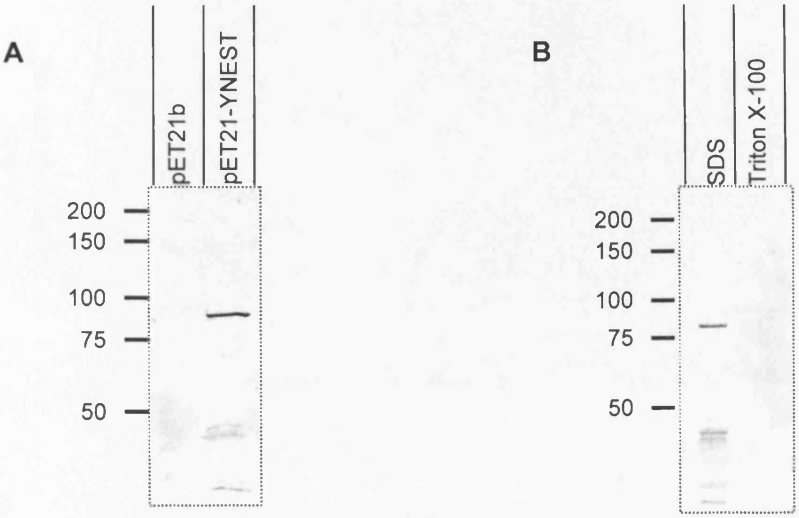

Figure 5.3. Phenyl valerate hydrolase activity of Yml059c at varying temperature and pH

Results of PV hydrolase assays carried out using particulate fractions of BY4743, BY4743 *yml059cΔ/Δ* and BY4743 P_{gal1}-GFP-*YML059c*/P_{gal1}-GFP-*YML059c* at varying pH (**A**) and temperature (**B**). All data taken from a single assay

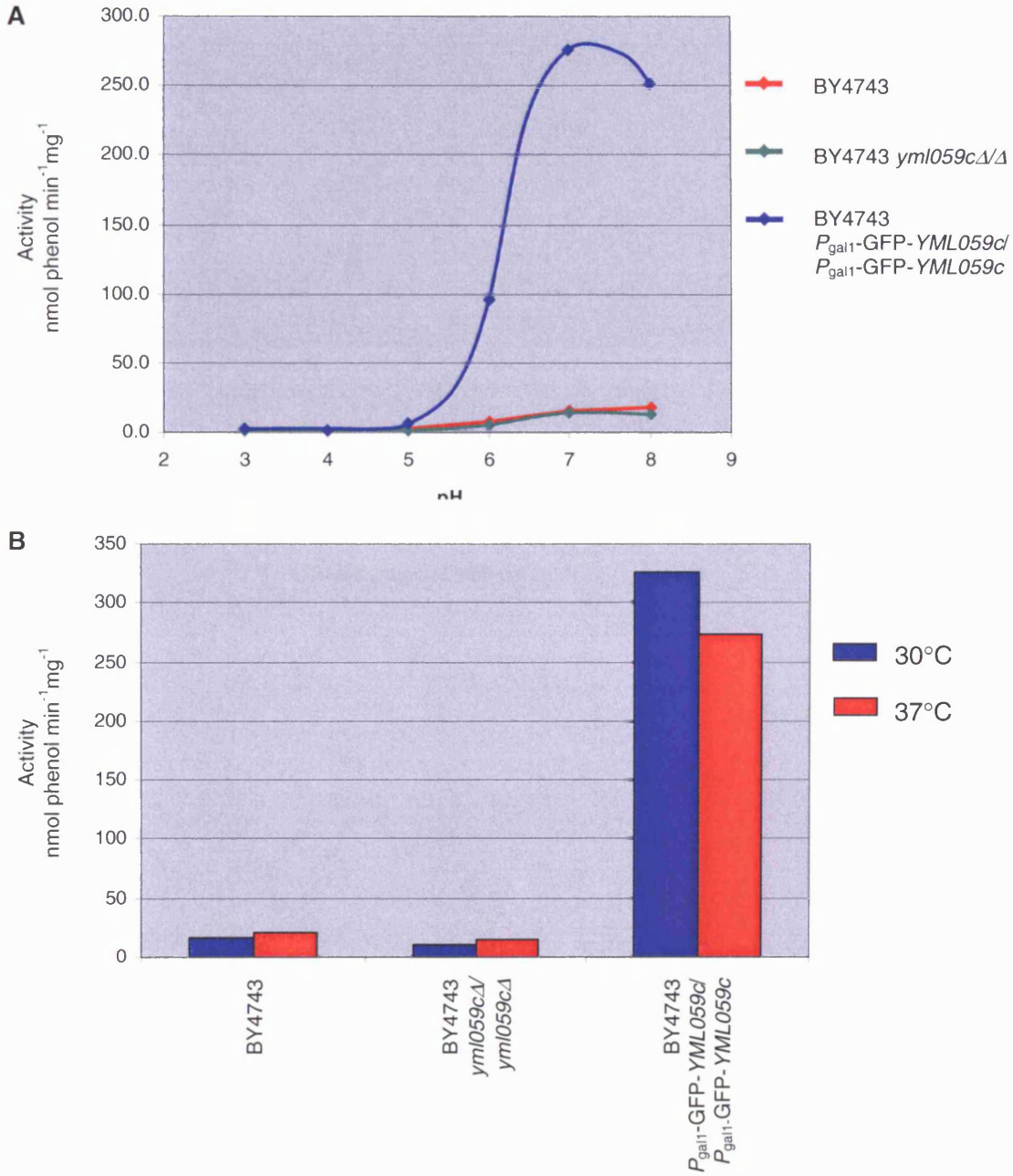

Figure 5.4. Inhibition of Yml059c esterase activity by known inhibitors of NTE

Results of PV hydrolase assays using particulate fractions of BY4743 P_{gal1}-GFP-*YML059c*/P_{gal1}-GFP-*YML059c* after a 20min preincubation with compounds known to inhibit NTE (Di-isopropylfluorophosphate, phenyl saligenin phosphate, Phenyl methylsulphonylfluoride and mipafox).

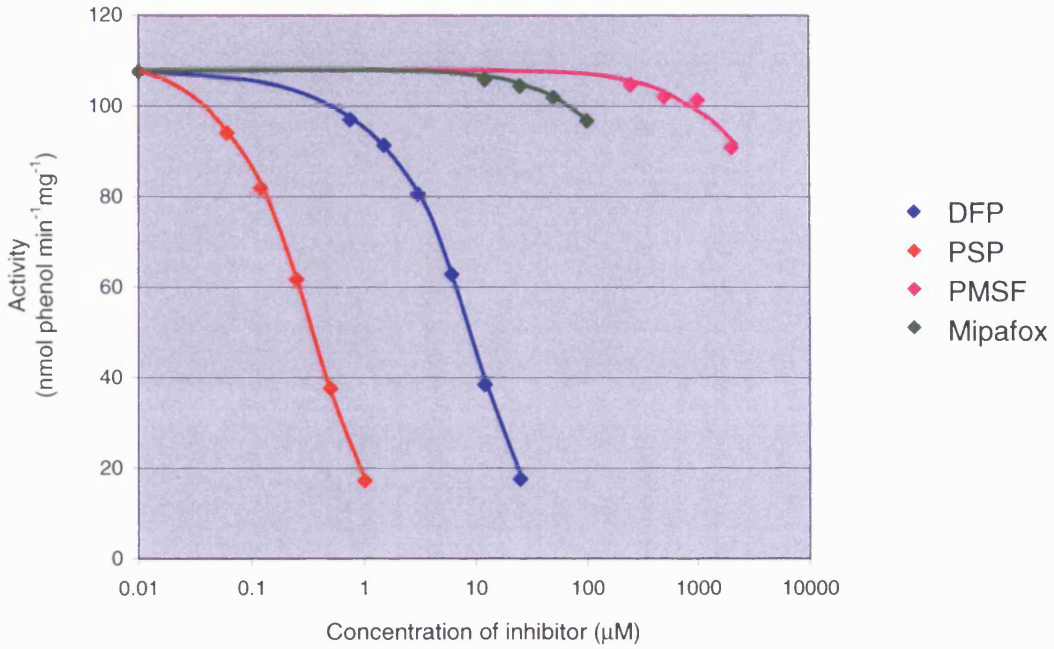

Figure 5.5. Western blot showing temperature stability of the GFP-Yml059c polypeptide

Result of western blot analysis of particulate fractions of BY4743, BY4743 *yml059cΔ/Δ*, and BY4743 P_{gal1}-GFP-*YML059c*/P_{gal1}-GFP-*YML059c* after 20 and 60min incubations with [^{3}H]DFP at 37°C. Samples from the BY4743 P_{gal1}-GFP-*YML059c*/P_{gal1}-GFP-*YML059c* overexpression strain are included in two lanes as zero time point controls. The expected location of the full length Yml059c polypeptide is shown.

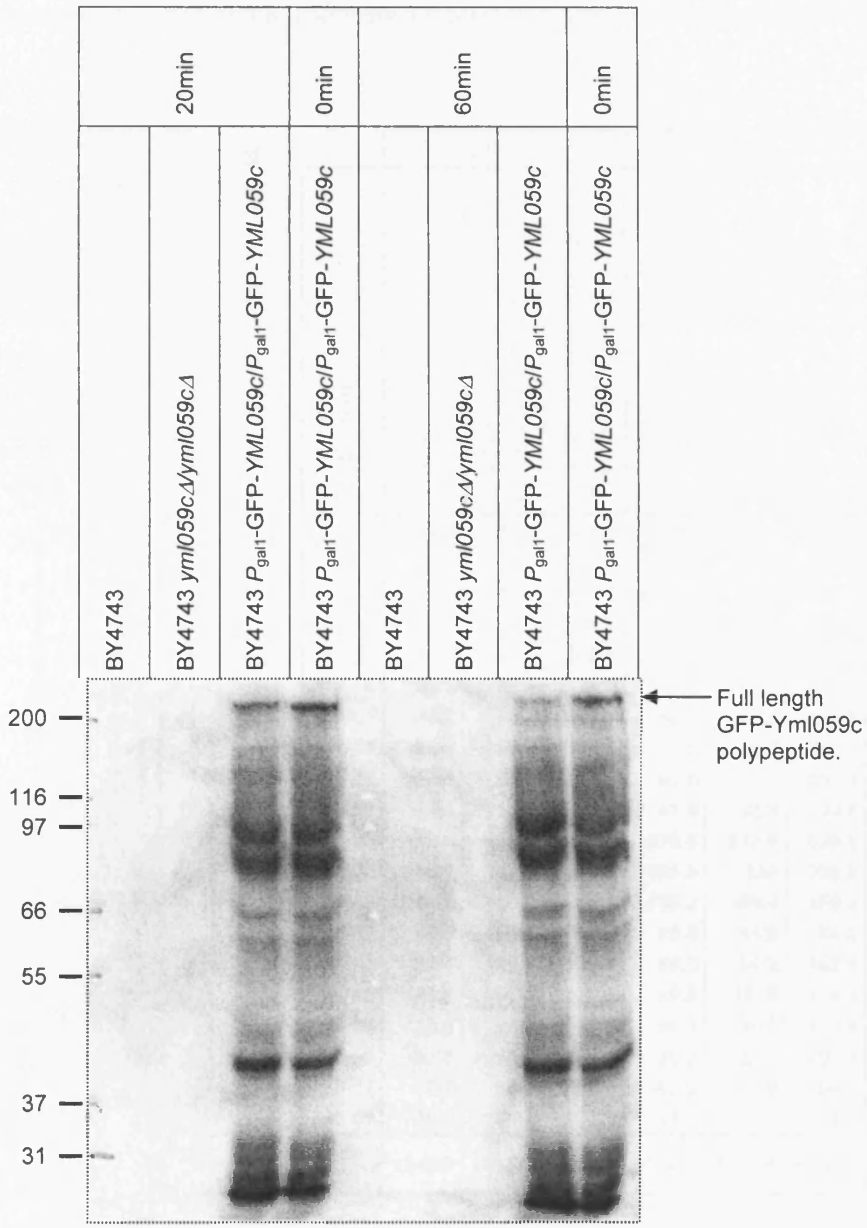

Figure 5.6. Imaging and quantification of [^{3}H]DFP-labelled yeast proteins

[^{3}H]DFP labelled particulate fractions were separated by SDS-PAGE before imaging using a micro-channel plate detector and quantifying by scintillation counting. **A.** Shows the image of the radiolabelled proteins **B.** Shows the results of scintillation counting in dpm (having subtracted the background counts). Results for each gel slice and the total counts in each lane are shown. The numbers to the right represent the size (in kDa) and relative position of the molecular weight markers. In each case the results are shown for both 20 and 60min incubations.

Indicates the predicted location of the full length GFP-Yml059c

Indicates the location of the unidentified protein that also reacts with [^{3}H]DFP

A

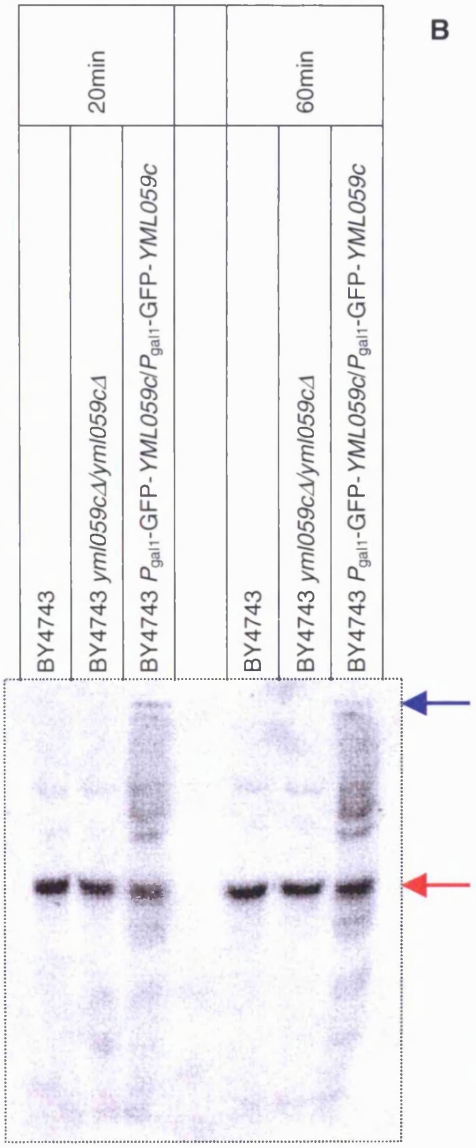

B

Gel Slice (mm)	20min			60min		
	BY4743	BY4743 *yml059cΔ/yml059cΔ*	BY4743 P_{gal1}-GFP-*YML059c*/ P_{gal1}-GFP-*YML059c*	BY4743	BY4743 *yml059cΔ/yml059cΔ*	BY4743 P_{gal1}-GFP-*YML059c*/ P_{gal1}-GFP-*YML059c*
1-3	57.8	18.3	407.3	53.3	48.7	390.4
4-6	48.1	57.1	275.8	48.8	25.9	652.5
7-9	17.5	40.8	732.0	56.2	41.3	594.3
10-12	22.7	6.3	302.7	87.1	44.8	574.1
13-15	52.5	41.0	300.4	60.6	57.3	440.0
16-18	48.9	52.9	255.3	18.8	60.0	549.3
19-21	65.2	73.3	379.4	63.8	67.8	457.8
22-24	52.5	37.6	318.1	72.6	35.3	348.5
25-27	36.5	21.1	241.6	57.6	33.5	153.9
28-30	64.8	13.9	56.4	41.9	32.9	94.8
31-33	459.8	472.0	433.7	219.8	512.6	629.9
34-36	136.6	124.6	370.2	421.9	152	258.6
37-39	69.6	46.0	248.3	125.3	80.4	159.3
40-42	48.9	15.1	63.7	25.8	44.8	64.0
43-45	22.4	29.0	102.6	64.0	56.2	163.4
46-48	41.8	57.1	172.1	49.8	14..6	119.1
49-51	10.5	24.5	114.7	44.9	39.4	130.4
52-54	57.6	65.6	76.4	30.2	22.7	107.2
55-57	6.5	56.3	80.7	65.5	10.9	84.4
58-60	26.0	64.7	153.5	61.1	107.7	134.3
Lane total	1346.2	1317.2	5084.9	1669.0	1488.8	6106.2

200
116
97
66
55
37
31

Figure 5.7. Yml059c hydrolyses PLPC

A. FFA liberated from PLPC was determined after a 3 min incubation with particulate fractions of BY4743, BY4743 *yml059cΔ/yml059cΔ* and BY4743 P_{gal1}-*GFP-YML059c*/P_{gal1}-*GFP-YML059c* **B.** Lineweaver-Burk transformations (1/v versus 1/s) of the data obtained from the overexpression strain allow the determination of kinetic values for the catalysis of FFA liberation from PLPC by Yml059c.
The x-axis intercept = $-1/K_m$
The gradient of the line = K_m/V_{max}

A

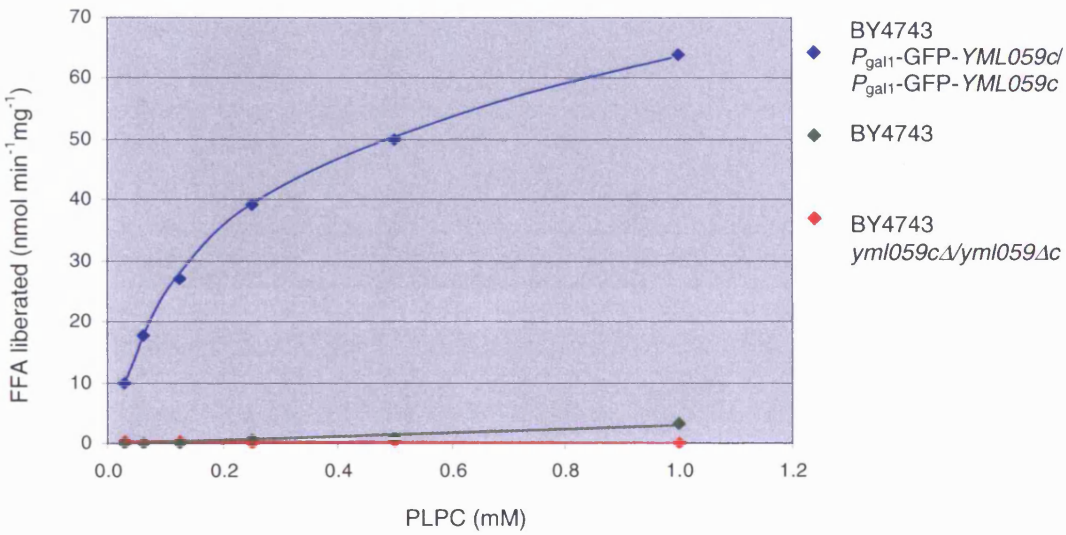

B

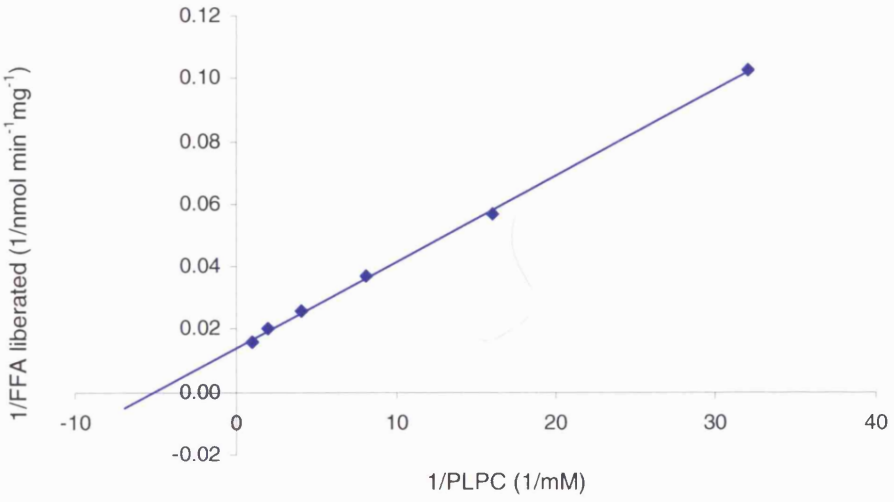

Figure 5.8. [^{3}H]cAMP-binding assay using a range of PKA-R1α concentrations

Decreasing quantities of PKA-R1α were assayed for [^{3}H]cAMP-binding in the presence of 0.2mg of BY4743 particulate fraction. The chart shows the bound [^{3}H]cAMP for each sample, minus the result (0.12pmol) for binding to yeast extract alone. Under these conditions as little as 0.2pmol of PKA-R1α can be detected. Data are means of duplicate determinations.

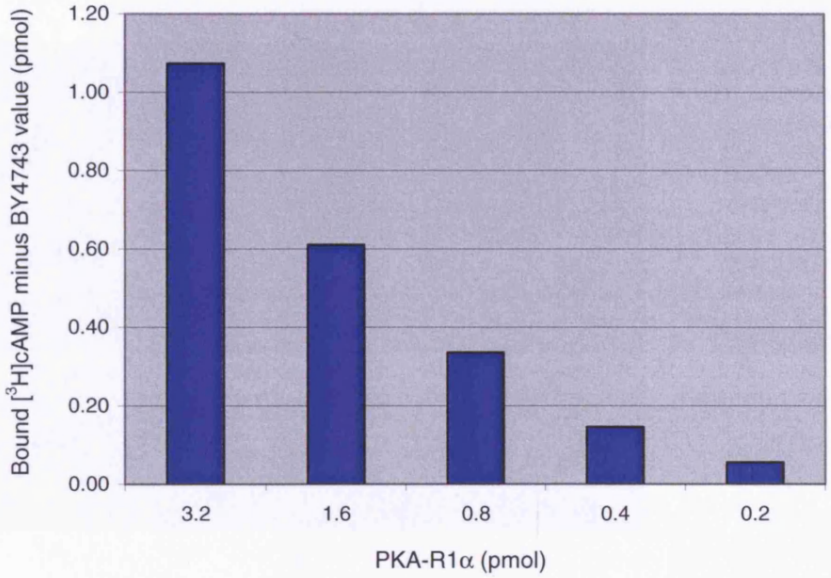

Figure 5.9. [^{3}H]cAMP binding filter assay

[^{3}H]cAMP binding assays were conducted using 0.2mg of particulate fractions for 0.1, 0.5, 1, 2.5, and 5 μM [^{3}H]cAMP concentrations. **A.** shows the bound [^{3}H]cAMP per mg of protein for each strain. **B.** [^{3}H]cAMP bound to Bcy1 was calculated by subtracting the result for the vector control from that carrying pYC2/CT-*BCY1*. **C.** [^{3}H]cAMP bound to Yml059c was calculated by subtracting the result for the null mutant from that of the *YML059c* overexpression strain. **D.** and **E.** show the respective Scatchard transformations.

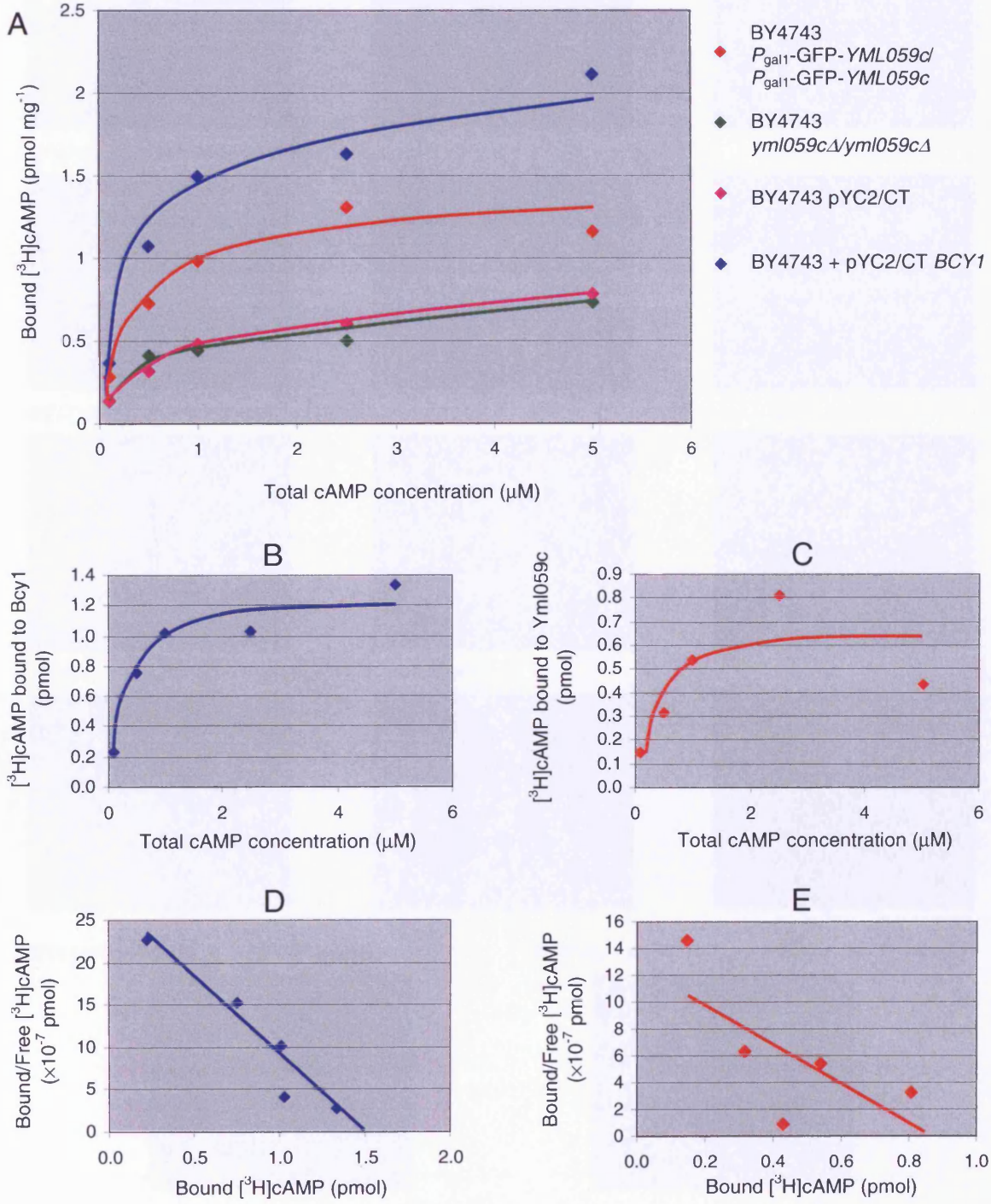

Figure 5.10. Confocal microscopy of GFP-tagged Yml059c in yeast

For each of the chromosomal overexpression strains a low-power image is shown (lefl) and two high-power images (centre and right). For all other strains only one low-power image is shown.

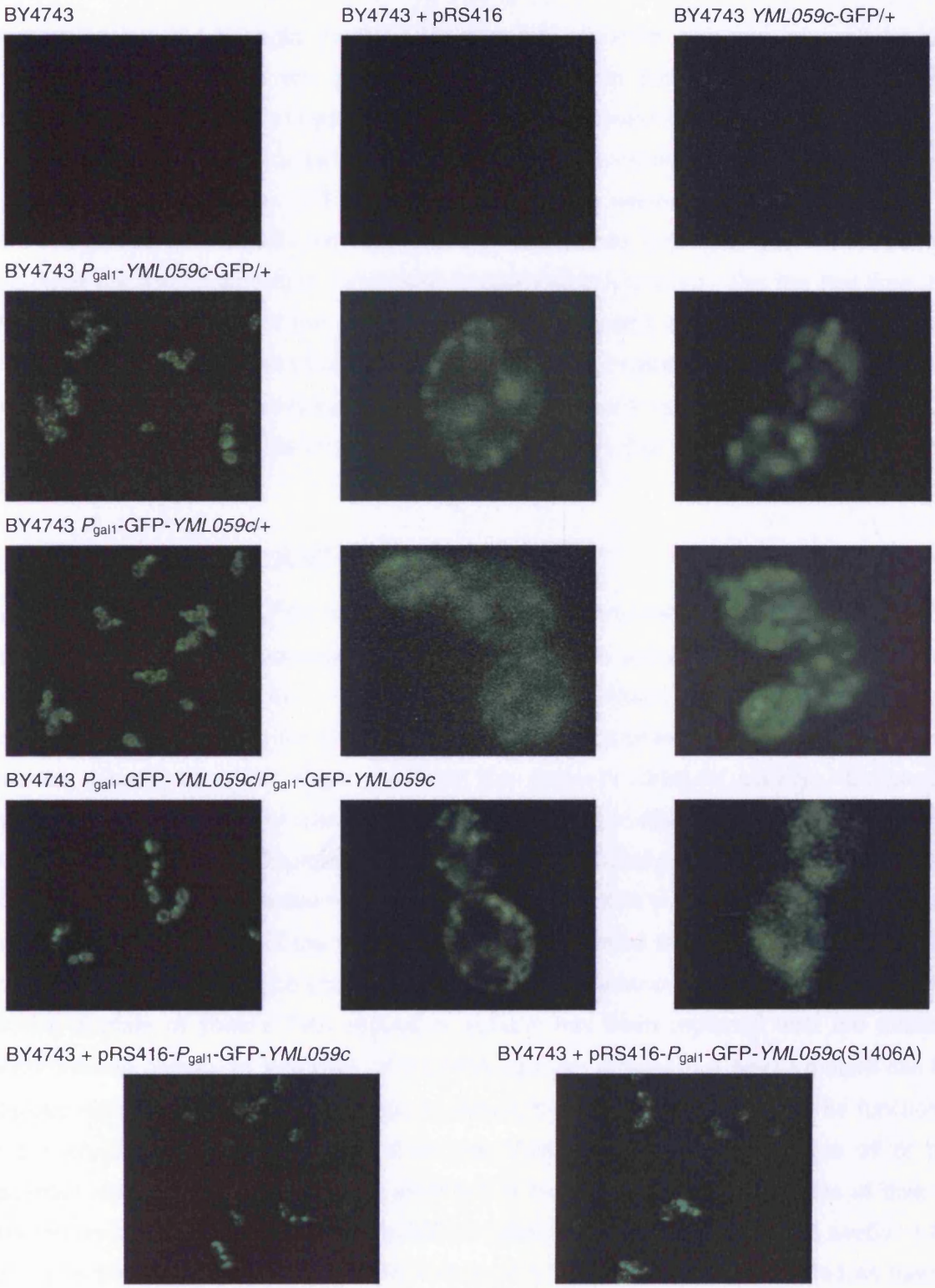

Chapter 6: General Discussion

6.1 Yml059c is the yeast homologue of NTE

Overexpression of full-length Yml059c in yeast has provided a means of exploring the biochemical properties of this previously uncharacterised protein. Using this method, Yml059c has been shown to hydrolyse the same artificial ester substrate as NTE *in vitro*, in a manner dependent upon a serine residue that lies in the corresponding location to NTE's essential active site serine. Like NTE, Yml059c has the same rank order to inhibition by OPs and can be labelled with radioactive DFP. Furthermore, both NTE and Yml059c avidly hydrolyse the lysophospholipid 1-palmitoyl-lysophosphatidylcholine. For the first time, the high sequence similarity of the most evolutionarily separated eukaryotic members of the NTE family has been shown to confer not only a conserved catalytic mechanism but also an overlapping substrate specificity. The tentative conclusion can now be drawn that the cellular role of NTE is to perform a biochemical function that is also conducted in yeast cells.

6.2 Regulation by cAMP

In this study, assays of [^{3}H]cAMP binding to yeast particulate fractions obtained from parental or *YML059c* overexpression strains were used to ascertain whether Yml059c has any cAMP binding capacity. Although not conclusive, these experiments suggest that Yml059c has some affinity for cAMP; therefore providing a possible regulatory mechanism whereby binding of cAMP might modulate this protein's catalytic activity. Conclusive evidence for this regulatory mechanism would represent a significant step forward in the characterisation of the NTE protein family. As stated previously, robust quantification of the binding of cAMP to the putative regulatory domain of Yml059c would require binding assays using the relevant region of the protein obtained in a purified form. A possible alternative qualitative approach might be achieved by generating a chimeric protein in which the cAMP-binding domain of yeast's PKA regulatory subunit has been replaced with the putative cAMP-binding domain of Yml059c. If the PKA catalytic activity of a *bcy1Δ* mutant can be glucose regulated when expressing this construct, then the binding site must be functional in this context. It certainly seems likely that Yml059c might bind cAMP as all of the essential residues for cAMP binding identified in the PKA regulatory subunits of diverse species are conserved in site 'B' of Yml059c's putative regulatory domain (see section 1.8). Also Yml059c is the only yeast protein besides Bcy1 that PSI-BLAST identified as having similarity to the cAMP binding site of PKA.

One of the *swiss cheese* mutant fly strains characterised by Kretzschmar *et al.* (1997) provides evidence supporting a requirement for cAMP binding for the function of this protein family. The strain carrying a G to A transition at base 1942 (relative to the start codon of *sws*) resulted in a mutant phenotype equal in severity to that of a mutant that expressed a truncated polypeptide lacking ¾ of its wild type length. This point mutation causes a glycine to arginine missense mutation at residue 648. This glycine lies within the putative regulatory domain and corresponds to one of the few invariant residues common to the cAMP binding sites of CAP, PKA-R and Epac and has been suggested to be an essential structural feature (Shabb and Corbin, 1992). That this mutation should result in as severe a phenotype as a major truncation of the protein indicates the importance of the regulatory domain to the protein's physiological function.

If the regulatory domain of Yml059c does bind to cAMP then the next question that must be addressed is whether this binding can modulate its catalytic activity and whether binding results in an up or down regulation. As previously stated, PKA activation requires binding of cAMP to its regulatory subunit; cAMP-binding also causes activation of CAP, Epac and the cyclic nucleotide-gated channels (de Rooij *et al.*, 2000; Bruckner and Titgemeyer, 2002; Kaupp and Seifert, 2002). Thus, in each case the regulatory domain inhibits the protein's effector activity until this inhibition is relieved by cAMP binding. In the case of NTE, the isolated catalytic domain, NEST, catalyses hydrolysis of phenyl valerate and lysophospholipid (van Tienhoven *et al.*, 2002). One might predict that that the regulatory domain would inhibit this hydrolytic activity unless cAMP were present. However, it has been shown that addition of cAMP to microsomes obtained from COS-7 cells overexpressing full-length NTE has no effect on hydrolysis of either phenyl valerate or lysophospholipid (Paul Glynn, unpublished work). An alternative approach to the question of putative cAMP regulation of Yml059c would be to uncover a cAMP-dependent phenotype which is altered in the *yml059cΔ* mutant.

6.3 The NTE protein family; essential in higher eukaryotes, superfluous in yeast?

Genetic mutation of either *sws* in the fruit fly (Kretzschmar *et al.*, 1997) or *Nte* in mice (Moser *et al.*, 2003) causes severe developmental consequences. However continuous dosing of adult chickens with non-neuropathic OPs effectively inhibits the catalytic activity of NTE without causing neuropathy (Johnson, 1974). It has therefore been postulated that the role of NTE is only critical during development, with no essential function in adult vertebrates. The only reported effect of decreased functional NTE protein levels in adult animals is a subtle increase in motor activity observed in mice dosed with the OP ethyl

octylphosphonofluoridate (EOPF) or carrying a heterozygous *Nte* deletion (Winrow *et al.*, 2003).

This study has shown that *YML059c* is a non-essential yeast gene whose disruption causes no obvious mutant phenotype. However, as for NTE, the function of Yml059c might only be critical under specific conditions that have not been investigated during this study.

If, as discussed in section 6.2, Yml059c is regulated by cAMP, then its cellular function might only be required when cAMP levels are high or low. Addition of glucose to yeast cells that are growing on a non-fermentable carbon source results in a rapid and transient increase in intracellular cAMP levels (van der Plaat, 1974). It is possible that the function of Yml059c is to act during this environmental transition and is positively regulated by the increased level of cAMP, possibly acting in concert with the cAMP-PKA pathway. Alternatively Yml059c might act only when cAMP levels are low. A number of cellular processes have been shown to require a decrease in the activity of the cAMP-PKA pathway, including response to stress conditions or nutrient exhaustion and sporulation in diploids (for a review see Broach and Deschenes, 1990). However these processes are not accompanied by a decrease in cAMP levels (Ma *et al.*, 1997) making them less likely candidates for processes that might require Yml059c.

Pseudohyphal differentiation has been shown to require a functional cAMP-PKA pathway and can be stimulated by the addition of exogenous cAMP (Lorenz and Heitman, 1997) making this a good candidate for a cellular process in which Yml059c might function. However, this study has shown that *YML059c* is not essential for the development of pseudohyphae.

If the cellular role of Yml059c is crucial only when cAMP levels are either high or low, then altering the cellular cAMP levels might expose a mutant or overexpression phenotype. As well as addition of glucose, the membrane depolarising agent dinitrophenol (DNP) is known to induce a rise in intracellular cAMP levels (Thevelein *et al.*, 1987). The cAMP rise caused by DNP is greater and more prolonged than that produced in response to glucose and may therefore offer greater potential as a strategy for identifying a cAMP-dependent phenotype. Other alternative approaches might be to reduce the breakdown of cAMP by incubating yeast in the presence of the phosphodiesterase inhibitor IBMX or to investigate the effect of *YML059c* knockout or overexpression in yeast lacking either of the yeast phosphodiesterases, *PDE1* and *PDE2*. Indeed, disruption of the high affinity phosphodiesterase *pde2* has been reported to increase the basal cAMP level and addition of exogenous cAMP to a *pde2*Δ mutant causes a rise in intracellular levels that is not seen

in a *PDE2*$^{+}$ strain (Wilson *et al.*, 1993). A *yml059cΔ pde2Δ* mutant strain has been generated for future investigation of the effects of an increased basal cAMP level (data not shown).

The NTE protein family has remained highly conserved amongst eukaryotes and as such must either perform an essential function or at least confer a selective advantage. This would certainly seem to be the case for mammalian NTE or Swiss cheese of fruit flies but neither appears true for Yml059c, as none of the tests performed in this study exposed any quantifiable phenotypic difference between the parental or *yml059cΔ* mutant strain. Perhaps an appropriate test has yet to be devised that would mimic the environmental conditions under which this protein would offer a selective advantage.

If a mutation confers no discernable phenotype under any conditions, it can be assumed that either another gene is present that can perform the same function or that an alternative metabolic pathway exists that can compensate for the mutation. As discussed in section 4.5, three putative proteins are encoded in the yeast genome with significant sequence similarity to the active site region of Yml059c (see Figure 4.2); these are Yor089c, Ykr089c and Ymr313c. However their level of similarity does not seem sufficiently high for their function to be redundant to that of Yml059c. Yor081c, Ykr089c and Ymr313c are only 749, 910, and 642 amino acids in length respectively; much shorter than the 1679 amino acid polypeptide of Yml059c. Unlike Yml059c they all lack equivalent residues to several of those found to be essential to the catalytic activity of NTE (Atkins and Glynn, 2000) and none possess the putative cAMP binding domain. Alternative explanations for a lack of mutant phenotype must be that either another metabolic pathway exists that can compensate or simply that the appropriate test has not been conducted that would expose a phenotype.

6.4 A possible function for Yml059c

This study has shown that Yml059c is a serine esterase capable of hydrolysing free fatty acid from lysophospholipid *in vitro*. The observation that overexpression of Yml059c causes a reduction in intracellular [^{14}C]-palmitate labelled lysophospholipid (Paul Glynn unpublished work) suggests that this reaction can also occur *in vivo*.

As described in section 1.11, only three other yeast proteins have been previously identified that catalyse the hydrolysis of lysophospholipid (Lee *et al.*, 1994; Fyrst *et al.*, 1999; Merkel *et al.*, 1999). It is possible that one or more of these phospholipase Bs (encoded by *PLB1*, *PLB2* and *PLB3*) has an overlapping function with that of Yml059c explaining the lack of a discernable phenotype in the *yml059c* mutant. However, the activities of Plb1, Plb2 and

Plb3 were reported to be at the plasma membrane (Merkel *et al.*, 1999), whereas Yml059c appears to localise to an intracellular organelle, possibly the ER.

No experiments have yet been performed in order to determine whether Yml059c has transacylase activity such as that associated with the three characterised yeast phospholipase Bs. Clearly Yml059c is able to hydrolyse lysophospholipid *in vitro* without the addition of cAMP; it may be the case that in a physiological context it acts as a transacylase and that this activity requires the presence of cAMP.

Recent evidence supports the existence of lipid rafts in cellular membranes. These are detergent insoluble domains formed by tightly packed clusters of the long saturated fatty acid chains of sphingolipids and cholesterol. Lipid rafts have since been shown to associate with a number of (GPI)-anchored proteins and are thought to be involved in various cellular processes (for a recent review see Pike, 2003). Lipid rafts consisting of sphingolipids and ergosterol have since been identified in yeast and appear to have a role in the delivery of some proteins from the ER to the plasma membrane (Bagnat *et al.*, 2000).

By investigating the clustering nature of cholesterol in vesicles of phosphatidylcholine with varying acyl chain unsaturations, Lagane *et al.* (2002) have shown that the relative saturation of the acyl chains of phospholipids may alter the formation of lipid rafts. Qualitative analysis by electrospray ionisation tandem mass spectrometry showed a disparity between the acyl chain saturation of individual phospholipid species in the plasma membrane compared to those of other organelles (Schneiter *et al.*, 1999). This suggests the existence of enzymes that remodel the saturated fatty acid content of phospholipids in specific organelles and leads to a possible hypothesis for the cellular function of Yml059c. If Yml059c has transacylase activity it may function to alter the proportions of phospholipids that contain saturated fatty acids in the ER membrane. If the transacylase activity is modulated by cAMP binding, this could provide a mechanism for the regulated recruitment of a specific group of ER proteins into lipid rafts for subsequent delivery to the plasma membrane. Perhaps the role of Yml059c is to assist in the delivery of proteins required at the plasma membrane during pseudohyphal development, or other cAMP regulated processes, and that the increased intracellular cAMP levels caused by growth on glucose provides the necessary signal that an appropriate carbon source is present. It is conceivable that this hypothetical environmental signalling mechanism in yeast has been adapted by evolution to control other cellular processes. Perhaps in mammalian neural development, cAMP activates NTE to assist in the delivery of appropriate proteins to the surface of neurons to ensure the correct interaction with glia.

6.5 Future work

A number of avenues of investigation could be explored in order to further characterise Yml059c and to substantiate or disprove the suggested hypothesis for its function.

If the lack of a detectable phenotype is due to an overlapping function with the one or more of the lysophospholipases encoded by the *PLB1*, *PLB2* and *PBL3* genes then disruption of *yml059c* in a *plb1 plb2 plb3* mutant background should elicit a phenotypic change. Disruption of these three lysophospholipases had resulted in sensitivity to lysophosphatidylcholine. The affect of lysophospholipid on a *yml059c* mutant or a *plb1 plb2 plb3 yml059c* quadruple mutant should also be explored, both in terms of sensitivity to these potentially harmful detergent-like molecules and whether they can be utilised as a source of fatty acid under anaerobic conditions.

If Yml059c is at its most active when cAMP levels are high then increasing the intracellular cAMP levels could provide a means of uncovering a mutant phenotype. Possible methods for which are discussed in section 6.3. As discussed in section 6.2, generation of a chimeric construct in which the cAMP binding domain of PKA has been replaced with that of Yml059c might provide a qualitative method for determining the functionality of its putative regulatory domain.

Functional characterisation of the three yeast proteins with sequence similarity to Yml059c (Yor081c, Ykr089c and Ymr313c) could determine to what extent they might perform a similar role to Yml059c. They may also provide insights as to its cellular function. It would be of interest to overexpress each of these three in order to determine if they, like Yml059c can hydrolyse phenyl valerate or lysophospholipid or react with [^{3}H]DFP. If these genes perform an overlapping function with *YML059c* this could be uncovered by generating mutants lacking combinations of these four genes.

Results of two-hybrid assays suggest that Yml059c interacts with Yfr021w, an uncharacterised protein that has a role in respiratory function (Georgakopoulos *et al.*, 2001). Any increase in respiratory deficiency caused by disruption of *yml059c* in a *yfr021wΔ* background would support the assertion that these proteins cooperate. Further investigations of any other possible protein interactions of Yml059c could be carried out using a yeast two-hybrid screen in which Yml059c is used as the bait. However, such a screen could be hampered by the membrane-associated nature of Yml059c. The alternative protein-protein interaction screen described by Stagljar *et al.* (1998) might prove more appropriate. This screen involves generating a fusion between the bait protein and

the C-terminal portion of ubiquitin, and a fusion between the prey and the N-terminal portion of ubiquitin. The bait fusion also carries a transcription factor that when released can enter the nucleus and activate a reporter gene such as *lacZ*. If the prey and bait interact they will bring together the two halves of ubiquitin; this is recognised and cleaved by ubiquitin specific proteases within the yeast cell, thereby releasing the transcription factor and activating the reporter. This method of screening has the potential to identify interactions involving membrane bound proteins.

A synthetic lethal screen such as that used by Karpova *et al.* (1993) may uncover a gene that performs a similar function to *YML059c*. Such a screen provides a method for identifying a gene that when disrupted causes *YML059c* to become essential to the cells viability. This could uncover a gene with overlapping function to *YML059c* and may be responsible for the apparent lack of a phenotype in the *yml059c* mutant.

Further quantification of the lipid content of the *yml059c* mutant should be performed in order to determine if disruption of this gene leads to a change in lysophospholipid under vegetative growth. If so, this would imply that Yml059c is functional while intracellular cAMP is at a basal level. This result would allow investigation of the affect of disrupting the putative regulatory domain, perhaps by site-directed mutagenesis of the arginine residue that is conserved amongst cAMP binding domains (see Figure 1.7). For this, the *in vivo* site-directed mutagenesis method described by Storici *et al.* (2001) could be used. Unlike a plasmid-based system, this method would ensure that wild type expression levels were preserved.

Experiments would need to be devised in order to investigate the hypothesis for the function of Yml059c, as discussed in 6.4. Firstly, it would be necessary to establish whether Yml059c has transacylase activity. This could be achieved by incubating particulate fractions of yeast overexpressing Yml059c, with lysophospholipid carrying a radioactively labelled fatty acid chain and assessing the production of labelled diacylphospholipids. Alternatively, the effect of genetic knockout or overexpression of *YML059c* on the subcellular localisation of proteins that are known to require lipid raft association might establish whether Yml059c has any role in lipid raft production. The proteins Pma1 or Gas1 are known to be associated with lipid rafts and might therefore be suitable candidates (Bagnat *et al.*, 2000).

References

Adachi, K., and Hamer, J. E. (1998). Divergent cAMP signaling pathways regulate growth and pathogenesis in the rice blast fungus *Magnaporthe grisea*. *Plant Cell* **10**, 1361-1374.

Aguilera, A. (1994). Formamide sensitivity: a novel conditional phenotype in yeast. *Genetics* **136**, 87-91.

Altschul, S. F., Madden, T. L., Schaffer, A. A., Zhang, J., Zhang, Z., Miller, W., and Lipman, D. J. (1997). Gapped BLAST and PSI-BLAST: a new generation of protein database search programs. *Nucleic Acids Res* **25**, 3389-3402.

Amieux, P. S., and McKnight, G. S. (2002). The essential role of RI alpha in the maintenance of regulated PKA activity. *Ann N Y Acad Sci* **968**, 75-95.

Ansari, K., Martin, S., Farkasovsky, M., Ehbrecht, I. M., and Kuntzel, H. (1999). Phospholipase C binds to the receptor-like Gpr1 protein and controls pseudohyphal differentiation in *Saccharomyces cerevisiae*. *J Biol Chem* **274**, 30052-30058.

Athenstaedt, K., Zweytick, D., Jandrositz, A., Kohlwein, S. D., and Daum, G. (1999). Identification and characterization of major lipid particle proteins of the yeast *Saccharomyces cerevisiae*. *J Bacteriol* **181**, 6441-6448.

Atkins, J., and Glynn, P. (2000). Membrane association of and critical residues in the catalytic domain of human neuropathy target esterase. *J Biol Chem* **275**, 24477-24483.

Atkins, J., Luthjens, L. H., Hom, M. L., and Glynn, P. (2002). Monomers of the catalytic domain of human neuropathy target esterase are active in the presence of phospholipid. *Biochem J* **361**, 119-123.

Bagnat, M., Keranen, S., Shevchenko, A., and Simons, K. (2000). Lipid rafts function in biosynthetic delivery of proteins to the cell surface in yeast. *Proc Natl Acad Sci U S A* **97**, 3254-3259.

Baldari, C., and Cesareni, G. (1985). Plasmids pEMBLY: new single-stranded shuttle vectors for the recovery and analysis of yeast DNA sequences. *Gene* **35**, 27-32.

Ballou, L., Hitzeman, R. A., Lewis, M. S., and Ballou, C. E. (1991). Vanadate-resistant yeast mutants are defective in protein glycosylation. *Proc Natl Acad Sci U S A* **88**, 3209-3212.

Banerjee, P., Dasgupta, A., Siakotos, A. N., and Dawson, G. (1992). Evidence for lipase abnormality: high levels of free and triacylglycerol forms of unsaturated fatty acids in neuronal ceroid-lipofuscinosis tissue. *Am J Med Genet* **42**, 549-554.

Bitter, G. A., and Egan, K. M. (1984). Expression of heterologous genes in *Saccharomyces cerevisiae* from vectors utilizing the glyceraldehyde-3-phosphate dehydrogenase gene promoter. *Gene* **32**, 263-274.

Boy-Marcotte, E., Perrot, M., Bussereau, F., Boucherie, H., and Jacquet, M. (1998). Msn2p and Msn4p control a large number of genes induced at the diauxic transition which are repressed by cyclic AMP in *Saccharomyces cerevisiae*. *J Bacteriol* **180**, 1044-1052.

Brachmann, C. B., Davies, A., Cost, G. J., Caputo, E., Li, J., Hieter, P., and Boeke, J. D. (1998). Designer deletion strains derived from *Saccharomyces cerevisiae* S288C: a useful set of strains and plasmids for PCR-mediated gene disruption and other applications. *Yeast* **14**, 115-132.

Broach, J. R. (1991). RAS genes in *Saccharomyces cerevisiae*: signal transduction in search of a pathway. *Trends Genet* **7**, 28-33.

Broach, J. R., and Deschenes, R. J. (1990). The function of ras genes in *Saccharomyces cerevisiae*. *Adv Cancer Res* **54**, 79-139.

Bruckner, R., and Titgemeyer, F. (2002). Carbon catabolite repression in bacteria: choice of the carbon source and autoregulatory limitation of sugar utilization. *FEMS Microbiol Lett* **209**, 141-148.

Bubis, J., Neitzel, J. J., Saraswat, L. D., and Taylor, S. S. (1988). A point mutation abolishes binding of cAMP to site A in the regulatory subunit of cAMP-dependent protein kinase. *J Biol Chem* **263**, 9668-9673.

Chemnitius, J. M., Haselmeyer, K. H., and Zech, R. (1984). Neurotoxic esterase: gel filtration and isoelectric focusing of carboxylesterases solubilized from hen brain. *Life Sci* **34**, 1119-1125.

Cho, R. J., Campbell, M. J., Winzeler, E. A., Steinmetz, L., Conway, A., Wodicka, L., Wolfsberg, T. G., Gabrielian, A. E., Landsman, D., Lockhart, D. J., and Davis, R. W. (1998). A genome-wide transcriptional analysis of the mitotic cell cycle. *Mol Cell* **2**, 65-73.

Chu, S., DeRisi, J., Eisen, M., Mulholland, J., Botstein, D., Brown, P. O., and Herskowitz, I. (1998). The transcriptional program of sporulation in budding yeast. *Science* **282**, 699-705.

Church, G. M., and Gilbert, W. (1984). Genomic sequencing. *Proc Natl Acad Sci U S A* **81**, 1991-1995.

Colombo, S., Ma, P., Cauwenberg, L., Winderickx, J., Crauwels, M., Teunissen, A., Nauwelaers, D., de Winde, J. H., Gorwa, M. F., Colavizza, D., and Thevelein, J. M. (1998). Involvement of distinct G-proteins, Gpa2 and Ras, in glucose- and intracellular acidification-induced cAMP signalling in the yeast *Saccharomyces cerevisiae*. *Embo J* **17**, 3326-3341.

Cooper, T. G. (1982). Nitrogen metabolism in *Saccharomyces cerevisiae*. In The molecular biology of the yeast Saccharomyces, J. N. Strathern, E. W. Jones, and J. R. Broach, eds. (Cold Spring Harbour, Cold Spring Harbour Laboratory Press), pp. 33-99.

Daum, G., Tuller, G., Nemec, T., Hrastnik, C., Balliano, G., Cattel, L., Milla, P., Rocco, F., Conzelmann, A., Vionnet, C., *et al.* (1999). Systematic analysis of yeast strains with possible defects in lipid metabolism. *Yeast* **15**, 601-614.

de la Rosa, L. A., Vilarino, N., Vieytes, M. R., and Botana, L. M. (2001). Modulation of thapsigargin-induced calcium mobilisation by cyclic AMP-elevating agents in human lymphocytes is insensitive to the action of the protein kinase A inhibitor H-89. *Cell Signal* **13**, 441-449.

de Rooij, J., Rehmann, H., van Triest, M., Cool, R. H., Wittinghofer, A., and Bos, J. L. (2000). Mechanism of regulation of the Epac family of cAMP-dependent RapGEFs. *J Biol Chem* **275**, 20829-20836.

de Rooij, J., Zwartkruis, F. J., Verheijen, M. H., Cool, R. H., Nijman, S. M., Wittinghofer, A., and Bos, J. L. (1998). Epac is a Rap1 guanine-nucleotide-exchange factor directly activated by cyclic AMP. *Nature* **396**, 474-477.

DeRisi, J. L., Iyer, V. R., and Brown, P. O. (1997). Exploring the metabolic and genetic control of gene expression on a genomic scale. *Science* **278**, 680-686.

Deutschbauer, A. M., Williams, R. M., Chu, A. M., and Davis, R. W. (2002). Parallel phenotypic analysis of sporulation and postgermination growth in *Saccharomyces cerevisiae*. *Proc Natl Acad Sci U S A* **99**, 15530-15535.

Doskeland, S. O., and Ogreid, D. (1988). Ammonium sulfate precipitation assay for the study of cyclic nucleotide binding to proteins. *Methods Enzymol* **159**, 147-150.

Eliasson, L., Ma, X., Renstrom, E., Barg, S., Berggren, P. O., Galvanovskis, J., Gromada, J., Jing, X., Lundquist, I., Salehi, A., *et al.* (2003). SUR1 Regulates PKA-independent cAMP-induced Granule Priming in Mouse Pancreatic B-cells. *J Gen Physiol* **121**, 181-197.

Feinberg, A. P., and Vogelstein, B. (1983). A technique for radiolabeling DNA restriction endonuclease fragments to high specific activity. *Anal Biochem* **132**, 6-13.

Ferea, T. L., Botstein, D., Brown, P. O., and Rosenzweig, R. F. (1999). Systematic changes in gene expression patterns following adaptive evolution in yeast. *Proc Natl Acad Sci U S A* **96**, 9721-9726.

Fillinger, S., Chaveroche, M. K., Shimizu, K., Keller, N., and d'Enfert, C. (2002). cAMP and ras signalling independently control spore germination in the filamentous fungus *Aspergillus nidulans*. *Mol Microbiol* **44**, 1001-1016.

Fyrst, H., Oskouian, B., Kuypers, F. A., and Saba, J. D. (1999). The *PLB2* gene of *Saccharomyces cerevisiae* confers resistance to lysophosphatidylcholine and encodes a phospholipase B/lysophospholipase. *Biochemistry* **38**, 5864-5871.

Gancedo, J. M. (2001). Control of pseudohyphae formation in *Saccharomyces cerevisiae*. *FEMS Microbiology Reviews* **25**, 107-123.

Gari, E., Piedrafita, L., Aldea, M., and Herrero, E. (1997). A set of vectors with a tetracycline-regulatable promoter system for modulated gene expression in *Saccharomyces cerevisiae*. *Yeast* **13**, 837-848.

Gasch, A. P., Huang, M., Metzner, S., Botstein, D., Elledge, S. J., and Brown, P. O. (2001). Genomic expression responses to DNA-damaging agents and the regulatory role of the yeast ATR homolog Mec1p. *Mol Biol Cell* **12**, 2987-3003.

Gasch, A. P., Spellman, P. T., Kao, C. M., Carmel-Harel, O., Eisen, M. B., Storz, G., Botstein, D., and Brown, P. O. (2000). Genomic expression programs in the response of yeast cells to environmental changes. *Mol Biol Cell* **11**, 4241-4257.

Gasperini, S., Crepaldi, L., Calzetti, F., Gatto, L., Berlato, C., Bazzoni, F., Yoshimura, A., and Cassatella, M. A. (2002). Interleukin-10 and cAMP-elevating agents cooperate to induce suppressor of cytokine signaling-3 via a protein kinase A-independent signal. *Eur Cytokine Netw* **13**, 47-53.

Georgakopoulos, T., Koutroubas, G., Vakonakis, I., Tzermia, M., Prokova, V., Voutsina, A., and Alexandraki, D. (2001). Functional analysis of the *Saccharomyces cerevisiae YFR021w/YGR223c/YPL100w* ORF family suggests relations to mitochondrial/peroxisomal functions and amino acid signalling pathways. *Yeast* **18**, 1155-1171.

Giaever, G., Chu, A. M., Ni, L., Connelly, C., Riles, L., Veronneau, S., Dow, S., Lucau-Danila, A., Anderson, K., Andre, B., *et al.* (2002). Functional profiling of the *Saccharomyces cerevisiae* genome. *Nature* **418**, 387-391.

Gietz, R. D., Schiestl, R. H., Willems, A. R., and Woods, R. A. (1995). Studies on the transformation of intact yeast cells by the LiAc/SS-DNA/PEG procedure. *Yeast* **11**, 355-360.

Gimeno, C. J., Ljungdahl, P. O., Styles, C. A., and Fink, G. R. (1992). Unipolar cell divisions in the yeast *S.cerevisiae* lead to filamentous growth: regulation by starvation and RAS. *Cell* **68**, 1077-1090.

Giots, F., Donaton, M. C., and Thevelein, J. M. (2003). Inorganic phosphate is sensed by specific phosphate carriers and acts in concert with glucose as a nutrient signal for activation of the protein kinase A pathway in the yeast *Saccharomyces cerevisiae*. *Mol Microbiol* **47**, 1163-1181.

Glynn, P. (2000). Neural development and neurodegeneration: two faces of neuropathy target esterase. *Prog Neurobiol* **61**, 61-74.

Glynn, P., Holton, J. L., Nolan, C. C., Read, D. J., Brown, L., Hubbard, A., and Cavanagh, J. B. (1998). Neuropathy target esterase: immunolocalization to neuronal cell bodies and axons. *Neuroscience* **83**, 295-302.

Glynn, P., Read, D. J., Guo, R., Wylie, S., and Johnson, M. K. (1994). Synthesis and characterization of a biotinylated organophosphorus ester for detection and affinity purification of a brain serine esterase: neuropathy target esterase. *Biochem J* **301**, 551-556.

Goffeau, A., Barrell, B. G., Bussey, H., Davis, R. W., Dujon, B., Feldmann, H., Galibert, F., Hoheisel, J. D., Jacq, C., Johnston, M., *et al.* (1996). Life with 6000 genes. *Science* **274**, 546, 563-547.

Gray, W. D. (1941). Studies on the alcohol tolerance of yeasts. *J Bacteriol* **42**, 561-574.

Gu, Z., Steinmetz, L. M., Gu, X., Scharfe, C., Davis, R. W., and Li, W. H. (2003). Role of duplicate genes in genetic robustness against null mutations. *Nature* **421**, 63-66.

Guthrie, C., and Fink, G. R. (1991). Guide to yeast genetics and molecular biology. In Methods in Enzymology (Academic Press).

Hairfield, M. L., Ayers, A. B., and Dolan, J. W. (2001). Phospholipase D1 is required for efficient mating projection formation in *Saccharomyces cerevisiae*. *FEMS Yeast Res* **1**, 225-232.

Hall, N. A., Lake, B. D., Dewji, N. N., and Patrick, A. D. (1991). Lysosomal storage of subunit c of mitochondrial ATP synthase in Batten's disease (ceroid-lipofuscinosis). *Biochem J* **275**, 269-272.

Hampsey, M. (1997). A review of phenotypes in *Saccharomyces cerevisiae*. *Yeast* **13**, 1099-1133.

Hanahan, D. (1983). Studies on transformation of *Escherichia coli* with plasmids. *J Mol Biol* **166**, 557-580.

Hartwell, L. H. (1974). *Saccharomyces cerevisiae* cell cycle. *Bacteriol Rev* **38**, 164-198.

Hasan, R., Leroy, C., Isnard, A. D., Labarre, J., Boy-Marcotte, E., and Toledano, M. B. (2002). The control of the yeast H_2O_2 response by the Msn2/4 transcription factors. *Mol Microbiol* **45**, 233-241.

Heisenberg, M., and Bohl, K. (1979). Isolation of anatomical brain mutants of *Drosophila* by histological means. *Z Naturforsch* **34**, 143-147.

Hixson, C. S., and Krebs, E. G. (1980). Characterization of a cyclic AMP-binding protein from bakers' yeast. Identification as a regulatory subunit of cyclic AMP-dependent protein kinase. *J Biol Chem* **255**, 2137-2145.

Hoffman, C. S. (1997). Rapid isolation of yeast chromosomal DNA. In Current protocols in molecular biology, F. M. Ausubel, R. Brent, R. E. Kingston, D. D. Moore, J. G. Seidman, J. A. Smith, and K. Struhl, eds. (New York, John Wiley and sons), pp. 13.11.12-13.11.14.

Hofmann, K., and Stoffel, W. (1993). TMbase - A database of membrane spanning proteins segments. *Biol Chem Hoppe-Seyler* **376**, 166.

Iacovelli, L., Capobianco, L., Salvatore, L., Sallese, M., D'Ancona, G. M., and De Blasi, A. (2001). Thyrotropin activates mitogen-activated protein kinase pathway in FRTL-5 by a cAMP-dependent protein kinase A-independent mechanism. *Mol Pharmacol* **60**, 924-933.

Ishikawa, Y., Chow, E., McNamee, M. G., McChesney, M., and Wilson, B. W. (1983). Separation of paraoxon and mipafox sensitive esterases by sucrose density gradient sedimentation. *Toxicol Lett* **17**, 315-320.

Jarvela, I., Lehtovirta, M., Tikkanen, R., Kyttala, A., and Jalanko, A. (1999). Defective intracellular transport of CLN3 is the molecular basis of Batten disease (JNCL). *Hum Mol Genet* **8**, 1091-1098.

Jarvela, I., Sainio, M., Rantamaki, T., Olkkonen, V. M., Carpen, O., Peltonen, L., and Jalanko, A. (1998). Biosynthesis and intracellular targeting of the CLN3 protein defective in Batten disease. *Hum Mol Genet* **7**, 85-90.

Johnson, K. E., Cameron, S., Toda, T., Wigler, M., and Zoller, M. J. (1987). Expression in *Escherichia coli* of *BCY1*, the regulatory subunit of cyclic AMP-dependent protein kinase from *Saccharomyces cerevisiae*. Purification and characterization. *J Biol Chem* **262**, 8636-8642.

Johnson, M. K. (1969a). The delayed neurotoxic effect of some organophosphorus compounds. Identification of the phosphorylation site as an esterase. *Biochem J* **114**, 711-717.

Johnson, M. K. (1969b). A phosphorylation site in brain and the delayed neurotoxic effect of some organophosphorus compounds. *Biochem J* **111**, 487-495.

Johnson, M. K. (1974). The primary biochemical lesion leading to the delayed neurotoxic effects of some organophosphorus esters. *J Neurochem* **23**, 785-789.

Johnson, M. K. (1977). Improved assay of neurotoxic esterase for screening organophosphates for delayed neurotoxicity potential. *Arch Toxicol* **37**, 113-115.

Johnson, M. K. (1982). The target for initiation of delayed neurotoxicity by organophosphorus esters: Biochemical studies and toxicological applications. *Rev Biochem Toxicol* **4**, 141-212.

Johnson, M. K. (1987). Organophosphate-induced delayed neuropathy: Anomalous data lead to advances in understanding. In Molecular Selectivity and Mechanisms of Toxicity, F. De Matteis, and E. A. Lock, eds. (New York, Macmillan Press), pp. 27-58.

Johnston, M., and Carlson, M. (1992). Regulation of carbon and phosphate utilisation. In The molecular and cellular biology of the yeast *Saccharomyces*, E. Jones, J. Pringle, and J. Broach, eds. (Cold Spring Harbour NY, Cold Spring Harbour Press), pp. 193-281.

Karpova, T. S., Lepetit, M. M., and Cooper, J. A. (1993). Mutations that enhance the *cap2* null mutant phenotype in *Saccharomyces cerevisiae* affect the actin cytoskeleton, morphogenesis and pattern of growth. *Genetics* **135**, 693-709.

Kashima, Y., Miki, T., Shibasaki, T., Ozaki, N., Miyazaki, M., Yano, H., and Seino, S. (2001). Critical role of cAMP-GEFII--Rim2 complex in incretin-potentiated insulin secretion. *J Biol Chem* **276**, 46046-46053.

Kaupp, U. B., and Seifert, R. (2002). Cyclic nucleotide-gated ion channels. *Physiol Rev* **82**, 769-824.

Koenig, H., McDonald, T., and Nellhaus, G. (1964). Morphological and histochemical studies of neurolipidosis by light and electron microscopy. *J Neuropathol Exp Neurol* **23**, 191-193.

Kraakman, L., Lemaire, K., Ma, P., Teunissen, A. W., Donaton, M. C., Van Dijck, P., Winderickx, J., de Winde, J. H., and Thevelein, J. M. (1999). A *Saccharomyces cerevisiae* G-protein coupled receptor, Gpr1, is specifically required for glucose activation of the cAMP pathway during the transition to growth on glucose. *Mol Microbiol* **32**, 1002-1012.

Kretzschmar, D., Hasan, G., Sharma, S., Heisenberg, M., and Benzer, S. (1997). The *swiss cheese* mutant causes glial hyperwrapping and brain degeneration in *Drosophila*. *J Neurosci* **17**, 7425-7432.

Kumar, A., Agarwal, S., Heyman, J. A., Matson, S., Heidtman, M., Piccirillo, S., Umansky, L., Drawid, A., Jansen, R., Liu, Y., *et al.* (2002). Subcellular localization of the yeast proteome. *Genes Dev* **16**, 707-719.

Kumar, A., Cheung, K. H., Ross-Macdonald, P., Coelho, P. S., Miller, P., and Snyder, M. (2000). TRIPLES: a database of gene function in *Saccharomyces cerevisiae*. *Nucleic Acids Res* **28**, 81-84.

Lagane, B., Mazeres, S., Le Grimellec, C., Cezanne, L., and Lopez, A. (2002). Lateral distribution of cholesterol in membranes probed by means of a pyrene-labelled cholesterol: effects of acyl chain unsaturation. *Biophys Chem* **95**, 7-22.

Lee, K. S., Patton, J. L., Fido, M., Hines, L. K., Kohlwein, S. D., Paltauf, F., Henry, S. A., and Levin, D. E. (1994). The *Saccharomyces cerevisiae PLB1* gene encodes a protein required for lysophospholipase and phospholipase B activity. *J Biol Chem* **269**, 19725-19730.

Lee, M. G., and Nurse, P. (1987). Complementation used to clone a human homologue of the fission yeast cell cycle control gene *cdc2*. *Nature* **327**, 31-35.

Lees, J. E., and Richards, P. G. (1999). Rapid, high-sensitivity imaging of radiolabeled gels with microchannel plate detectors. *Electrophoresis* **20**, 2139-2143.

Lehrach, H., Diamond, D., Wozney, J. M., and Boedtker, H. (1977). RNA molecular weight determinations by gel electrophoresis under denaturing conditions, a critical reexamination. *Biochemistry* **16**, 4743-4751.

Li, Y., Dinsdale, D., and Glynn, P. (2003). Protein domains, catalytic activity and subcellular distribution of neuropathy target esterase in mammalian cells. *J Biol Chem* **278**, 8820-8825.

Liu, H., Styles, C. A., and Fink, G. R. (1996). *Saccharomyces cerevisiae* S288C has a mutation in *FLO8*, a gene required for filamentous growth. *Genetics* **144**, 967-978.

Longtine, M. S., McKenzie, A., Demarini, D. J., Shah, N. G., Wach, A., Brachat, A., Philippsen, P., and Pringle, J. R. (1998). Additional modules for versatile and economical PCR-based gene deletion and modification in *Saccharomyces cerevisiae*. *Yeast* **14**, 953-961.

Lorenz, M. C., Cutler, N. S., and Heitman, J. (2000). Characterization of alcohol-induced filamentous growth in *Saccharomyces cerevisiae*. *Mol Biol Cell* **11**, 183-199.

Lorenz, M. C., and Heitman, J. (1997). Yeast pseudohyphal growth is regulated by *GPA2*, a G protein alpha homolog. *Embo J* **16**, 7008-7018.

Lotti, M. (1991). The pathogenesis of organophosphate polyneuropathy. *Crit Rev Toxicol* **21**, 465-487.

Lowry, O. H., Rosbrough, N. J., Farr, A. L., and Randall, R. J. (1951). Protein measurement with the Folin phenol reagent. *J Biol Chem* **193**, 265-275.

Lush, M. J., Li, Y., Read, D. J., Willis, A. C., and Glynn, P. (1998). Neuropathy target esterase and a homologous *Drosophila* neurodegeneration-associated mutant protein contain a novel domain conserved from bacteria to man. *Biochem J* **332**, 1-4.

Lyons, T. J., Gasch, A. P., Gaither, L. A., Botstein, D., Brown, P. O., and Eide, D. J. (2000). Genome-wide characterization of the Zap1p zinc-responsive regulon in yeast. *Proc Natl Acad Sci U S A* **97**, 7957-7962.

Ma, P., Goncalves, T., Maretzek, A., Dias, M. C., and Thevelein, J. M. (1997). The lag phase rather than the exponential-growth phase on glucose is associated with a higher cAMP level in wild-type and cAPK-attenuated strains of the yeast *Saccharomyces cerevisiae*. *Microbiology* **143**, 3451-3459.

Mandel, M., and Higa, A. (1970). Calcium-dependent bacteriophage DNA infection. *J Mol Biol* **53**, 159-162.

Matsumoto, K., Uno, I., and Ishikawa, T. (1983). Initiation of meiosis in yeast mutants defective in adenylate cyclase and cyclic AMP-dependent protein kinase. *Cell* **32**, 417-423.

McCusker, J. H., and Haber, J. E. (1988). Cycloheximide-resistant temperature-sensitive lethal mutations of *Saccharomyces cerevisiae*. *Genetics* **119**, 303-315.

McKay, D. B., Weber, I. T., and Steitz, T. A. (1982). Structure of catabolite gene activator protein at 2.9-A resolution. Incorporation of amino acid sequence and interactions with cyclic AMP. *J Biol Chem* **257**, 9518-9524.

Merkel, O., Fido, M., Mayr, J. A., Pruger, H., Raab, F., Zandonella, G., Kohlwein, S. D., and Paltauf, F. (1999). Characterization and function *in vivo* of two novel phospholipases B/lysophospholipases from *Saccharomyces cerevisiae*. *J Biol Chem* **274**, 28121-28127.

Moser, M., Dahmen, S., Kretzschmar, D., Kluge, R., Li, Y., Glynn, P., and Buettner, R. (2003). Neuropathy Target Esterase (NTE) is required for cell survival during embryonic development. (submitted to Mol Biol Cell).

Moser, M., Stempfl, T., Li, Y., Glynn, P., Buettner, R., and Kretzschmar, D. (2000). Cloning and expression of the murine sws/NTE gene. *Mech Dev* **90**, 279-282.

Muller, G., and Bandlow, W. (1991). Two lipid-anchored cAMP-binding proteins in the yeast *Saccharomyces cerevisiae* are unrelated to the R subunit of cytoplasmic protein kinase A. *Eur J Biochem* **202**, 299-308.

Muller, G., Schubert, K., Fiedler, F., and Bandlow, W. (1992). The cAMP-binding ectoprotein from *Saccharomyces cerevisiae* is membrane-anchored by glycosyl-phosphatidylinositol. *J Biol Chem* **267**, 25337-25346.

Nitiss, J., and Wang, J. C. (1988). DNA topoisomerase-targeting antitumor drugs can be studied in yeast. *Proc Natl Acad Sci U S A* **85**, 7501-7505.

Norbeck, J., and Blomberg, A. (2000). The level of cAMP-dependent protein kinase A activity strongly affects osmotolerance and osmo-instigated gene expression changes in *Saccharomyces cerevisiae*. *Yeast* **16**, 121-137.

Nurse, P., and Bissett, Y. (1981). Gene required in G1 for commitment to cell cycle and in G2 for control of mitosis in fission yeast. *Nature* **292**, 558-560.

Nurse, P., Thuriaux, P., and Nasmyth, K. (1976). Genetic control of the cell division cycle in the fission yeast *Schizosaccharomyces pombe*. *Mol Gen Genet* **146**, 167-178.

Ogawa, N., DeRisi, J., and Brown, P. O. (2000). New components of a system for phosphate accumulation and polyphosphate metabolism in *Saccharomyces cerevisiae* revealed by genomic expression analysis. *Mol Biol Cell* **11**, 4309-4321.

Ogreid, D., Doskeland, S. O., Gorman, K. B., and Steinberg, R. A. (1988). Mutations that prevent cyclic nucleotide binding to binding sites A or B of type I cyclic AMP-dependent protein kinase. *J Biol Chem* **263**, 17397-17404.

Ossipov, D., Schroder-Kohne, S., and Schmitt, H. D. (1999). Yeast ER-Golgi v-SNAREs Bos1p and Bet1p differ in steady-state localization and targeting. *J Cell Sci* **112**, 4135-4142.

Palmer, D. N., Fearnley, I. M., Walker, J. E., Hall, N. A., Lake, B. D., Wolfe, L. S., Haltia, M., Martinus, R. D., and Jolly, R. D. (1992). Mitochondrial ATP synthase subunit c storage in the ceroid-lipofuscinoses (Batten disease). *Am J Med Genet* **42**, 561-567.

Pan, X., and Heitman, J. (1999). Cyclic AMP-dependent protein kinase regulates pseudohyphal differentiation in *Saccharomyces cerevisiae*. *Mol Cell Biol* **19**, 4874-4887.

Pearce, D. A., Ferea, T., Nosel, S. A., Das, B., and Sherman, F. (1999). Action of *BTN1*, the yeast orthologue of the gene mutated in Batten disease. *Nat Genet* **22**, 55-58.

Pearce, D. A., and Sherman, F. (1997). BTN1, a yeast gene corresponding to the human gene responsible for Batten's disease, is not essential for viability, mitochondrial function, or degradation of mitochondrial ATP synthase. *Yeast* **13**, 691-697.

Pearce, D. A., and Sherman, F. (1998). A yeast model for the study of Batten disease. *Proc Natl Acad Sci U S A* **95**, 6915-6918.

Pike, L. J. (2003). Lipid Rafts: Bringing Order to Chaos. *J Lipid Res.*

Pope, C. N., and Padilla, S. (1989a). Modulation of neurotoxic esterase activity *in vitro* by phospholipids. *Toxicol Appl Pharmacol* **97**, 272-278.

Pope, C. N., and Padilla, S. S. (1989b). Chromatographic characterization of neurotoxic esterase. *Biochem Pharmacol* **38**, 181-188.

Rehmann, H., Prakash, B., Wolf, E., Rueppel, A., De Rooij, J., Bos, J. L., and Wittinghofer, A. (2003). Structure and regulation of the cAMP-binding domains of Epac2. *Nat Struct Biol* **10**, 26-32.

Richardson, R. J., Davis, C. S., and Johnson, M. K. (1979). Subcellular distribution of marker enzymes and of neurotoxic esterase in adult hen brain. *J Neurochem* **32**, 607-615.

Roberts, C. J., Nelson, B., Marton, M. J., Stoughton, R., Meyer, M. R., Bennett, H. A., He, Y. D., Dai, H., Walker, W. L., Hughes, T. R., *et al.* (2000). Signaling and circuitry of multiple MAPK pathways revealed by a matrix of global gene expression profiles. *Science* **287**, 873-880.

Robertson, L. S., and Fink, G. R. (1998). The three yeast A kinases have specific signaling functions in pseudohyphal growth. *Proc Natl Acad Sci U S A* **95**, 13783-13787.

Roncero, C., Valdivieso, M. H., Ribas, J. C., and Duran, A. (1988). Isolation and characterization of *Saccharomyces cerevisiae* mutants resistant to Calcofluor white. *J Bacteriol* **170**, 1950-1954.

Rose, K., Rudge, S. A., Frohman, M. A., Morris, A. J., and Engebrecht, J. (1995). Phospholipase D signaling is essential for meiosis. *Proc Natl Acad Sci U S A* **92**, 12151-12155.

Rose, M. D., Winston, F., and Hieter, P., eds. (1990). Methods in yeast genetics: A laboratory course manual (New York, Cold Spring Harbour Press).

Ross-Macdonald, P., Coelho, P. S., Roemer, T., Agarwal, S., Kumar, A., Jansen, R., Cheung, K. H., Sheehan, A., Symoniatis, D., Umansky, L., *et al.* (1999). Large-scale analysis of the yeast genome by transposon tagging and gene disruption. *Nature* **402**, 413-418.

Rubin-Bejerano, I., Mandel, S., Robzyk, K., and Kassir, Y. (1996). Induction of meiosis in *Saccharomyces cerevisiae* depends on conversion of the transcriptional repressor Ume6 to a positive regulator by its regulated association with the transcriptional activator Ime1. *Mol Cell Biol* **16**, 2518-2526.

Ruffer-Turner, M. E., Read, D. J., and Johnson, M. K. (1992). Purification of neuropathy target esterase from avian brain after prelabelling with [^{3}H]diisopropyl phosphorofluoridate. *J Neurochem* **58**, 135-141.

Sagee, S., Sherman, A., Shenhar, G., Robzyk, K., Ben-Doy, N., Simchen, G., and Kassir, Y. (1998). Multiple and distinct activation and repression sequences mediate the regulated transcription of *IME1*, a transcriptional activator of meiosis-specific genes in *Saccharomyces cerevisiae*. *Mol Cell Biol* **18**, 1985-1995.

Sambrook, J., Fritsch, E. F., and Maniatis, T. (1989). Molecular Cloning: A laboratory manual. Second edition (New York, Cold Spring Harbour Press).

Sawai, H., Okamoto, Y., Luberto, C., Mao, C., Bielawska, A., Domae, N., and Hannun, Y. A. (2000). Identification of *ISC1* (*YER019w*) as inositol phosphosphingolipid phospholipase C in *Saccharomyces cerevisiae*. *J Biol Chem* **275**, 39793-39798.

Schmitt, A. P., and McEntee, K. (1996). Msn2p, a zinc finger DNA-binding protein, is the transcriptional activator of the multistress response in *Saccharomyces cerevisiae*. *Proc Natl Acad Sci U S A* **93**, 5777-5782.

Schmitt, M. E., Brown, T. A., and Trumpower, B. L. (1990). A rapid and simple method for preparation of RNA from *Saccharomyces cerevisiae*. *Nucleic Acids Res* **18**, 3091-3092.

Schneiter, R., Brugger, B., Sandhoff, R., Zellnig, G., Leber, A., Lampl, M., Athenstaedt, K., Hrastnik, C., Eder, S., Daum, G., *et al.* (1999). Electrospray ionization tandem mass spectrometry (ESI-MS/MS) analysis of the lipid molecular species composition of yeast subcellular membranes reveals acyl chain-based sorting/remodeling of distinct molecular species en route to the plasma membrane. *J Cell Biol* **146**, 741-754.

Schnell, N., and Entian, K. D. (1991). Identification and characterization of a *Saccharomyces cerevisiae* gene (*PAR1*) conferring resistance to iron chelators. *Eur J Biochem* **200**, 487-493.

Sen, B. H., Akdeniz, B. G., and Denizci, A. A. (2000). The effect of ethylenediamine-tetraacetic acid on *Candida albicans*. *Oral Surg Oral Med Oral Pathol Oral Radiol Endod* **90**, 651-655.

Shabb, J. B., and Corbin, J. D. (1992). Cyclic nucleotide-binding domains in proteins having diverse functions. *J Biol Chem* **267**, 5723-5726.

Shenhar, G., and Kassir, Y. (2001). A positive regulator of mitosis, Sok2, functions as a negative regulator of meiosis in *Saccharomyces cerevisiae*. *Mol Cell Biol* **21**, 1603-1612.

Shilo, V., Simchen, G., and Shilo, B. (1978). Initiation of meiosis in cell cycle initiation mutants of *Saccharomyces cerevisiae*. *Exp Cell Res* **112**, 241-248.

Shimizu, S., Tani, Y., Yamada, H., Tabata, M., and Murachi, T. (1980). Enzymatic determination of serum-free fatty acids: a colorimetric method. *Anal Biochem* **107**, 193-198.

Simanis, V., and Nurse, P. (1986). The cell cycle control gene *cdc2+* of fission yeast encodes a protein kinase potentially regulated by phosphorylation. *Cell* **45**, 261-268.

Smith, A., Ward, M. P., and Garrett, S. (1998). Yeast PKA represses Msn2p/Msn4p-dependent gene expression to regulate growth, stress response and glycogen accumulation. *Embo J* **17**, 3556-3564.

Smith, M. I., Elvove, E., and Frazier, W. H. (1930). The pharmacological action of certain phenol esters with special reference to the etiology of so-called ginger paralysis. *Public Health Reports* **45**, 2509-2524.

Southern, E. M. (1975). Detection of specific sequences among DNA fragments separated by gel electrophoresis. *J Mol Biol* **98**, 503-517.

Spellman, P. T., Sherlock, G., Zhang, M. Q., Iyer, V. R., Anders, K., Eisen, M. B., Brown, P. O., Botstein, D., and Futcher, B. (1998). Comprehensive identification of cell cycle-regulated genes of the yeast *Saccharomyces cerevisiae* by microarray hybridization. *Mol Biol Cell* **9**, 3273-3297.

Sreenivas, A., Patton-Vogt, J. L., Bruno, V., Griac, P., and Henry, S. A. (1998). A role for phospholipase D (Pld1p) in growth, secretion, and regulation of membrane lipid synthesis in yeast. *J Biol Chem* **273**, 16635-16638.

Stagljar, I., Korostensky, C., Johnsson, N., and te Heesen, S. (1998). A genetic system based on split-ubiquitin for the analysis of interactions between membrane proteins *in vivo*. *Proc Natl Acad Sci U S A* **95**, 5187-5192.

Steinmetz, L. M., Scharfe, C., Deutschbauer, A. M., Mokranjac, D., Herman, Z. S., Jones, T., Chu, A. M., Giaever, G., Prokisch, H., Oefner, P. J., and Davis, R. W. (2002). Systematic screen for human disease genes in yeast. *Nat Genet* **31**, 400-404.

Storici, F., Lewis, L. K., and Resnick, M. A. (2001). *In vivo* site-directed mutagenesis using oligonucleotides. *Nat Biotechnol* **19**, 773-776.

Su, Y., Dostmann, W. R., Herberg, F. W., Durick, K., Xuong, N. H., Ten Eyck, L., Taylor, S. S., and Varughese, K. I. (1995). Regulatory subunit of protein kinase A: structure of deletion mutant with cAMP binding domains. *Science* **269**, 807-813.

The International Batten Disease Consortium (1995). Isolation of a novel gene underlying Batten disease, CLN3. *Cell* **82**, 949-957.

Thevelein, J. M. (1984). Regulation of trehalose mobilization in fungi. *Microbiol Rev* **48**, 42-59.

Thevelein, J. M. (1991). Fermentable sugars and intracellular acidification as specific activators of the RAS-adenylate cyclase signalling pathway in yeast: the relationship to nutrient-induced cell cycle control. *Mol Microbiol* **5**, 1301-1307.

Thevelein, J. M. (1994). Signal transduction in yeast. *Yeast* **10**, 1753-1790.

Thevelein, J. M., Beullens, M., Honshoven, F., Hoebeeck, G., Detremerie, K., den Hollander, J. A., and Jans, A. W. (1987). Regulation of the cAMP level in the yeast *Saccharomyces cerevisiae*: intracellular pH and the effect of membrane depolarizing compounds. *J Gen Microbiol* **133**, 2191-2196.

Thevelein, J. M., and de Winde, J. H. (1999). Novel sensing mechanisms and targets for the cAMP-protein kinase A pathway in the yeast *Saccharomyces cerevisiae*. *Mol Microbiol* **33**, 904-918.

Thomas, P. S. (1980). Hybridization of denatured RNA and small DNA fragments transferred to nitrocellulose. *Proc Natl Acad Sci U S A* **77**, 5201-5205.

Thomas, T. C., Ishikawa, Y., McNamee, M. G., and Wilson, B. W. (1989). Correlation of neuropathy target esterase activity with specific tritiated di-isopropyl phosphorofluoridate-labelled proteins. *Biochem J* **257**, 109-116.

Thomas, T. C., Szekacs, A., Hammock, B. D., Wilson, B. W., and McNamee, M. G. (1993). Affinity chromatography of neuropathy target esterase. *Chem Biol Interact* **87**, 347-360.

Thomas, T. C., Szekacs, A., Rojas, S., Hammock, B. D., Wilson, B. W., and McNamee, M. G. (1990). Characterization of neuropathy target esterase using trifluoromethyl ketones. *Biochem Pharmacol* **40**, 2587-2596.

Thompson, J. D., Higgins, D. G., and Gibson, T. J. (1994). CLUSTAL W: improving the sensitivity of progressive multiple sequence alignment through sequence weighting, position-specific gap penalties and weight matrix choice. *Nucleic Acids Res* **22**, 4673-4680.

Toda, T., Cameron, S., Sass, P., Zoller, M., and Wigler, M. (1987). Three different genes in *S.cerevisiae* encode the catalytic subunits of the cAMP-dependent protein kinase. *Cell* **50**, 277-287.

Toda, T., Uno, I., Ishikawa, T., Powers, S., Kataoka, T., Broek, D., Cameron, S., Broach, J., Matsumoto, K., and Wigler, M. (1985). In yeast, RAS proteins are controlling elements of adenylate cyclase. *Cell* **40**, 27-36.

Towbin, H., Staehelin, T., and Gordon, J. (1979). Electrophoretic transfer of proteins from polyacrylamide gels to nitrocellulose sheets: procedure and some applications. *Proc Natl Acad Sci U S A* **76**, 4350-4354.

van der Plaat, J. B. (1974). Cyclic 3',5'-adenosine monophosphate stimulates trehalose degradation in baker's yeast. *Biochem Biophys Res Commun* **56**, 580-587.

Van Haastert, P. J. (1985). The modulation of cell surface cAMP receptors from *Dictyostelium discoideum* by ammonium sulfate. *Biochim Biophys Acta* **845**, 254-260.

van Tienhoven, M., Atkins, J., Li, Y., and Glynn, P. (2002). Human neuropathy target esterase catalyzes hydrolysis of membrane lipids. *J Biol Chem* **277**, 20942-20948.

Wach, A., Brachat, A., Alberti-Segui, C., Rebischung, C., and Philippsen, P. (1997). Heterologous *HIS3* marker and GFP reporter modules for PCR-targeting in *Saccharomyces cerevisiae*. *Yeast* **13**, 1065-1075.

Wach, A., Brachat, A., Pohlmann, R., and Philippsen, P. (1994). New heterologous modules for classical or PCR-based gene disruptions in *Saccharomyces cerevisiae*. *Yeast* **10**, 1793-1808.

Wagner, S., and Paltauf, F. (1994). Generation of glycerophospholipid molecular species in the yeast *Saccharomyces cerevisiae*. Fatty acid pattern of phospholipid classes and selective acyl turnover at *sn*-1 and *sn*-2 positions. *Yeast* **10**, 1429-1437.

Wang, A., Yang, H. C., Friedman, P., Johnson, C. A., and Dennis, E. A. (1999a). A specific human lysophospholipase: cDNA cloning, tissue distribution and kinetic characterization. *Biochim Biophys Acta* **1437**, 157-169.

Wang, D. Y., Kumar, S., and Hedges, S. B. (1999b). Divergence time estimates for the early history of animal phyla and the origin of plants, animals and fungi. *Proc R Soc Lond B Biol Sci* **266**, 163-171.

Weber, I. T., and Steitz, T. A. (1987). Structure of a complex of catabolite gene activator protein and cyclic AMP refined at 2.5 A resolution. *J Mol Biol* **198**, 311-326.

Wickner, R. B. (1994). [*URE3*] as an altered *URE2* protein: evidence for a prion analog in *Saccharomyces cerevisiae*. *Science* **264**, 566-569.

Williams, D. G., and Johnson, M. K. (1981). Gel-electrophoretic identification of hen brain neurotoxic esterase, labelled with tritiated di-isopropyl phosphorofluoridate. *Biochem J* **199**, 323-333.

Wilson, R. B., Renault, G., Jacquet, M., and Tatchell, K. (1993). The *PDE2* gene of *Saccharomyces cerevisiae* is allelic to *RCA1* and encodes a phosphodiesterase which protects the cell from extracellular cAMP. *FEBS Lett* **325**, 191-195.

Winrow, C. J., Hemming, M. L., Allen, D. M., Quistad, G. B., Casida, J. E., and Barlow, C. (2003). Loss of neuropathy target esterase in mice links organophosphate exposure to hyperactivity. *Nat Genet*.

Winzeler, E. A., Shoemaker, D. D., Astromoff, A., Liang, H., Anderson, K., Andre, B., Bangham, R., Benito, R., Boeke, J. D., Bussey, H., *et al.* (1999). Functional characterization of the *S.cerevisiae* genome by gene deletion and parallel analysis. *Science* **285**, 901-906.

Woodford, T. A., Correll, L. A., McKnight, G. S., and Corbin, J. D. (1989). Expression and characterization of mutant forms of the type I regulatory subunit of cAMP-dependent protein kinase. The effect of defective cAMP binding on holoenzyme activation. *J Biol Chem* **264**, 13321-13328.

Wu, S. Y., and Casida, J. E. (1992). Neuropathy target esterase inhibitors: 2-alkyl-, 2-alkoxy-, and 2-(aryloxy)-4H-1,3,2-benzodioxaphosphorin 2-oxides. *Chem Res Toxicol* **5**, 680-684.

Wyrick, J. J., Holstege, F. C., Jennings, E. G., Causton, H. C., Shore, D., Grunstein, M., Lander, E. S., and Young, R. A. (1999). Chromosomal landscape of nucleosome-dependent gene expression and silencing in yeast. *Nature* **402**, 418-421.

Zahringer, H., Holzer, H., and Nwaka, S. (1998). Stability of neutral trehalase during heat stress in *Saccharomyces cerevisiae* is dependent on the activity of the catalytic subunits of cAMP-dependent protein kinase, Tpk1 and Tpk2. *Eur J Biochem* **255**, 544-551.

Zahringer, H., Thevelein, J. M., and Nwaka, S. (2000). Induction of neutral trehalase Nth1 by heat and osmotic stress is controlled by STRE elements and Msn2/Msn4 transcription factors: variations of PKA effect during stress and growth. *Mol Microbiol* **35**, 397-406.